UNIVERSITY OF CALIFORNIA, SAN DIEGO

Evaluating low oxygen and pH variation and its effects on invertebrate early life stages on upwelling margins

A dissertation submitted in partial satisfaction of the requirements
for the degree Doctor of Philosophy

in

Oceanography

by

Christina A. Frieder

Committee in charge:

Professor Lisa A. Levin, Chair
Professor Andrew G. Dickson
Professor Amro Hamdoun
Professor David A. Holway
Professor James J. Leichter
Professor Todd R. Martz

2013

The Dissertation of Christina A. Frieder is approved, and it is acceptable in quality and form for publication on microfilm and electronically.

Chair

University of California, San Diego

2013

EPIGRAPH

Your preparation for the real world is not in the answers you've learned,

but in the questions you've learned how to ask.

- Bill Watterson

TABLE OF CONTENTS

LIST OF TABLES

LIST OF FIGURES

ACKNOWLEDGEMENT

First, and foremost, I would like to acknowledge the inspirational and insightful nature of my adviser, Lisa Levin. Additionally, all members of the Levin lab have had a profound impact on my journey at Scripps both from a scientific and personal perspective. This includes my big scientific brothers Andrew Thurber and Geoff Cook along with all current graduate students, Ben Grupe, Mike Navarro, Kirk Sato and Natasha Gallo. Without Jen Gonzalez I would have completed just a fraction of the studies within my dissertation. She was instrumental in maintaining larval cultures and assistance with the multi-elemental analysis of larval shells.

My Biological Oceanography cohort has also been a source of constant learning and support. With Ally Pasulka, Aly Fleming, Karli Merkens, Tara Whitty, and my officemate Rebecca Asch we have built strong relationships to last a lifetime, and dabbled in various scientific pursuits that have resulted in collaborations. I am also very gracious for collaborations initiated by the San Diego Coastal Expedition, a two-part UC Ship Funds cruise led by myself with other Scripps graduate students. From this adventure I have and continue to learn a great deal from physical oceanographer SungHyun Nam and marine chemists Yui Takeshita and Emily Bockmon.

I have greatly benefited from access to both Andrew Dickson and Todd Martz's laboratory facilities. My innate skills do not translate well into being a savvy chemist, but Andrew Dickson and Todd Martz along with their lab members have taught me the necessary skills to critically consider accuracy and precision, along with creative solutions for finicky fancy electronics.

Those classes at Scripps with the greatest influence are those that were out of the classroom and in the field. Of course these were Paul Dayton courses. This includes both the Natural History field course and the first implementation of the Subtidal Natural History course. The subtidal course was based on SCUBA diving various habitats along the San Diego coastline. All local, scientific divers should get to Mia's Reef at least once, preferably during epic visibility. Further related to diving, I owe extensive thanks to my fellow diving support. Most notable are Phil Zerofski who let me swim with large animals, Mike Navarro who made me dive deep, Geoff Cook who introduced me to subtidal San Diego, Emily Kelly who I thoroughly rely on for stellar photos, and Eddie Kisfaludy who taught me how to make moorings.

This dissertation would not have been possible without the support of the National Science Foundation, the Science to Achieve Results – Environmental Protection Agency graduate student fellowship, California Sea Grant, the Scripps Director's Fellowship, the Tegner and Mullin Research Grants, UC Ship Funds, CenCal Diving, and the Training Award for New Investigators from ChEss.

Lastly, I would not be where I am today if it weren't for the support of my parents. They always encouraged and provided an environment for perpetual learning.

Chapter 2, in part, is a reprint of the material as it appears in Biogeosciences. Frieder, Christina A., Nam, SungHyun, Martz, Todd R., Levin, Lisa A., 2012. The dissertation author was the primary investigator and author of this paper.

Chapter 3, in part, is currently being prepared for submission for publication of the material. Frieder, Christina A. The dissertation author was the primary investigator and author of this material.

Chapter 4, in part, is currently being prepared for submission for publication of the material. Frieder, Christina A.; Gambi, M. Cristina; Levin, Lisa A. The dissertation author was the primary investigator and author of this material.

Chapter 5, in full, has been submitted for publication of the material as it may appear in Global Change Biology, 2013, Frieder, Christina A.; Gonzalez, Jennifer P.; Bockmon, Emily A.; Navarro, Michael O.; Levin, Lisa A. The dissertation author was the primary investigator and author of this material.

Chapter 6, in part, is currently being prepared for submission for publication of the material. Frieder, Christina A.; Levin, Lisa A. The dissertation author was the primary investigator and author of this material.

VITA

2006 Bachelor of Science, University of California, Santa Barbara

2013 Doctor of Philosophy, University of California, San Diego

PUBLICATIONS

EE Bockmon, CA Frieder, MO Navarro, LA White-Kershek and AG Dickson (2013) Technical note: Controlled experimental aquarium system for multi-stressor investigation of carbonate chemistry, oxygen saturation, and temperature. *Biogeosciences* 10, 5967-5975.

EA Sperling, CA Frieder, AV Raman, PR Giruis, LA Levin, AH Knoll (2013) Oxygen, ecology, and the Cambrian radiation of animals. *Proc. Natl. Acad. Sci.* 110, 13446-13451

CA Frieder, SH Nam, TR Martz and LA Levin (2012) High temporal and spatial variability of dissolved oxygen and pH in a nearshore California kelp forest. *Biogeosciences* 9, 3917-3930.

GE Hofmann, JE Smith, KS Johnson, U Send, LA Levin, F Micheli, A Paytan, NN Price, B Peterson, Y Takeshita, PG Matson, ED Crook, KJ Kroeker, MC Gambi, EB Rivest, CA Frieder, PC Yu and TR Martz (2011) High-frequency dynamics of ocean pH: a multi-ecosystem comparison. *PLoS ONE* 6(12): e28983.

ABSTRACT OF THE DISSERTATION

Evaluating low oxygen and pH variation and its effects on invertebrate early life stages on upwelling margins

by

Christina A. Frieder

Doctor of Philosophy in Oceanography

University of California, San Diego, 2013

Professor Lisa A. Levin, Chair

Along upwelling margins, pH and oxygen vary on multiple temporal and spatial scales, and in many places levels are decreasing with climate change. Continuous monitoring in nearshore settings along an upwelling-influenced margin revealed strong, semidiurnal fluctuations, week-long reduction events, and a tight positive correlation between oxygen and pH. Laboratory experiments were conducted to assess implications of pH and oxygen changes for invertebrate gamete and larval performance. At levels reflecting nearshore conditions, there were effects of low pH on fertilization success in echinoids and larval development and size of two *Mytilus* mussel species, but there was

no apparent effect of low oxygen alone or in combination with pH. Fertilization experiments indicated that pH variability present within the habitat of *Strongylocentrotus franciscanus* could hinder fertilization success when timing of spawning coincides with low pH conditions. The incorporation of semidiurnal pH fluctuations, the dominant scale of observed temporal variability, into laboratory experiments alleviated negative effects of reduced pH in both *Mytilus* species studied. Furthermore, at lower pH, high variance in echinoid sperm performance and in larval size of *Mytilus* spp. suggests the raw material exists for evolutionary adaptation to reduced pH. Population variance in combination with temporal and spatial variation in pH may be increasingly important in future, low-pH oceans. Additionally, the observation of species-specific responses to pH among congeneric echinoids and mytilid mussels implies that we cannot assume similar sensitivity to reduced pH based on taxonomic relatedness. Further understanding of responses to ocean acidification may be aided by knowledge of larval pH-exposure history. The development of a larval-based geochemical proxy revealed that U/Ca in larval shells reflected differing pH exposures of mussel larvae. Application to outplanted larvae developing along the San Diego coastline demonstrated that higher U/Ca in larval shells can reflect upwelling and exposure to low pH. Notably, present-day pH conditions are at times low enough to elicit significant effects on fertilization in *S. franciscanus*, on larval development of *Mytilus* spp., and on the geochemical composition of larval shells. These effects could influence the sustainability and persistence of these commercially harvested species as ocean acidification intensifies along upwelling margins.

CHAPTER 1

Introduction

Most benthic invertebrates are broadcast spawners, releasing their gametes into the external environment where fertilization occurs. Embryos become planktonic larvae developing and dispersing in the pelagic realm. This life stage is terminated when competent larvae undergo metamorphosis and join benthic populations as juveniles (Fig. 1.1). In the plankton, gamete and larval performance is an integration of many environmental drivers (Pechenik, 1987). Often the highest mortality rates in marine populations occur during this early life stage (Rumrill, 1990). This population bottleneck has cultivated a rich history of larval ecology investigations on how varying environmental conditions influence gamete performance, fertilization success and larval performance in the plankton (Young, 1990).

More recently, research on early life stage success in the pelagic realm has shifted focus to climate change parameters (Byrne, 2012). A threat of recent concern is ocean acidification (Doney *et al.*, 2009). Another is ocean deoxygenation (Keeling *et al.*, 2010; Gruber, 2011). Together they could serve as an accelerating threat to the early life stages of marine invertebrates, particularly along upwelling margins where pH and dissolved oxygen ($[O_2]$) covary (Booth *et al.*, 2012; Frieder *et al.*, 2012) and conditions of low pH and $[O_2]$ shoal into the nearshore environment during upwelling events (Feely *et al.*, 2008).

Ocean Acidification

Since the industrial revolution, human activities have altered the earth's biogeochemical cycles to such an extent that the ocean is undergoing climatic changes. Thirty percent of anthropogenic CO_2 emitted over the last 250 years has been absorbed by the ocean (Sabine *et al.*, 2004), and pH in open-ocean surface waters has dropped about 0.1 pH units over this time period (Bates *et al.*, 2012). CO_2 in seawater forms carbonic acid and reacts with carbonate ion to form two bicarbonate ions resulting in the release of protons, which reduces the pH. This is concomitant with a decrease in the concentration of carbonate ion and thus lowers the saturation state with regard to the mineral phases of $CaCO_3$. Biological responses to ocean acidification can therefore be a function of one or many changes in the inorganic carbon chemistry. Studies to date indicate that fertilization in most, but not all, broadcast spawners is rather robust to ocean acidification (Byrne, 2012), and sensitivity is usually detected only at extremely low pH values (e.g., Kurihara & Shirayama, 2004). Among the later larval developmental stages, calcifying larvae are most sensitive to ocean acidification (Kurihara, 2008; Byrne, 2012).

Ocean Deoxygenation

Ocean deoxygenation is primarily a consequence of the ocean's heat uptake (Keeling *et al.*, 2010). Increased temperatures reduce oxygen solubility in seawater, and increased stratification results from ocean warming, causing interior $[O_2]$ levels to drop. Long-term loss of $[O_2]$ has been observed in the open ocean (Stramma *et al.*, 2008), and along upwelling margins (Whitney *et al.*, 2007; Chan *et al.*, 2008; Bograd *et al.*, 2008; Crawford & Peña, 2013). It is unclear whether decreasing trends along upwelling margins

are secular or part of low-frequency multi-decadal cycles (McClatchie *et al.*, 2010). While there is confidence that ocean deoxygenation will continue into the future, reliable projections for where and how much are less well developed (Gruber, 2011). Decreasing [O_2] is of concern for organisms that require a certain minimum level for survival. Experiments exposing larvae to hypoxic conditions have revealed tolerance levels that are taxon-specific (Eerkes-Medrano *et al.*, 2013). Tolerance levels also vary as a function of larval size, with smaller and younger larvae being more sensitive than larger and older larvae (Widdows *et al.*, 1989; Wang & Widdows, 1991).

The Role of Natural Spatial and Temporal Environmental Variability

While decreased pH and [O_2] elicit biological sensitivities, there are uncertainties with how these threats play out in environments that undergo short-term fluctuations that regularly exceed long-term predictions. Coastal water pH often undergoes strong daily and seasonal changes that are much greater than those changes in the open ocean (Hofmann *et al.*, 2011), and strong spatial gradients exist in [O_2] and pH along upwelling margins (Feely *et al.*, 2008). This variability could be a source of stress alleviation or exacerbation under present-day and future conditions. Elucidating the role of variability in modulating responses of early life stages to ocean acidification is a persistent theme within my dissertation.

pH and [O_2] are also considered in combination because a strong positive correlation exists between the two along upwelling margins. During upwelling events, the inner-shelf is exposed to deep seawater depleted in [O_2] and enriched in pCO_2 from remineralization of organic matter (Feely *et al.*, 2008). In addition to upwelling, the

inner-shelf undergoes multiple scales of environmental variability resulting in high-frequency (largely semidiurnal and diurnal) excursions of [O_2] and pH (Booth *et al.*, 2012; Frieder *et al.*, 2012).

Regional Setting for the Dissertation

The San Diego margin is situated within the Southern California Bight (SCB). The SCB is characterized by water masses from the subarctic through the California Current and the tropical Pacific via the California Undercurrent (Bray *et al.*, 1999; Dong *et al.*, 2009). Seasonal upwelling is strongest during the spring when equatorward currents lift isopycnal surfaces and bring low [O_2] and low pH water from intermediate depths onto the continental shelf (Bray *et al.*, 1999; Feely *et al.*, 2008). During July and December of 2012, a two-part student-led research cruise, the San Diego Coastal Expedition, characterized the structure of oxygen and carbonate chemistry in nearshore and offshore waters of San Diego. [O_2] and pH gradients with depth in the upper 200 m were much stronger during July than December, concurrent with seasonal upwelling patterns (Fig. 1.2). Oxygen concentrations within this depth range were as great as 300 μmol kg^{-1} and as low as 50 μmol kg^{-1}. pH was as great as 8.1 and as low as 7.6. These sharp gradients in the upper water column are the source of extensive variability in inner-shelf habitats. Furthermore, long-term changes in the depth gradients of oxygen and pH in offshore settings will influence conditions over the margin.

The SCB also harbors one of the world's fastest growing primary producers, the giant kelp *Macrocystis pyrifera*. Kelp forests are the foundation for diverse and energy-rich habitats of great ecological and economic importance (Graham *et al.*, 2007).

Invertebrate life events and stages studied during my dissertation occur within the kelp forest, and more generally, in nearby nearshore habitats. The SCB is a relevant and important setting for studying the effects of multiple, interacting stressors on marine organisms because upwelling margins have been suggested as particularly vulnerable habitats for climate change (Gruber, 2011), there is existing evidence for changes in the $[O_2]$ and pH structure of the region, along with region-specific projections for acidification (Bograd *et al.*, 2008; Hauri *et al.*, 2013), and the nearshore habitats have a rich history of investigation.

The Thesis: Introductory Remarks

When I began my dissertation in 2007 there was a paucity of data documenting present-day, nearshore $[O_2]$ and pH dynamics. This type of information is particularly necessary when predicting the effects of ocean acidification in local and regional settings. For example, baseline conditions and scales of variability for kelp forests, an ecologically and economically important habitat, did not exist aside from a handful of discrete measurements (e.g., Delille *et al.*, 2009). This led to the deployment of the first two "SeapHOx" instrument packages that provide high-frequency and reliable $[O_2]$, pH, salinity and temperature data. Chapter 2, published as Frieder et al. (2012), characterizes the time and space scales of variability of $[O_2]$ and pH in the La Jolla Kelp Forest and adjacent nearshore settings using SeapHOx instrumentation. Emphasis was placed on documenting changes with depth, cross-shore and alongshore direction. Understanding of present-day variability regimes and underlying drivers of $[O_2]$ and pH change will influence how nearshore habitats along upwelling margins are considered in the context

of climate change. Information resulting from these deployments provided key information for the latter chapters of my dissertation.

Marine organism sensitivity to pH and [O_2] is often species- and habitat-specific. Chapter 3 examines the effects of pH on fertilization in four species of temperate echinoids. Three of the species were congeners of *Strongylocentrotus*, the fourth was the sand dollar, *Dendraster excentricus*. These species vary in habitat overlap, depth distributions and relative genetic relatedness. These species were selected to determine whether fertilization in additional *Strongylocentrotus* urchin species were sensitive to reductions in pH as has been shown for *S. franciscanus* (Reuter *et al.*, 2011), and whether fertilization in another echinoid from similar depths was sensitive to pH. Fertilization assays were carried out to determine at which sperm-egg ratios fertilization success was sensitive to reduced pH, if at all. Multiple sperm-egg ratios need to be incorporated into fertilization tests because they are the most important determinant of fertilization success (Vogel *et al.*, 1982). When there are too few sperm relative to eggs than fertilization is near-zero, oversaturation of sperm relative to eggs and fertilization rates are so high that any effect of the environment is often masked. Incorporating sperm-limiting conditions into laboratory experiments is also important because natural spawning events for some echinoids can be sperm limited (Levitan, 2004). Further experimental tests developed pH response curves for *Strongylocentrotus purpuratus* and *S. franciscanus*. Since *S. franciscanus* fertilization was the most sensitive to pH reductions, pH data were collected from the natural habitat of *S. franciscanus* during its reproductive season to determine whether fertilization success could be influenced by present-day pH conditions.

Extending the scrutiny of pH effects from fertilization to early developmental stages, CO_2-induced acidification experiments have revealed many sublethal effects on echinoid larvae. In general, development is slower and the pluteus arms are smaller at reduced pH (Kurihara, 2008; Dupont *et al.*, 2010; Ross *et al.*, 2011; Byrne, 2012). While all experimental observations to date are based on laboratory-controlled experiments, unique field laboratories exist where effects of CO_2-induced reductions in pH are a result of volcanic venting. Such sites exist in the Mediterranean, and interestingly, adult urchins are absent from regions of high venting and very low pH. Chapter 4 utilizes an in-situ larval culturing technique to expose laboratory-spawned echinoid larvae of *Paracentrotus lividus* and *Arbacia lixula* to natural gradients in pH. The experiments tested whether the size of larval sea urchins were smaller or more variable at reduced pH sites. *A. lixula* embryos were exposed to venting for two days and developed into 4-arm pluteus. *P. lividus* larvae were reared for ten days in the laboratory and transferred to the venting sites for three days to investigate the sensitivity of 'older' larvae to changes in pH. This study represents the first test of larval responses to reduced pH in natural field settings. One of the benefits of field experiments is that they incorporate natural variability associate with light, temperature, currents and food cycles.

Incorporating cycles of natural variability and multiple stressors into laboratory experiments are rare. Chapter 5 describes laboratory studies in which pH, $[O_2]$ and semidiurnal pH fluctuations were manipulated to test their effects on early development and growth in *Mytilus californianus* and *M. galloprovincialis.* Values of pH, $[O_2]$ and semidiurnal pH ranges chosen for these experiments reflected observations from shallow, nearshore settings (Chapter 2; Frieder et al. 2012) along with region-specific acidification

scenarios (Hauri *et al.*, 2013). The objectives of this chapter were to investigate the singular and interactive effects of (1) low pH and low [O_2], and (2) semidiurnal pH fluctuations relative to stable pH, on the survivorship, development, and size of mytilid larvae. The relative role of [O_2] and pH in structuring larval performance was tested by manipulating them alone and in combination. I adopted *Mytilus californianus* and *M. galloprovincialis* larvae as model species because they play key ecological roles in the rocky intertidal, have been shown to be sensitive to low pH (Kurihara *et al.*, 2008; Gaylord *et al.*, 2011), larval development patterns are similar between the two species, adults coexist but dominate in different environments, and peak spawning periods are different for the two species exposing them to different upwelling regimes (Carson *et al.*, 2010).

More often than not, pH and [O_2] experienced by planktonic larvae are unknown due to difficulties in tracking larval abundance and distributions in the field. Natural geochemical proxies in larval carbonate structures are one means by which environmental conditions can be estimated. The most reliable [O_2] or carbonate chemistry proxy would be primarily controlled by physicochemical processes that have limited influence from endogenous factors. Chapter 6 probes for such a geochemical proxy in larval carbonates of *Mytilus californianus* and *M. galloprovincialis*. The shell material utilized for this chapter was generated during experiments described in Chapter 5. The objectives of this chapter were (1) to determine if aragonitic mytilid larval shells precipitated in varying [O_2] and pH conditions have distinct single- or multi-element signatures, (2) to evaluate whether element accumulation was influenced by ontogenetic effects, represented by larval shell size, and (3) to compare element signatures of

experimentally cultured larval shells with those of field-cultured larval shells with either known pH and [O_2] exposure histories or known spatial gradients in upwelling intensity.

The final chapter, Chapter 7, summarizes and integrates the findings of this dissertation and their implications.

References

Bates NR, Best MHP, Neely K, Garley R, Dickson AG, Johnson RJ (2012) Detecting anthropogenic carbon dioxide uptake and ocean acidification in the North Atlantic Ocean. *Biogeosciences*, **9**, 2509–2522.

Bograd SJ, Castro CG, Di Lorenzo E, Palacios DM, Bailey H, Gilly W, Chavez FP (2008) Oxygen declines and the shoaling of the hypoxic boundary in the California Current. *Geophysical Research Letters*, **35**, L12607.

Booth JAT, McPhee-Shaw EE, Chua P, *et al.* (2012) Natural intrusions of hypoxic, low pH water into nearshore marine environments on the California coast. *Continental Shelf Research*, **45**, 108–115.

Bray NA, Keyes A, Morawitz WML (1999) The California Current system in the Southern California Bight and the Santa Barbara Channel. *Journal of Geophysical Research*, **104**, 7695.

Byrne M (2012) Global change ecotoxicology: Identification of early life history bottlenecks in marine invertebrates, variable species responses and variable experimental approaches. *Marine Environmental Research*, **76**, 3–15.

Carson HS, López-Duarte PC, Rasmussen L, Wang D, Levin LA (2010) Reproductive timing alters population connectivity in marine metapopulations. *Current Biology*, **20**, 1926–31.

Chan F, Barth JA, Lubchenco J, Kirincich A, Weeks H, Peterson WT, Menge BA (2008) Emergence of anoxia in the California current large marine ecosystem. *Science*, **319**, 920.

Crawford WR, Peña MA (2013) Declining oxygen on the British Columbia continental shelf. *Atmosphere-Ocean*, **51**, 88–103.

Delille B, Borges AV, Delille D (2009) Influence of giant kelp beds (*Macrocystis pyrifera*) on diel cycles of pCO_2 and DIC in the Sub-Antarctic coastal area. *Estuarine, Coastal and Shelf Science*, **81**, 114–122.

Doney SC, Fabry VJ, Feely RA, Kleypas JA (2009) Ocean acidification: The other CO_2 problem. *Annual Review of Marine Science*, **1**, 169–192.

Dong C, Idica EY, McWilliams JC (2009) Circulation and multiple-scale variability in the Southern California Bight. *Progress in Oceanography*, **82**, 168–190.

Dupont S, Ortega-Martínez O, Thorndyke M (2010) Impact of near-future ocean acidification on echinoderms. *Ecotoxicology*, **19**, 449–62.

Eerkes-Medrano D, Menge BA, Sislak C, Langdon CJ (2013) Contrasting effects of hypoxic conditions on survivorship of planktonic larvae of rocky intertidal invertebrates. *Marine Ecology Progress Series*, **478**, 139–151.

Feely RA, Sabine CL, Hernandez-Ayon JM, Ianson D, Hales B (2008) Evidence for upwelling of corrosive "acidified" water onto the continental shelf. *Science*, **320**, 1490–2.

Frieder CA, Nam SH, Martz TR, Levin LA (2012) High temporal and spatial variability of dissolved oxygen and pH in a nearshore California kelp forest. *Biogeosciences*, **9**, 3917–3930.

Gaylord B, Hill TM, Sanford E, *et al.* (2011) Functional impacts of ocean acidification in an ecologically critical foundation species. *The Journal of Experimental Biology*, **214**, 2586–94.

Graham MH, Vásquez JA, Buschmann AH (2007) Global ecology of the giant kelp Macrocystis: From ecotypes to ecosystems. *Oceanography and Marine Biology: An Annual Review*, **45**, 39-88.

Gruber N (2011) Warming up, turning sour, losing breath: Ocean biogeochemistry under global change. *Philosophical Transactions of the Royal Society A*, **369**, 1980–96.

Hauri C, Gruber N, Vogt M, *et al.* (2013) Spatiotemporal variability and long-term trends of ocean acidification in the California Current System. *Biogeosciences*, **10**, 193–216.

Hofmann GE, Smith JE, Johnson KS, *et al.* (2011) High-frequency dynamics of ocean pH: A multi-ecosystem comparison. (W-C Chin, Ed.). *PloS ONE*, **6**, e28983.

Keeling RF, Körtzinger A, Gruber N (2010) Ocean deoxygenation in a warming world. *Annual Review of Marine Science*, **2**, 199–229.

Kurihara H (2008) Effects of CO_2-driven ocean acidification on the early developmental stages of invertebrates. *Marine Ecology Progress Series*, **373**, 275–284.

Kurihara H, Asai T, Kato S, Ishimatsu A (2008) Effects of elevated pCO_2 on early development in the mussel *Mytilus galloprovincialis*. *Aquatic Biology*, **4**, 225–233.

Kurihara H, Shirayama Y (2004) Effects of increased atmospheric CO_2 on sea urchin early development. *Marine Ecology Progress Series*, **274**, 161–169.

Levitan DR (2004) Density-dependent sexual selection in external fertilizers: Variances in male and female fertilization success along the continuum from sperm limitation to sexual conflict in the sea urchin *Strongylocentrotus franciscanus*. *The American Naturalist*, **164**, 298–309.

McClatchie S, Goericke R, Cosgrove R, Auad G, Vetter R (2010) Oxygen in the Southern California Bight: Multidecadal trends and implications for demersal fisheries. *Geophysical Research Letters*, **37**, L19602.

Pechenik JA (1987) Environmental influences on larval survival and growth. In: *Reproduction of Marine Invertebrates, Vol. 9* (eds: Giese AC, Pearse JS), pp551–608. New York, Blackwell Scientific.

Reuter KE, Lotterhos KE, Crim RN, Thompson CA, Harley CDG (2011) Elevated pCO_2 increases sperm limitation and risk of polyspermy in the red sea urchin *Strongylocentrotus franciscanus*. *Global Change Biology*, **17**, 163–171.

Ross PM, Parker L, O'Connor WA, Bailey EA (2011) The impact of ocean acidification on reproduction, early development and settlement of marine organisms. *Water*, **3**, 1005–1030.

Rumrill SS (1990) Natural mortality of marine invertebrate larvae. *Ophelia*, **32**, 163–198.

Sabine CL, Feely RA, Gruber N, *et al.* (2004) The oceanic sink for anthropogenic CO_2. *Science*, **305**, 367–71.

Stramma L, Johnson GC, Sprintall J, Mohrholz V (2008) Expanding oxygen-minimum zones in the tropical oceans. *Science*, **320**, 655–8.

Vogel H, Czihak G, Chang P, Wolf W (1982) Fertilization kinetics of sea urchin eggs. *Mathemetical Biosciences*, **58**, 189–216.

Wang W, Widdows J (1991) Physiological responses of mussel larvae *Mytilus edulis* to environmental hypoxia and anoxia. *Marine Ecology Progress Series*, **70**, 223–236.

Whitney FA, Freeland HJ, Robert M (2007) Persistently declining oxygen levels in the interior waters of the eastern subarctic Pacific. *Progress in Oceanography*, **75**, 179–199.

Widdows J, Newell RIE, Mann R (1989) Effects of hypoxia and anoxia on survival, energy metabolism, and feeding of oyster larvae (*Crassostrea virginica*, Gmelin). *Biological Bulletin*, **177**, 154–166.

Young CM (1990) Larval ecology of marine invertebrates: A sesquicentennial history. *Ophelia*, **32**, 1–48.

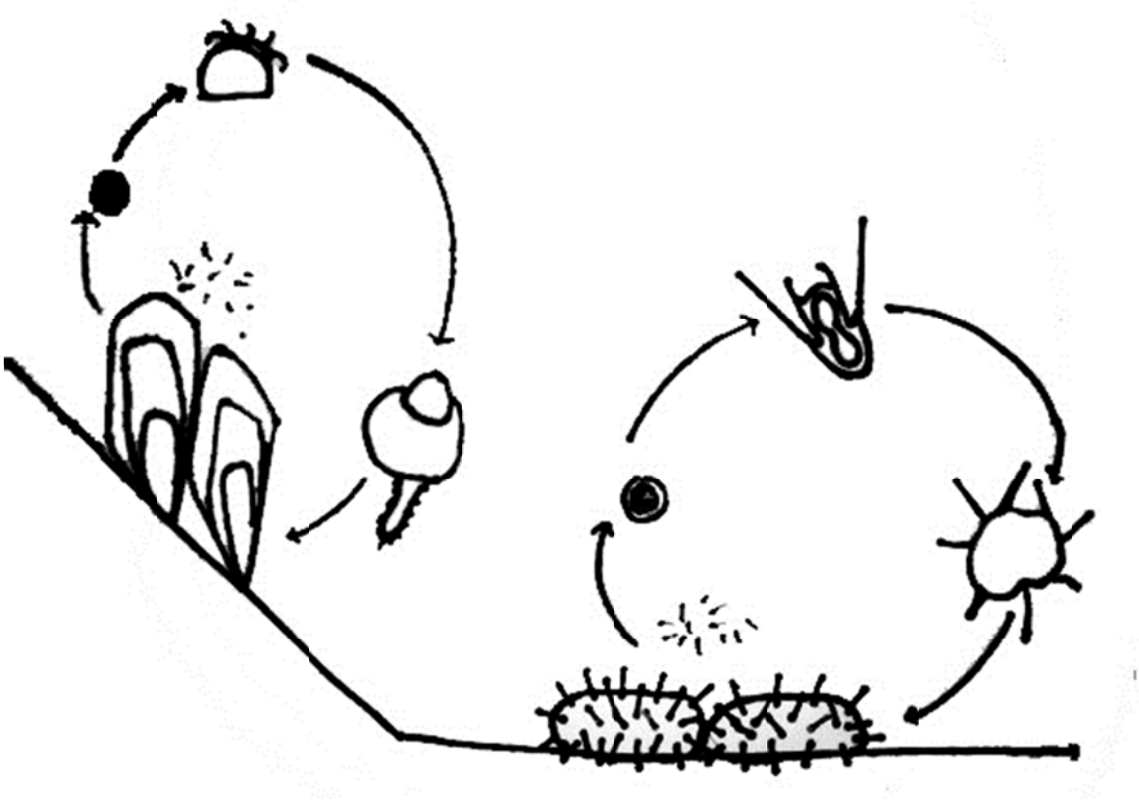

Figure 1.1. Life cycle diagram of mytilid mussels and echinoid urchins. Both taxa are broadcast spawners, fertilization occurs externally, embryos develop into larvae, undergo continued growth and metamorphose into juveniles and return to the benthos.

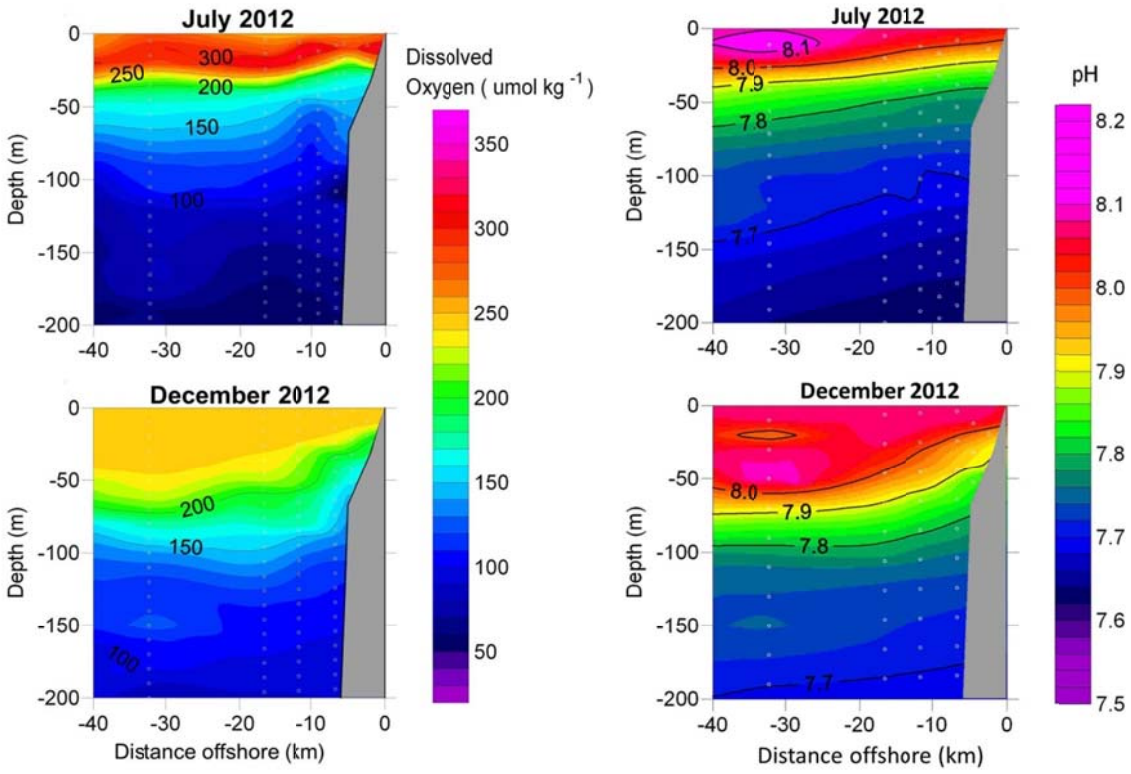

Figure 1.2. Section plots of dissolved oxygen and pH during July and December 2012 along the San Diego margin.

CHAPTER 2

High temporal and spatial variability of dissolved oxygen and pH in a nearshore California kelp forest

Synopsis

This chapter examines the temporal and spatial variability of pH and dissolved oxygen ($[O_2]$) along the southern California coast, with an emphasis on kelp forests. Information about $[O_2]$ and carbonate chemistry was sought in order to understand the range of environmental conditions influencing fertilization potential of broadcast spawners and to determine the exposure histories of planktonic larvae originating both within kelp forests and in nearby settings.

This chapter is presented as a paper. "High spatial and temporal variability of dissolved oxygen and pH in a nearshore California kelp forest," published in Biogeoscienes in 2012, characterizes $[O_2]$ and pH gradients in an alongshore, cross-shore, and depth direction over multiple temporal scales from hours to months.

Biogeosciences, 9, 3917–3930, 2012
www.biogeosciences.net/9/3917/2012/
doi:10.5194/bg-9-3917-2012

Biogeosciences

High temporal and spatial variability of dissolved oxygen and pH in a nearshore California kelp forest

C. A. Frieder[1], S. H. Nam[2], T. R. Martz[3], and L. A. Levin[1,4]

[1]Integrative Oceanography Division, Scripps Institution of Oceanography, University of California San Diego, 9500 Gilman Drive, 92093–0218 La Jolla, CA, USA
[2]Climate, Atmospheric Science and Physical Oceanography, Scripps Institution of Oceanography, University of California San Diego, 9500 Gilman Drive, 92093–0230 La Jolla, CA, USA
[3]Geosciences Research Division, Scripps Institution of Oceanography, University of California San Diego, 9500 Gilman Drive, 92093–0244 La Jolla, CA, USA
[4]Center for Marine Biodiversity and Conservation, Scripps Institution of Oceanography, University of California San Diego, 9500 Gilman Drive, 92093–0218 La Jolla, CA, USA

Correspondence to: C. A. Frieder (cfanner@ucsd.edu)

Received: 13 March 2012 – Published in Biogeosciences Discuss.: 30 March 2012
Revised: 30 August 2012 – Accepted: 10 September 2012 – Published: 12 October 2012

Abstract. Predicting consequences of ocean deoxygenation and ocean acidification for nearshore marine ecosystems requires baseline dissolved oxygen (DO) and carbonate chemistry data that are both high-frequency and high-quality. Such data allow accurate assessment of environmental variability and present-day organism exposure regimes. In this study, scales of DO and pH variability were characterized over one year in a nearshore kelp forest ecosystem in the Southern California Bight. DO and pH were strongly, positively correlated, revealing that organisms on this upwelling shelf are not only exposed to low pH but also to low DO. The dominant scale of temporal DO and pH variability occurred on semi-diurnal, diurnal and event (days–weeks) time scales. Daily ranges in DO and pH at 7 m water depth (13 mab) could be as large as 220 μmol kg^{-1} and 0.36 units, respectively. Sources of pH and DO variation include photosynthesis within the kelp forest ecosystem, which can elevate DO and pH by up to 60 μmol kg^{-1} and 0.1 units over one week following the intrusion of high-density, nutrient-rich water. Accordingly, highly productive macrophyte-based ecosystems could serve as deoxygenation and acidification refugia by acting to elevate DO and pH relative to surrounding waters. DO and pH exhibited greater spatial variation over a 10 m increase in water depth (from 7 to 17 m) than along a 5 km stretch of shelf in a cross-shore or alongshore direction. Over a three-month time period, mean DO and pH at 17 m water depth were 168 μmol kg^{-1} and 7.87, respectively. These values represent a 35% decrease in mean DO and 37% increase in $[H^+]$ relative to near-surface waters. High-frequency variation was also reduced at depth. The mean daily range in DO and pH was 39% and 37% less, respectively, at 17 m water depth relative to 7 m. As a consequence, the exposure history of an organism is largely a function of its depth of occurrence within the kelp forest. With knowledge of local alkalinity conditions and high-frequency temperature, salinity, and pH data, we estimated pCO_2 and calcium carbonate saturation states with respect to calcite and aragonite (Ω_{calc} and Ω_{arag}) for the La Jolla kelp forest at 7 m and 17 m water depth. pCO_2 ranged from 246 to 1016 μatm, Ω_{calc} was always supersaturated, and Ω_{arag} was undersaturated at the beginning of March for five days when pH was less than 7.75 and DO was less than 115 μmol kg^{-1}. These findings raise the possibility that the benthic communities along eastern boundary current systems are currently acclimatized and adapted to natural, variable, and low DO and pH. Still, future exposure of coastal California populations to even lower DO and pH may increase as upwelling intensifies and hypoxic boundaries shoal, compressing habitats and challenging the physiological capacity of intolerant species.

1 Introduction

Increased levels of atmospheric carbon dioxide (CO_2) have reduced subsurface oxygen concentrations and increased acidity of surface waters (Gruber, 2011; Doney et al., 2012). Ocean deoxygenation is due to a combination of warming, increased stratification and altered ocean circulation (Keeling et al., 2010). Ocean acidification is an increase in oceanic CO_2 uptake and the concomitant decrease in seawater pH and saturation states of calcium carbonate (Ω; Doney et al., 2009). Much of what has been learned about carbonate chemistry and dissolved oxygen (DO) trends and trajectories in the ocean is based upon open-ocean conditions measured via ship-based hydrographic time series that sample quarterly, annually or even less often. This limits our understanding of DO and carbonate chemistry dynamics in nearshore settings.

The coastal environment is a highly variable system. Fluctuations in temperature, salinity, air–sea gas exchange, mixing processes and biogeochemical processes can have large influences on DO and pH. There are contemporary nearshore environments, particularly eastern boundary current systems, which are exposed to low pH, high pCO_2, and low Ω conditions during upwelling events (Feely et al., 2008; Hofmann et al., 2011b). Deoxygenation and acidification are of particular concern in tandem in ocean regions where DO and inorganic carbon are tightly linked through local primary production and/or remineralization of organic matter (Cai et al., 2011; Gruber, 2011; Hofmann et al., 2011a). Understanding the nature and drivers of DO and carbonate chemistry dynamics along eastern boundary current systems, which harbor ecologically and economically important species, will provide insight into the relative sensitivity of these systems to a changing ocean climate.

There has been much emphasis on understanding the physical characteristics of nearshore waters in upwelling systems, and different scales of variability have been identified and associated with specific processes. Sources of variability in temperature and nutrients, for example, include El Niño-Southern Oscillation (ENSO), seasonal and temporal upwelling, coastally trapped waves, coastal sea breeze, and internal tidal waves and bores (Pineda, 1999; Lerczak et al., 2001; Lluch-Cota et al., 2001; Kaplan et al., 2003; Pringle and Riser, 2003), but there is presently limited information regarding DO and pH dynamics in relation to these different scales of variability. Recent studies have found that the upper horizon of the hypoxic boundary (defined as 60 μmol kg^{-1}) in the Southern California Bight (SCB) has shoaled by almost 100 m near the coastline since the 1980s (Bograd et al., 2008), with consequences for benthic fishes (McClatchie et al., 2010). ENSO cycles also influence DO over the SCB shelf. The 2010 La Niña event led to a 38–50 % decline in DO relative to the normal seasonal mean (Nam et al., 2011). Strong upwelling events also bring low pH water toward the surface along the eastern Pacific margin, with pH_{sws} values falling below 7.7 near the coastline (Feely et al., 2008). Some high-frequency variability in pH has been reported in nearshore habitats (Hofmann et al., 2011b; Yu et al., 2011; Booth et al., 2012). Results indicate that pH signatures are ecosystem and site-specific with characteristic diel, semidiurnal, and stochastic patterns of varying amplitudes. Kelp forests in upwelling regions can exhibit large fluctuations in pH conditions due to a combination of mixing, tidal excursions, upwelling, and biological activity (Hofmann et al., 2011b).

The SCB is characterized by water masses from the subarctic and tropical Pacific through the California Current and California Undercurrent (Bray et al., 1999; Dong et al., 2009). Seasonal upwelling is strongest during the spring when equatorward currents lift isopycnal surfaces and bring low DO and low pH water from intermediate depths onto the continental shelf (Bray et al., 1999; Feely et al., 2008). The complex bathymetry and coastline of the SCB drives extensive variability in circulation features, and coastal regions are affected by both locally and coastally propagated remote forcing that drives temporal upwelling events at timescales of a few days to weeks (Pringle and Riser, 2003; Dong et al., 2009; Send and Nam, 2012). The SCB also harbors one of the world's fastest growing primary producers, the giant kelp *Macrocystis pyrifera*. Kelp forests are abundant along the SCB coast (North et al., 1993), and serve as the foundation for diverse and energy-rich habitats of great ecological and economic importance (Graham et al., 2007). Understanding the DO and pH dynamics within kelp forests will provide detailed information regarding the corresponding exposure histories for a diversity of valued species of molluscs, echinoderms, crustaceans and fishes. Additionally, it is important to identify present-day carbonate chemistry conditions in coastal macrophyte-dominated ecosystems, as recent evidence suggests that under high-CO_2 scenarios kelps have variable but often positive responses to elevated CO_2 (Swanson and Fox, 2007; Roleda et al., 2012). A working hypothesis for kelps in the SCB is that they may respond positively to the direct and indirect effects of ocean acidification but negatively to the direct and indirect effects of warming (Harley et al., 2012). Still, other evidence suggests that under high-CO_2 scenarios canopy-forming macroalgae could experience greater competition with noncalcareous turf species (Connell and Russell, 2010; Hepburn et al., 2011).

Here, we characterize variability of DO and pH in the La Jolla kelp forest (LJKF) and adjacent nearshore settings. We deployed two sensors in a variety of configurations in order to ask the following questions: What are the dominant short-term scales of pH and DO variability? Is there spatial variation in pH and DO within the kelp forest linked to depth, alongshore direction, or cross-shore direction? What is the relationship between pH and DO in the kelp forest and is the relationship stable in time and space? To constrain the carbonate system in nearshore settings, two of the four possible parameters must be directly measured or estimated with robust empirical relationships (Cullison Gray et al., 2011; Alin

et al., 2012). With knowledge of local alkalinity conditions and the high-frequency pH, salinity and temperature data, we estimated pCO_2 and Ω for two forms of $CaCO_3$, calcite and aragonite (Ω_{calc} and Ω_{arag}, respectively), and consider how spatial and temporal heterogeneity in carbonate chemistry and DO may influence different levels of biological organization and organism exposure histories.

2 Methods

2.1 Field measurements

We used moorings deployed on the inner shelf, located within and around the LJKF to explore cross-shore, alongshore and water depth effects on DO and pH between July 2010 and November 2011 (Fig. 1). The shelf in this region is 8 km wide and the kelp forest, at its fullest extent, is 8 km long and up to 1.5 km wide. Time-series data were collected with a sampling rate of 15 min using two instruments placed in different configurations among moorings (Fig. 1). Data were nearly continuously collected from mooring A (32.81° N 117.29° W; 20 m bottom depth) within the LJKF. The sensor was attached 13 m above bottom (mab or 7 m water depth) to explore variability in DO and pH over multiple temporal scales (Fig. 1a). Changes in DO and pH with water depth were investigated by comparing concurrent data from mooring A at 7 m and 17 m (3 mab) below the surface (Fig. 1b). Alongshore changes in DO and pH were explored by comparing sensor data from 7 m water depth from mooring A and mooring D (32.85° N 117.28° W; 20 m bottom depth), which was located 5 km to the north in an alongshore direction and still within the LJKF (Fig. 1c). Cross-shore changes in DO and pH were explored by comparing sensor data from 7 m water depth at different locations along an east–west transect perpendicular to the local coastline (Fig. 1d). In 2010, the paired moorings were mooring B, 3.5 km from the coast (32.81° N 117.31° W; 30 m bottom depth), and mooring A, 1.9 km from the coast. Mooring B is located offshore of the kelp forest. In 2011, the paired moorings were mooring A (1.9 km from the coast) and mooring C, 1.4 km from the coast (32.81° N 117.28° W; 15 m bottom depth). Concurrent DO and pH data exist for all deployments except that no pH data were available from August to November 2011 at mooring A due to a sensor malfunction.

Data were collected using two "SeapHOx" instrument packages. The SeapHOx consists of a Honeywell Durafet III pH sensor (Martz et al., 2010), an Aanderaa 3835 oxygen optode, and an SBE-37 MicroCAT CTD. One of the MicroCAT CTDs was equipped with a pressure sensor. We compared LJKF data with current speed and direction measured in the upper 30 m of the water column (100 m bottom depth) from the Del Mar mooring located 14 km to the NW (DM Buoy: 32.94° N 117.32° W). Current data were obtained every 7.5 min at 5 m intervals from 5 to 100 m using

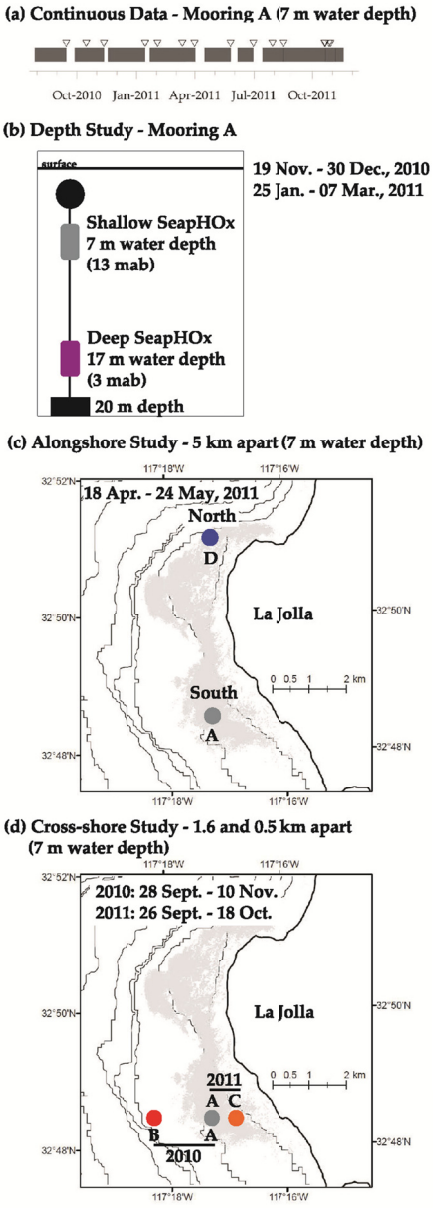

Fig. 1. Placement of SeapHOx sensors among moorings to characterize DO and pH differences **(a)** over time, **(b)** with depth, **(c)** in an alongshore direction, and **(d)** in a cross-shore direction. Bathymetric contours are in 10 m increments (10–60 m depth). At least one discrete sample (upside-down triangles) was taken per SeapHOx deployment to calibrate the pH sensor. Color scheme of moorings corresponds with subsequent figures. Grey shading in **(c)** and **(d)** depicts maximum extent of the La Jolla Kelp Forest based on aerial surveys from 1989–2009 (California Department of Fish and Game).

a down-looking 300 kHz acoustic Doppler current profiler (ADCP).

2.2 Calibrations

To calibrate the pH sensors, discrete water samples were taken during each SeapHOx deployment for the determination of total alkalinity (TA) and total dissolved inorganic carbon (DIC) (Fig. 1a). The calibration samples were collected via SCUBA next to the sensor with a 5 l Niskin bottle during the middle and/or end of the sensor deployment. This was not done at the beginning of the deployment because we found the pH sensor requires a day before providing stabilized data. The collected seawater was transferred to a 500 ml clean borosilicate glass bottle with a ground glass neck and stopper. The samples were poisoned with a saturated mercuric chloride solution. TA measurements were determined using an open-cell, potentiometric titration (Dickson et al., 2007). DIC measurements were determined by acid extraction and coulometric detection of CO_2 (Dickson et al., 2007). pH was calculated from TA and DIC using the Matlab version of CO2SYS (van Heuven et al., 2011) with dissociation constants from Mehrbach et al. (1973) as refitted by Dickson and Millero (1987). The calculated pH at in situ temperature from the calibration sample was used to determine the electrode-specific calibration coefficients. When two calibration samples were taken during the same SeapHOx deployment, they were averaged since we did not find significant evidence of drift and these sensors have been shown to be stable for months at a time (Martz et al., 2010). The calibration sample produced a pH accuracy of 0.01 units for each SeapHOx instrument. The oxygen sensors were factory calibrated by Aanderaa, and before each deployment a two-point (0 % and 100 % saturation) offset was applied as recommended in the manual. Data from SeapHOx deployments presented in this paper are available at http://osprey.bco-dmo.org.

2.3 Data analysis

DO and pH data from the SeapHOx sensors were analyzed as either unfiltered data in order to illustrate the extremes and rates of change or a 2-d running mean was applied to raw data. pH is reported on the total hydrogen ion scale at in situ temperature. Extreme salinity outliers (≥ 3 SD) were removed, and density was calculated from salinity and temperature data. Time in all figures is shown in Coordinated Universal Time (UTC). Although uptake and release of dissolved inorganic carbon leads to a slightly nonlinear relationship between pH and DO, for the purposes of our statistical description a simple linear fit between the two was sufficient to distinguish underlying patterns, and the use of higher-order functions was deemed unnecessary. Accordingly, the relationship between DO and pH was determined with a Model-II least squares fit for all concurrent data of DO and pH. Spectral analyses were calculated on detrended datasets using a fast fourier transform. Spectra of temperature, DO and pH were averaged over four 16-d windows from the longest continuous deployment at mooring A, 7 m below the surface from 25 January 2011–31 March 2011. Pressure data were not available during this time period. Instead, spectra were averaged over four 11.5-d windows from 29 July 2010–13 September 2010, and averaging yielded a typical power spectrum of pressure for this region. To explore DO, pH, and temperature cycles at semidiurnal and diurnal timescales, a fast fourier transform was applied to data and desired frequencies were bandpass filtered (e.g., $DO_{f=1}$ or $DO_{f=2}$, frequency of once per day or twice per day). Current data obtained from the DM mooring were decomposed into cross-shore (u) and alongshore (v) components, and both were smoothed with a 2-d running mean. Equatorward phases were designated as time periods when the alongshore current velocity at all depths between 5 and 30 m was southward, e.g., $v < 0$, and poleward phases were designated as time periods when alongshore current velocity at all depths between 5 and 30 m was northward, e.g., $v > 0$.

pCO_2, Ω_{arag}, and Ω_{calc} were estimated from the high-frequency pH, temperature, and salinity data generated by the SeapHOx at 7 m and 17 m water depth at mooring A, along with upper and lower estimates of TA for the LJKF. The lower and upper values chosen for TA were 2225 and 2260 µmol kg^{-1}. These values are 5 µmol kg^{-1} beyond that observed from the minimum and maximum values from all discrete samples ($n = 18$) taken for SeapHOx calibration purposes. Additionally, these values fall within the range reported by Alin et al. (2012) for TA < 100 m water depth. Carbonate chemistry parameters were calculated using the Matlab version of CO2SYS (van Heuven et al., 2011). Using the upper and lower limit of TA for this system along with pH, temperature and salinity data resulted in an average range for each calculated value of pCO_2 of 8 µatm. The average ranges for each calculated value of Ω were 0.031 for Ω_{arag} and 0.049 for Ω_{calc}.

3 Results

3.1 Temporal variability in dissolved oxygen and pH

3.1.1 Diurnal and semidiurnal scales of dissolved oxygen and pH variability

Two time scales of periodic variability were identified within one year at mooring A: semidiurnal and diurnal. The average daily range (peak-to-peak) in DO and pH were 63 µmol O_2 kg^{-1} ($n = 249$ d; SD = 39.4) and 0.11 pH units ($n = 169$ d; SD = 0.07). The daily range could be as great as 220 µmol O_2 kg^{-1} and 0.36 pH urits. DO, pH, temperature and pressure at 7 m water depth exhibited energetic variance at both the semidiurnal and diurnal frequencies (Fig. 2). Semidiurnal variance was greater than diurnal

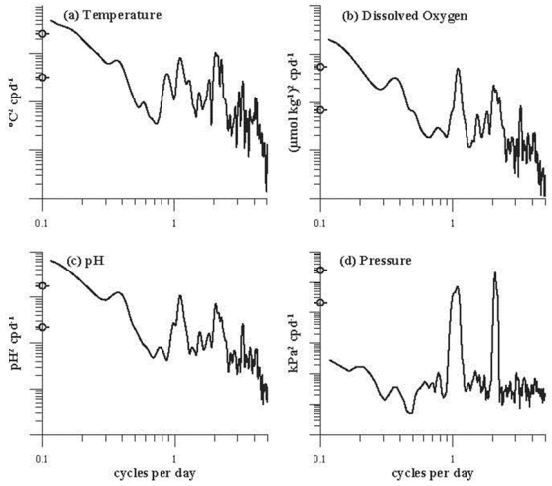

Fig. 2. Frequency power spectra (cycles per day) from mooring A at 7 m water depth for **(a)** temperature, **(b)** dissolved oxygen, **(c)** pH and **(d)** pressure. The circles on the left side of each graph denote the critical scale for 95 % confidence in energy peaks.

variance for temperature and pressure, but diurnal variance was greater than semidiurnal variance for DO and pH. Semidiurnal and diurnal DO and pH fluctuations had differing proportions of physical and biological forcing. Semidiurnal fluctuations in DO and pH were well correlated with temperature, suggesting that the primary source of semidiurnal variability was physical isothermal fluctuations ($DO_{f=2} = 19.2 \times temp_{f=2}$, $R^2 = 0.85$, $P < 0.001$; $pH_{f=2} = 0.03 \times temp_{f=2}$, $R^2 = 0.74$, $P < 0.001$). DO and pH were less correlated with temperature at the diurnal band ($DO_{f=1} = 16.4 \times temp_{f=1}$, $R^2 = 0.55$, $P < 0.001$; $pH_{f=1} = 0.03 \times temp_{f=1}$, $R^2 = 0.53$, $P < 0.001$). A decrease in correlation at the diurnal bandwidth indicates that diurnal isothermal fluctuations either play less of a role in diurnal forcing of DO and pH, or other mechanisms (e.g., diel scales of production and respiration, and/or air–sea gas exchange associated with diurnal land–sea breeze) are opposing diurnal modulations in DO and pH forced by temperature. These observed high-frequency scales of fluctuations in the LJKF are not only persistent through time, but also encompass a large range of DO and pH conditions.

3.1.2 Event-scale variability in dissolved oxygen and pH

Overall increases and decreases in DO and pH, and intermittent amplifications of higher-frequency (e.g., diurnal and semidiurnal) fluctuations lasting from days to weeks, were observed in the LJKF. Here we define changes in pH and DO lasting more than one day to multiple weeks as event-scale variability.

Mean increases in DO and pH: Notable increases in DO and pH were observed for approximately a week following the occasional intrusion of high-density (deep, cold, and nutrient-rich) water. High-density waters were defined as $\sigma > 25.1\,kg\,m^{-3}$. This value has been suggested to reflect water containing the threshold concentration of nitrate required for kelp growth (Parnell et al., 2010). During 2010–2011 there were seven events (observed among all moorings) when high-density seawater shoaled to 7 m water depth (Table 1). These events fueled primary production and increased DO and pH with the exception of the August 2010 event at mooring B, when high mean DO ($290\,\mu mol\,kg^{-1}$) existed prior to the intrusion of high-density seawater. ΔDO and ΔpH were calculated as the difference between the mean value for seven days before the intrusion of high-density seawater and the mean value for seven days after the intrusion of high-density seawater. The magnitude of the regional water velocity after the event (v after) explained 62 % of the variation in ΔpH ($\Delta pH = 0.012 \times v$ after $- 0.02$, $R^2 = 0.62$, $P = 0.035$). The greatest ΔDO and ΔpH values occurred when alongshore currents transitioned from equatorward to strong poleward currents. As an illustrative example, such an event occurred during late April to early May 2011 at mooring D (Fig. 3). Mean DO at $\sigma < 25.1$ prior to the event was $247\,\mu mol\,kg^{-1}$, and mean DO at $\sigma < 25.1$ the subsequent week was $309\,\mu mol\,kg^{-1}$, reflecting a 20 % increase in DO. The corresponding mean pH before and after the event was 8.07 and 8.17, respectively. Similar observations were made during the same time period in south LJKF (mooring A). Mean DO before the event was $249\,\mu mol\,kg^{-1}$, and mean DO after the event was $312\,\mu mol\,kg^{-1}$. The corresponding mean pH before and after the event at mooring A was 8.05 and 8.15, respectively. The influx of high-density, nutrient-replete water masses occurred when alongshore current direction was equatorward and was followed by a strong poleward reversal that stimulated biological production within the LJKF, causing a release of DO, uptake of CO_2, and thus increased pH.

Mean decreases in DO and pH: Event-scale mean decreases in DO and pH were rare at 7 m water depth but were observed during Fall 2010 and 2011 (Table 2). In 2010, mean DO and pH dropped below $200\,\mu mol\,kg^{-1}$ and 7.9 units for an extended period of time on two occasions. The first event lasted for two days from 4–5 September 2010, and the end of the second event was not captured but lasted > 1.4 d. In 2011, mean DO dropped below $200\,\mu mol\,kg^{-1}$ four times (corresponding pH data not available). Each event lasted between one and five days.

Changes in DO and pH variability regimes: We have documented large daily ranges in pH and DO, with magnitudes corresponding to alongshore current direction. Daily DO and pH ranges were greatly enhanced when alongshore currents were equatorward (Fig. 4). As an example, between 29 September 2010–9 November 2010, DO and pH varied up to $113\,\mu mol\,kg^{-1}\,d^{-1}$ and $0.22\,units\,d^{-1}$, respectively. When

Table 1. Event-scale mean increases in dissolved oxygen (ΔDO) and pH (ΔpH) proceeding intrusion of high-density water ($\sigma > 25.1\,kg\,m^{-3}$) at 7 m water depth. v and u indicate the mean velocity ($cm\,s^{-1}$) of alongshore and cross-shore currents, respectively, between 5 and 30 m for 7 d before and after the event. Negative values are equatorward or offshore for v and u, respectively. Positive values of ΔDO and ΔpH indicate mean increases from before to after the event. Events are ordered by magnitude of ΔDO.

Event start	Mooring	v before	v after	u before	u after	ΔDO	ΔpH
14 Jul 2010	B	−1.6	4.3	0.5	1.0	66	0.07
26 Apr 2011	A	−3.8	10.9	0.7	2.5	63	0.10
26 Apr 2011	D	−3.8	10.9	0.7	2.5	62	0.10
27 Nov 2010	A	−4.4	5.9	1.2	0.8	35	0.03
31 Jul 2011	A	0.8	0.0	1.2	3.4	35	0.01
21 Aug 2010	A	0.3	4.2	−0.7	0.1	25	0.03
21 Aug 2010	B	0.3	4.2	−0.7	0.1	−2	−0.02

Table 2. Low dissolved oxygen (ΔDO) and pH (ΔpH) events at 7 m water depth at mooring A. Event start date is day that low-pass filtered DO and pH fell below 200 $\mu mol\,kg^{-1}$ and 7.9 units, respectively. nd = no data.

Event start	Duration	Mean DO	Mean pH	Mean density
04 Sep 2010	1.8	136	7.82	25.5
12 Sep 2010	> 1.4	157	7.88	25.0
03 Sep 2011	4.5	180	nd	25.0
21 Sep 2011	2.3	189	nd	25.0
01 Oct 2011	1.1	184	nd	25.0
16 Oct 2011	3.1	184	nd	25.0

alongshore currents were directed poleward, the maximum daily range in DO and pH was reduced to 40 $\mu mol\,kg^{-1}$ and 0.01 units, respectively.

3.2 Spatial variability in dissolved oxygen and pH

3.2.1 Changes in dissolved oxygen and pH with water depth

Simultaneous measurements at 7 and 17 m documented large differences in mean DO and pH over small depth scales within the kelp forest (Fig. 5). Mean DO and pH in shallow water were 259 $\mu mol\,kg^{-1}$ and 8.07, respectively. Only 10 m deeper, mean DO and pH were 168 $\mu mol\,kg^{-1}$ and 7.87. These represent a 35% decrease and 37% increase in DO and $[H^+]$, respectively, from 7 to 17 m. Deep DO and pH were below 130 $\mu mol\,kg^{-1}$ and 7.8 for 20% of the time, and the minimum DO and pH observed were 86 $\mu mol\,kg^{-1}$ and 7.67, respectively. Over this 10 m depth range, the average DO and pH gradients were 9 $\mu mol\,kg^{-1}\,m^{-1}$ and 0.02 pH units m^{-1}. The large differences between the DO and pH environment were related to the strength of density stratification (Fig. 6a and b). When the water column was well-stratified, DO and pH decreased with increasing depth. A density difference of 0.2–1 $kg\,m^{-3}$ could

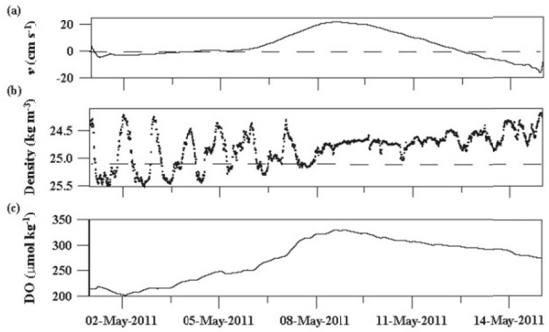

Fig. 3. Event-scale increases in dissolved oxygen (DO) following the intrusion of high-density seawater ($\sigma > 25.1\,kg\,m^{-3}$) at 7 m below the surface at mooring D. **(a)** Mean alongshore current velocity between 5 and 30 m at the Del Mar buoy, **(b)** time series of density and **(c)** time series of 2-d smoothed DO from 26 April 2011–16 May 2011. Density scale is reversed. Positive alongshore velocities indicate poleward flow.

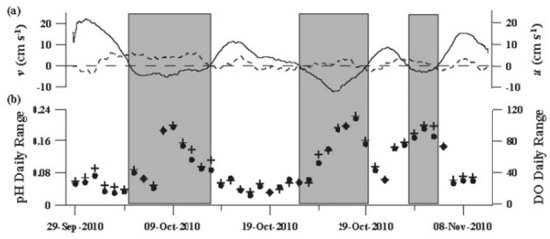

Fig. 4. (a) Mean alongshore current velocity (v: solid) and mean cross-shore current velocity (u: dotted) between 5 and 30 m from the Del Mar buoy and **(b)** daily range in pH (circles) and dissolved oxygen (DO: crosses) from mooring A at 7 m water depth. Grey-shaded rectangles indicate time periods when alongshore velocities are equatorward (negative). See Fig. 8 for corresponding time series of density, DO and pH.

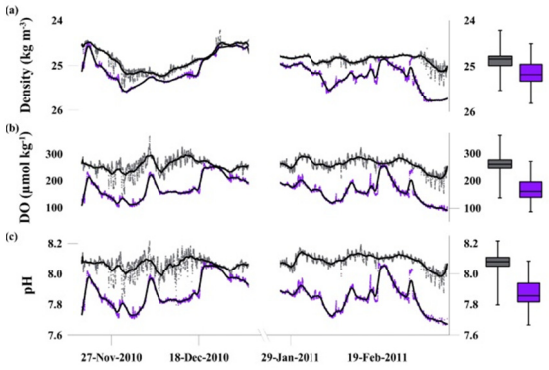

Fig. 5. Density, dissolved oxygen (DO) and pH comparisons between 7 m (grey) and 17 m (purple) at mooring A during two separate deployments. Time series and corresponding box plots of **(a)** density, **(b)** dissolved oxygen and **(c)** pH. Black solid lines are 2-d smoothed data. Density scale is reversed. Box plots at right depict the minimum, maximum, median, lower quartile and upper quartile for corresponding time-series data.

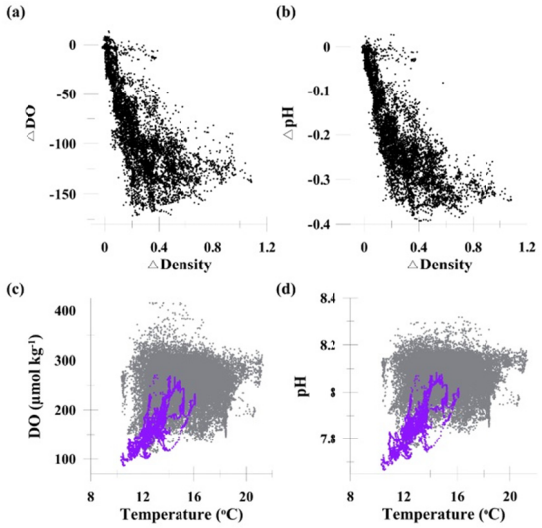

Fig. 6. Scatter plots of **(a)** density difference (ΔDensity) and dissolved oxygen difference (ΔDO) between 7 and 17 m at mooring A, and **(b)** ΔDensity and pH difference (ΔpH) between 7 and 17 m at mooring A. Includes all data from Fig. 5. Scatter plots of **(c)** temperature and DO, and **(d)** temperature and pH at 7 m (grey hatches) and 17 m (purple hatches) below the surface from all SeapHOx deployments from 10 July 2010–19 October 2011.

equate to a 0.4 unit decrease in pH and a DO reduction of 170 µmol kg^{-1}. On one occasion, starting on 19 December 2010, the water column was well-mixed, but on the fourth day DO and pH steadily decreased at 17 m while remaining stable near the surface; there was no apparent stratification between depths ($\sigma_{7\,m} \approx \sigma_{17\,m}$, Fig. 5). This suggests that the photosynthesis to respiration ratio ($P : R$) in deep water was below one. Variability patterns were also different in deep and shallow water. The mean change per hour in DO in shallow water was 4 µmol kg^{-1} h^{-1} (SD = 7.04), whereas in deep water the mean rate of change was 2.5 µmol kg^{-1} h^{-1} (SD = 4.43). In shallow water the mean change per hour in pH was 0.01 units h^{-1} (SD = 0.02); in deep water the mean rate of change was only 0.006 units h^{-1} (SD = 0.01). Thus, the near-surface DO and pH conditions were more variable on semidiurnal and diurnal timescales, while near-bottom depths (17 m; 3 mab) exhibited more stable conditions at high frequencies and large changes were associated with the structure of the water column over event time scales.

3.2.2 Alongshore changes in dissolved oxygen and pH within the kelp forest

Differences in DO and pH within the kelp forest were examined 5 km apart in an alongshore direction at 7 m water depth. The moorings were located in north and south LJKF. There were minimal but significant differences in DO and pH during the study period (Fig. 7). Mean DO was 258 versus 252 µmol kg^{-1} ($t = 5.8$, $d.f. = 2469$, $P < 0.001$) and mean pH was 8.10 versus 8.05 in north LJKF (mooring D) versus south LJKF (mooring A), respectively ($t = 17.5$, $d.f. = 2469$, $P < 0.001$). The average gradient from north to south in DO and pH were negligible (e.g., < 1.5 µmol kg^{-1} km^{-1} and 0.01 units km^{-1}). Temporal variability was also similar at both sites. Concordant high-frequency, large excursions in DO and pH occurred on diurnal and semidiurnal frequencies at both moorings. Event-scale increases in DO and pH resulting from biological production in response to the intrusion of high-density, high-nutrient seawater were observed in both the north and south LJKF, and magnitudes of change were very similar (Table 1; event start = 26 April 2011). This suggests that the spatial scale of these events can span the entire length of the kelp forest (≥ 5 km). However, beginning 16 May 2011 higher density waters, with a low pH and DO signature, were observed in south LJKF but not in north LJKF for two days. At that time, the gradient in DO and pH from south to north significantly increased to 20 µmol kg^{-1} km^{-1} and 0.05 units km^{-1}, respectively. Mean temperature was 1 °C cooler in south LJKF versus north LJKF. This discrepancy between north and south LJKF was also observed earlier in the month, between 1 May and 6 May 2011. Thus, in general there was a great deal of coherence in DO and pH in north and south LJKF but minor differences existed and were likely related to different local forcing dynamics.

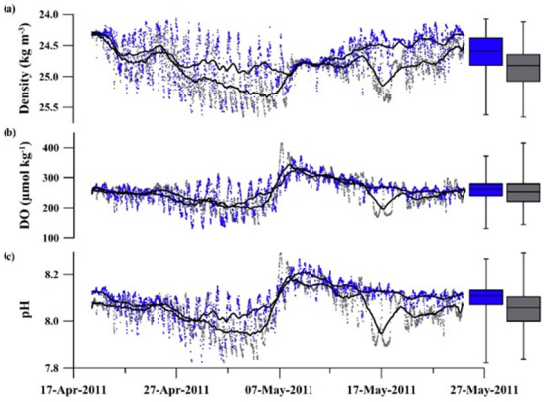

Fig. 7. Alongshore comparisons in density, dissolved oxygen (DO) and pH in the south and north La Jolla kelp forest. Time series and corresponding box plots of **(a)** density, **(b)** DO and **(c)** pH at south LJKF (mooring A; grey) and north LJKF (mooring D; blue) at 7 m below the surface. Black solid lines are 2-d smoothed data. Density scale is reversed. Box plot depicts the minimum, maximum, median, lower quartile and upper quartile for corresponding time-series data.

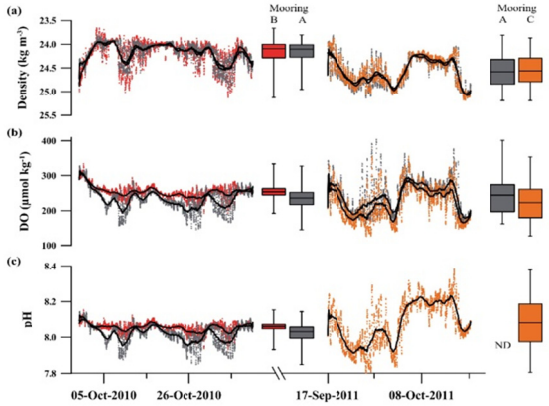

Fig. 8. Cross-shore differences in time series and corresponding box plots of **(a)** density, **(b)** dissolved oxygen (DO) and **(c)** pH. From 28 September 2010–10 November 2010, one SeapHOx was deployed at mooring B, 3.5 km from the coast (red), and the other SeapHOx was deployed at mooring A, 1.9 km from the coast (grey). From 26 September 2011–18 October 2011, one SeapHOx was deployed at mooring A, 1.9 km from the coast (grey), and the other SeapHOx was deployed at mooring C, 1.4 km from the coast (orange). Black solid lines are 2-d smoothed data. Density scale is reversed. Box plot depicts the minimum, maximum, median, lower quartile and upper quartile for corresponding time-series data. ND = no data.

3.2.3 Cross-shore changes in dissolved oxygen and pH on the inner shelf

DO and pH conditions varied strongly with proximity to shore. Mean DO and pH at 7 m decreased with decreasing distance from shore, suggesting that isopleths of DO and pH slope up towards the coast (Fig. 8). Two measurement experiments were conducted during the same months (September–November) in 2010 and 2011 along a zonal transect (Fig. 1). During 2010, mean DO was 20 µmol kg^{-1} lower at 1.9 km versus 3.5 km from the coast ($t = 37.3$, $d.f. = 4117$, $P < 0.001$), resulting in a DO gradient of -13 µmol kg^{-1} km^{-1} (towards the coastline). Mean pH was 0.03 units lower ($t = 38.5$, $d.f. = 4117$, $P < 0.001$), and the gradient was -0.02 units km^{-1}. These differences could not be attributed to water mass as the density gradient between moorings was negligible (< 0.01 kg m^{-3} km^{-1}), and there was no significant difference in density conditions ($P > 0.05$). The same trend emerged during 2011. Mean DO was 19 µmol kg^{-1} lower at 1.4 km versus 1.9 km from the coast ($t = 15.5$, $d.f. = 3064$, $P < 0.001$), and resulted in a gradient of -38 µmol kg^{-1} km^{-1}. A pH comparison was not available for 2011. Density was greater at the outer mooring ($t = 3.27$, $d.f. = 4117$, $P < 0.002$). The expectation would be that DO and pH would be greater closer to shore if considering only physical water excursion, but the opposite trend has emerged.

The decoupling between DO and pH with density was investigated by comparing the changes in the linear relationship between DO and pH with density with respect to distance from shore. At a given density, DO and pH were lower inshore relative to offshore, particularly at high density values. This phenomenon was corroborated by changes in the linear relationship between density and DO or pH with varying distance from shore. There was a significant decrease in the intercept of the linear relationship between density and DO with decreasing distance from shore during both years (2010: $t = 33.7$, $d.f. = 8231$, $P < 0.001$; 2011: $t = 14.2$, $d.f. = 6125$, $P < 0.001$). There was also a significant decrease in the intercept of the linear relationship between density and pH with decreasing distance from shore during 2010 ($t = 14.6$, $d.f. = 8231$, $P < 0.001$). These relationships illustrate that the change in the DO and pH environment with proximity to shore was due to shoaling isopleths that were decoupled from isopycnals.

3.3 Relationship between dissolved oxygen and pH

There was a significant, positive linear relationship between DO and pH for all data collected at 7 and 17 m water depths (pH = 0.002 × DO + 7.50, $R^2 = 0.96$, $P < 0.001$; Fig. 9). The linear relationship between DO and pH was more stable at depth than near the surface (7 m: $R^2 = 0.85$, $P < 0.001$; 17 m: $R^2 = 0.97$, $P < 0.001$), and the strong relationship between DO and pH indicates a mechanistic link. There were no significant linear relationships between DO or pH and temperature at 7 m water depth ($P > 0.05$;

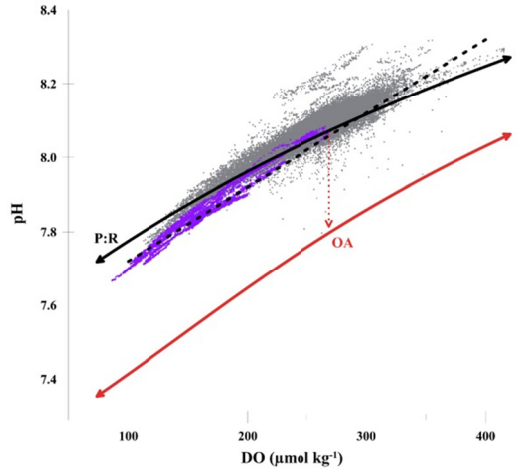

Fig. 9. Scatter plot of dissolved oxygen (DO) and pH at 7 m (grey hatches) and 17 m (purple hatches) water depth from all SeapHOx deployments from 10 July 2010–19 October 2011. Dashed black line is the linear relationship between pH and DO for all data regardless of depth. Solid black line represents expected changes in DO and pH with production and respiration ($P:R$) at present-day conditions (384 ppm CO_2). Future changes in pH due to ocean acidification are modeled at oxygen saturation and CO_2 levels of 800 ppm (OA; dashed red line) along with the corresponding changes in the $P:R$ relationship (solid red line).

Fig. 6c and d), but at 17 m there were positive linear relationships ($DO = 32.9 \times temp - 2.6$, $R^2 = 0.62$, $P < 0.001$; $pH = 0.08 \times temp + 6.88$, $R^2 = 0.67$, $P < 0.001$). The positive relationship between temperature and DO or pH can be best explained by biologically-driven gradients and is opposite to thermodynamically-predicted changes in temperature with DO or pH. The stronger correlation at depth suggests that physically forced changes via water movement are more important in driving changes in DO and pH in deeper waters, while local biochemical processes and air–sea gas exchange dominate at the surface.

Low DO and pH were linked, but high DO and pH were not. The minimum pH and DO values during this study were observed simultaneously at 17 m water depth on 30 December 2010; these were 7.67 and 86 µmol kg^{-1} (31 % saturation), respectively. The maximum pH value observed was 8.38 at 7 m water depth on 15 October 2011, whereas the maximum DO value observed was 415 µmol kg^{-1} (165 % saturation) at 7 m water depth on 7 May 2011. These findings indicate that low DO and pH are persistently linked in the LJKF benthic environment.

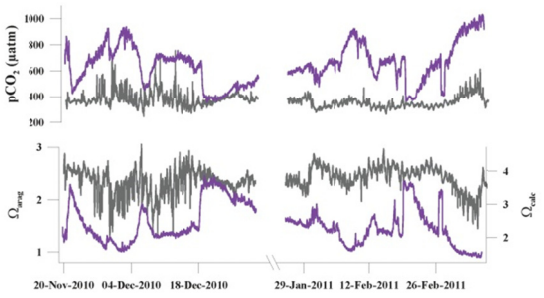

Fig. 10. Estimates of pCO_2 and saturation state of aragonite and calcite (Ω_{arag} and Ω_{calc}) at 7 m (grey) and 17 m (purple) water depth at mooring A during two separate deployments. The width of the line at each point represents the range estimated for pCO_2 or Ω as calculated from pH, temperature, and salinity measured by the SeapHOx sensor and a TA range of 2225–2260 µmol kg^{-1}.

3.4 Estimates of pCO_2 and saturation state in the LJKF

pCO_2, Ω_{arag}, and Ω_{calc} were estimated using sensor data collected at 7 m and 17 m during the depth experiment (data used corresponds with Fig. 5) along with TA ranges specific to this system. At 7 m water depth, estimated pCO_2 ranged between 246 and 820 µatm, and between 353 and 1016 µatm at 17 m water depth (Fig. 10). Estimated Ω_{arag} ranged between 1.15 and 3.05 at 7 m water depths, and between 0.90 and 2.45 at 17 m water depth (Fig. 10). Estimated Ω_{calc} ranged between 1.81 and 4.78 at 7 m water depth, and between 1.41 and 3.83 at 17 m water depth (Fig. 10). The highest pCO_2 and lowest Ω corresponded with the lowest DO and pH conditions observed.

4 Discussion

4.1 Temporal scales of dissolved oxygen and pH variability

Large ranges in DO and pH were observed on semidiurnal, diurnal and event time scales in the LJKF. This is not unexpected given that short-term fluctuations in many nearshore environments, including the California inner shelf, have been previously documented for many variables including temperature, nutrients, pH and DO (Kaplan et al., 2003; McPhee-Shaw et al., 2007; Moore et al., 2009; Jiang et al., 2011; Hofmann et al., 2011b; Booth et al., 2012). These dynamics are likely to be representative of all nearshore environments that are under strong influence of winds, tides, and upwelling, such as the major eastern boundary current (Benguela, California, Canary, Humboldt Current) systems. We expected to observe a prominent diel signal from production and respiration of the kelp forest ecosystem as has been observed in other kelp forests (Delille et al., 2009), but diel modulations

of DO and pH were not the dominant forcing observed in the LJKF. This could be due to strong water advection that may dampen the productivity signal by continually replenishing kelp forest waters, or the signal could have been counteracted by strong modulations from temperature. Diurnal changes in cross-shore advection can easily dominate in this study area due to intermittently enhanced diurnal winds associated with diurnal land–sea breeze (Pidgeon and Winant, 2005), wind- and tide-driven diurnal waves (Lerczak et al., 2001; Nam and Send, 2011), and sea/land breeze-driven resonant oscillations (Nam and Send, 2012).

The observed strong modulations of diurnal DO and pH fluctuations under equatorward currents (Fig. 4) are consistent with previous studies on the concentration and trapping of near-inertial (close to diurnal frequency in study location) internal wave energy under upwelling rather than downwelling conditions (Federiuk and Allen, 1996; Chant, 2001; Lerczak et al., 2001). Such internal waves are a primary mechanism supplying nitrate to kelp forests (McPhee-Shaw et al., 2007), and are important for sustaining kelp growth. During this study, kelp forest ecosystem production in response to high-density, high-nutrient seawater led to elevated DO and pH on event time scales encompassing a few days to weeks; mean increases in DO and pH were related to alongshore current direction and velocity (Fig. 4, Table 1). Poleward flow following upwelling advects low DO (and low pH) water along the shelf and results in event-scale DO and pH changes that can be as significant as the effects of isopycnal shoaling on DO and pH (Send and Nam, 2012). Our observations provide additional evidence for the significant role of alongshore currents in event-scale DO and pH variability. In particular, biological production is expected to regulate mean DO and pH conditions for weeks at a time. High-density waters were present while alongshore current direction was equatorward. The transition from strong equatorward to poleward currents corresponded with the accumulation of DO, and uptake of CO_2, yielding increases in pH. Ecosystem production in response to the intrusion of high-density waters to shallow depths was evident in the DO and pH records at multiple times throughout the year (Table 1).

4.2 Spatial scales of dissolved oxygen and pH variability

The largest gradients in DO and pH in this study occurred with changes in water depth. pH values not expected until 2100 at the surface in open ocean settings were observed frequently at 17 m depth in the LJKF (Caldeira and Wickett, 2003). The structure of the DO and pH gradient with depth was linked to the density structure of the water column, and so future changes in stratification will alter the duration and frequency over which benthic communities are exposed to low DO and pH conditions.

Cross-shore gradients in DO and pH were greater than alongshore gradients. These results correspond to previously documented long alongshore correlation scales in currents (Winant, 1983; Lentz and Winant, 1986), water properties, and nutrients (McPhee-Shaw et al., 2007). This suggests that fewer time series stations are needed in an alongshore direction relative to the cross-shore direction to accurately describe DO and pH dynamics.

DO and pH conditions at a given density decreased with decreasing distance from the shore. Mechanisms driving the cross-shore discrepancy among density, DO and pH warrant further investigation. The relationship between DO and pH was maintained at various distances from shore, but DO and pH decreased at a given density towards the shore. Anomalies in the DO and density relationships have been previously observed on the San Diego margin. DO and pH isopleths shoaled towards the coast at a greater rate than isopycnals. The mechanisms that explained the DO anomaly at the Del Mar buoy included decreased subsurface primary production and strengthened poleward flows by the California Undercurrent (Nam et al., 2011), yet the extent to which these processes account for the nearshore anomalies in density with DO or pH observed during this study in the LJKF is unknown. The greatest cross-shore gradients in DO and pH were observed during 2011. The observations were made further inshore (15 and 20 m bottom depth) than during 2010 (20 and 30 m bottom depth). At shallower bottom depths, benthic respiration may play a greater role in shoaling isopleths because benthic respiration processes are integrated over a smaller volume of water.

4.3 Relationship between dissolved oxygen and pH

The linear relationship between DO and pH was stable and coherent with depth, alongshore, and cross-shore directions in the context of this study (Fig. 9). The relationship was stronger with depth, and at high DO and high pH values there was nonlinearity. This nonlinearity may be explained by the expected changes in DO and pH with biological production and respiration ($P : R$) (Fig. 9), which are nonlinear. At high values of DO and pH, production generates a greater increase in DO than pH. The $P : R$ model was produced with mean temperature (14.8 °C), TA (2240 µmol kg^{-1}), and salinity (33.4) conditions. It assumes an $O_2 : CO_2$ Redfield ratio of $-150 : 106$ and a $TA : CO_2$ ratio of $-18 : 106$. The overlap of the $P : R$ model with the DO and pH relationship indicates that the biochemical consumption and production of O_2 is primarily responsible for the corresponding changes in DO and pH observed in the LJKF, and that calcification and dissolution of calcium carbonate play a more minor role. The $P : R$ model was then run under future atmospheric CO_2 conditions at 800 ppm (year 2100) using the same alkalinity, salinity, and temperature conditions but with an increase in DIC (+112 µmol kg^{-1}) at oxygen saturation. This model attributes all of the change in pH to anthropogenic CO_2 intrusion. At DO saturation, pH is expected to decrease by 0.20 units, while at low DO values, pH could be as low as 7.35, a decrease of 0.37 pH units from present low pH

conditions. The additional drop in pH at low DO is a consequence of the nonlinear nature of the carbonate system (Cai et al., 2011; Melzner et al., 2012). Nearshore CO_2-enriched habitats are expected to experience greater changes in pCO_2 than the open surface ocean and have been suggested to be particularly vulnerable habitats in a changing ocean climate (Brewer and Peltzer, 2009; Thomsen et al., 2010; Cai et al., 2011).

There was no significant linear relationship between temperature and DO or pH at shallow depths in contrast to the firm relationship at deeper depths in the region (e.g., Figs. 6c, d and S1 in Nam et al., 2011). DO and pH are more affected by biochemical processes at shallow versus deep depths, and these processes may account for the large deviations in the relationships between temperature and DO or pH.

4.4 Estimates of pCO_2 and saturation state in the LJKF

Increasing evidence suggests that species responses to ocean acidification vary for different carbonate system constituents (Fabry et al., 2008; Doney et al., 2009). Thus, full constraint of the carbonate system, beyond just pH measurements, is critical for defining this nearshore system and the potential sensitivity or resilience of its residents to ocean acidification. The observed range in TA in the LJKF (35 $\mu mol\,kg^{-1}$) has relatively little influence on variability in pCO_2 in this system; instead, changes in pCO_2 are driven by large DIC gradients. Ω_{arag} was undersaturated at 17 m for a short period of time at the end of February and early March 2011. This also corresponded with the lowest DO concentrations observed (Fig. 5). While emphasis has been placed on the strong relationship between DO and pH, low DO also corresponds with low Ω_{arag}, low Ω_{calc}, and high pCO_2.

4.5 Biological implications of dissolved oxygen and pH trends

pH and DO in the LJKF vary on multiple timescales with large ranges; biological responses to pH and DO also unfold over a range of timescales. Rapid pH and DO changes can disturb an organism's extracellular and intracellular acid–base balance; in the LJKF these changes can be as great as 62 $\mu mol\,O_2\,kg^{-1}\,h^{-1}$ and 0.16 pH units h^{-1}. Different taxa react differently to these rapid excursions. For example, mussels cannot control extracellular pH (Thomsen et al., 2010), sea urchins take several days to adjust (Stumm p et al., 2012), and many fish and decapod crustaceans are able to rapidly regulate extracellular and intracellular pH (Heisler, 1984). The biological significance of these low values of DO and pH observed at 17 m water depth in the LJKF is unknown. However, these low values of DO ($< 90\ \mu mol\,kg^{-1}$) are considered to be sublethal thresholds for coastal species of fishes, crustaceans, and bivalves (Vaquer-Sunyer and Duarte, 2008). These groups are common and diverse within the kelp forest at depths deeper than 17 m where even lower DO concentrations occur (Parnell et al., 2006).

It is unclear which aspect of the DO and carbonate chemistry signals will shape ecological patterns and how these aspects are changing over time. Changes in the extremes, ranges, or patterns of variability need to be considered in the context of organismal sensitivity. Knowledge of DO thresholds and responses to low DO events by shelf animals in this region is limited and in need of further study, while our present understanding of organism and ecosystem sensitivity to carbonate chemistry is in relation to mean conditions. Laboratory studies have revealed that some species that are found within this study region, and particularly their early life stages, are sensitive to the pH values observed in and around the LJKF during this study at 17 m. For example, larvae of the mussel *Mytilus californianus*, a foundation species common on rocky shorelines in our study region, precipitated weaker, thinner, and smaller shells and had lower tissue mass at pH_{tot} values of 7.83 and 7.63 versus 7.95 (Gaylord et al., 2011; pH values converted from the National Bureau of Standards (NBS) scale to total scale at 15 °C). pH was observed below 7.83 in the LJKF in deeper waters 32 % of the time. Thus, it is possible that *M. californianus* larvae are exposed to pH conditions in the present day that may elicit laboratory-observed biological responses to low pH. Also, the echinoplutei of the sea urchin *Lytechinus pictus* were smaller and had altered gene expression in pH_{tot} treatments of 7.75 and 7.66 versus control conditions of 7.81 (O'Donnell et al., 2010; pH values converted from NBS to total scale at 18.5 °C). pH conditions less than 7.75 were observed 10 % of the time in the LJKF at 17 m water depth. These examples highlight the potential importance of vertical positioning for invertebrate larvae developing within the kelp forest. Another study on a resident urchin, *Strongylocentrotus franciscanus*, investigated the potential for evolutionary response in larval development to ocean acidification, and found that *S. franciscanus* larvae were smaller but that phenotypic and genetic variation could allow evolutionary responses within 50 yr in response to a pH decrease of 0.31–0.33 units (Sunday et al., 2011). Full understanding of implications will require integration of DO and pH dynamics with research on how oxygen and pH influence energetics, calcification, sinking and swimming behavior.

Our $P : R$ model predicts that under future scenarios of ocean acidification pH could be as low as 7.35 (corresponding pCO_2 of approximately 2100 µatm) at low DO concentrations. This drop could mean that carbonate chemistry will play a larger role in structuring marine ecosystems than DO if DO conditions remain the same over this time period. Yet, while pH may reach extreme low levels, the variability associated with these mean changes is unknown. When just considering changes in the pH and oxygen relationship due to ocean acidification, high-frequency in pH variability would increase relative to present-day variability. This is because in this system, changes in pH are largely driven by changes

in DIC. The same change in DIC at high concentrations will produce a greater change in pH than at low concentrations of DIC.

Still, there are many other processes that may change over the coming decades that will structure pH and oxygen dynamics. These include changes in water-column stability, the $P : R$ ratio, upwelling dynamics (e.g., timing and intensity), wind patterns, and the sources and chemical properties of water that are advected horizontally and vertically into upwelling margins. Model simulations of the California Current System indicate that the seafloor (50–120 m) will become exposed to year-round aragonite undersaturation by 2050 (Gruber et al., 2012). Additionally, future changes in upwelling dynamics in the SCB remain a critical topic for further research. Evidence suggests a general intensification of wind-driven coastal upwelling in major upwelling regions as greenhouse gas concentrations increase (Bakun et al., 2010; Narayan et al., 2010). These results suggest that DO could reach hypoxic values at increasingly shallower depths and result in habitat compression (or expansion) for intolerant (or tolerant) species. We suggest that in eastern boundary current systems biological sensitivity to changes in DO and pH will largely derive from changes that carry low DO and pH waters from depth into nearshore benthic habitats (Feely et al., 2008; Gruber, 2011; Hofmann et al., 2011a).

5 Conclusions

In this study, we show that DO and pH in an eastern Pacific kelp forest can be highly variable, tightly correlated, and reflect influences from many different processes including alongshore-current direction, internal tidal dynamics, and biological production. All of these features invoked large ranges in DO and pH, as well as in pCO_2, Ω_{arag}, and Ω_{calc}. The most extreme and consistent temporal scales of variation in DO and pH were semidiurnal and diurnal. The high productivity of the kelp forest can increase DO and pH on event time scales in response to nutrient-replete water intrusion. This phenomenon may serve to alleviate biological stress following low DO and pH events. Thus, kelp forests and similar macrophyte regions might provide temporary refugia from acidification and deoxygenation when high levels of productivity elevate DO and pH values relative to surrounding waters. The spatial distribution of DO and pH in the LJKF was largely uniform in an alongshore direction, there were minor differences in the cross-shore direction, and there were drastic depth effects that are largely related to stratification of the water column. Future changes in warming and upwelling in the SCB will have implications for the exposure, duration, and frequency of low DO and pH experienced by benthic species and their early life stages. It is likely that nearshore communities along eastern boundary current systems are preadapted to the range of pH and DO observed during this study. However, communities may respond to rapid transitions at sharply defined critical thresholds rather than experience an extended transition to decreased pH. There is a need for more continuous monitoring of DO and pH along with relevant corresponding physical and biochemical variables, particularly where hypoxia lies near the shelf (Hofmann et al., 2011a). Such data will facilitate a mechanistic understanding of DO and pH trends in highly variable and potentially vulnerable coastal ecosystems.

Acknowledgements. We would like to acknowledge B. Peterson and Y. Takeshita, who provided assistance with SeapHOx development and maintenance. We thank Andrew Dickson for providing access to his laboratory facilities to run DIC and TA samples. The ADCP data collected from the DM Buoy were provided by Uwe Send and the SIO Ocean Time Series Group (http://mooring.ucsd.edu). We thank all those who assisted with field and diving support, especially P. Zerofski, M. Navarro and G. Cook. We thank D. Holway, J. Leichter, and A. Dickson for comments on earlier drafts of this manuscript, and F. Melzner and an anonymous reviewer for helpful comments on the submitted manuscripts. This research was supported by NSF-OCE Award Nos. 0927445 and 1041062. This publication was developed under a Science to Achieve Results (STAR) Fellowship Assistance Agreement No. FP916973 awarded by the US Environmental Protection Agency (EPA). It has not been formally reviewed by the EPA. The views expressed in this publication are solely those of the authors.

Edited by: L. C. da Cunha

References

Alin, S. R., Feely, R. A., Dickson, A. G., Hernández-Ayón, J. M., Juranek, L. W., Ohman, M. D., and Goericke, R.: Robust empirical relationships for estimating the carbonate system in the southern California System and application to CalCOFI hydrographic cruise data (2005–2011), J. Geophys. Res., 117, C05033, doi:10,1029/2011JC007511, 2012.

Bakun, A., Field, D. B., Redondo-Rodriguez, A., and Weeks, S. J.: Greenhouse gas, upwelling-favorable winds, and the future of coastal ocean upwelling ecosystems, Glob. Change Biol., 16, 1213–1228, doi:10.1111/j.1365-2486.2009.02094.x, 2010.

Bograd, S. J., Castro, C. G., Di Lorenzo, E., Palacios, D. M., Bailey, H., Gilly, W., and Chavez, F. P.: Oxygen declines and the shoaling of the hypoxic boundary in the California Current, Geophys. Res. Lett., 35, L12607, doi:10.1029/2008GL034185, 2008.

Booth, J. A. T., McPhee-Shaw, E. E., Chua, P., Kingsley, E., Denny, M., Phillips, R., Bograd, S. J., Zeidberg, L. D., and Gilly, W. F.: Natural intrusions of hypoxic, low pH water into nearshore marine environments on the California coast, Cont. Shelf Res., 45, 108–115, doi:10.1016/j.csr.2012.06.009, 2012.

Bray, N. A., Keyes, A., and Morawitz, W. M. L.: The California Current system in the Southern California Bight and the Santa Barbara Channel, J. Geophys. Res., 104, 7695–7714, 1999.

Brewer, P. G. and Peltzer, E. T.: Limits to marine life, Science, 324, 347–348, doi:10.1126/science.1170756, 2009.

Cai, W.-J., Hu, X., Huang, W.-J., Murrell, M. C., Lehrter, J. C., Lohrenz, S. E., Chou W.-C., Zhai, W., Hollibaugh, J. T., Wang, Y., Zhao, P., Guo, X., Gundersen, K., Dai, M., and Gong, G.-C.: Acidification of subsurface coastal waters enhance by eutrophication, Nat. Geosci., 4, 766–770, doi:10.1038/NGEO1297, 2011.

Caldeira, K. and Wickett, M. E.: Anthropogenic carbon and ocean pH, Nature, 425, p. 365, 2003.

Chant, R. J.: Evolution of near-inertial waves during an upwelling event on the New Jersey inner shelf, J. Phys. Oceanogr., 31, 746–764, 2001.

Connell, S. D. and Russell, B. D.: The direct effects of increasing CO_2 and temperature on non-calcifying organisms: increasing the potential for phase shifts in kelp forests, P. R. Soc. B, 277, 1409–1415, doi:10.1098/rspb.2009.2069, 2010.

Cullison Gray, S. E., DeGrandpre, M. D., Moore, T. S., Martz, T. R., Friederich, G. E., and Johnson, K. S.: Application of *in situ* pH measurements for inorganic carbon calculations, Mar. Chem., 125, 82–90, 2011.

Delille, B., Borges, A. V., and Delille, D.: Influence of giant kelp beds (*Macrocystis pyrifera*) on diel cycles of pCO_2 and DIC in the Sub-Antarctic coastal area, Estuar. Coast. Shelf S., 81, 114–122, 2009.

Dickson, A. G. and Millero, F. J.: A comparison of the equilibrium constants for the dissociation of carbonic acid in seawater media, Deep-Sea Res., 34, 1733–1743, 1987.

Dickson, A. G., Sabine, C. L., and Christian, J. R.: Guide to best practices for ocean CO_2 measurements, Vol. 3, 374 PICES Spec. Publ., Sidney, British Columbia, 2007.

Doney, S. C., Fabry, V. J., Feely, R. A., and Kleypas, J. A.: Ocean acidification: The other CO_2 problem, Annu. Rev. Mar. Sci., 1, 169–192, doi:10.1146/annurev.marine.010908.163834, 2009.

Doney, S. C., Ruckelshaus, M., Duffy, J. E., Barry, J. P., Chan, F., English, C. A., Galindo, H. M., Grebmeier, J. M., Hollowed, A. B., Knowlton, N., Polovina, J., Rabalais, N. N., Sydeman, W. J., and Talley, L. D.: Climate change impacts on marine ecosystems, Annu. Rev. Mar. Sci., 4, 11–37, doi:10.1146/annurev-marine-041911-111611, 2012.

Dong, C., Idica, E. Y., and McWilliams, J. C.: Circulation and multiple-scale variability in the Southern California Bight, Prog. Oceanogr., 82, 168–190, 2009.

Fabry, V. J., Seibel, B. A., Feely, R. A., and Orr, J. C.: Impacts of ocean acidification on marine fauna and ecosystem processes, ICES J. Mar. Sci., 65, 414–432, 2008.

Federiuk, J. and Allen, J. S.: Model studies of near-inertial waves in flow over the Oregon continental shelf, J. Phys. Oceanogr., 26, 2053–2075, 1996.

Feely, R. A., Sabine, C. L., Hernandez-Ayon, J. M., Ianson, D., and Hales, B.: Evidence for upwelling of corrosive "acidified" water onto the continental shelf, Science, 320, 1490–1492, doi:10.1126/science.1155676, 2008.

Gaylord, B., Hill, T. M., Sanford, E., Lenz, E. A., Jacobs, L. A., Sato, K. N., Russel A. D., and Hettinger, A.: Functional impacts of ocean acidification in an ecologically critical foundation species, J. Exp. Biol., 214, 2586–2594, 2011.

Graham, M. H., Vásquez, J. A., and Buschmann, A. H.: Global ecology of the giant kelp *Macrocystis*: From ecotypes to ecosystems, Oceanogr. Mar. Biol., 45, 39–88, 2007.

Gruber, N.: Warming up, turning sour, losing breath: ocean biogeochemistry under global change, Phil. T. R. Soc. A, 369, 1980–1996, doi:10.1098/rsta.2011.0003, 2011.

Gruber, N., Hauri, C., Lachkar, Z., Loher, D., Frölicher, T. L., and Plattner, G.-K.: Rapid progression of ocean acidification in the California Current System, Science, 337, 220–223, 2012.

Hurley, C. D. G., Anderson, K. M., Demes, K. W., Jorve, J. P., Kordas, R. L., and Coyle, T. A.: Effects of climate change on global seaweed communities, J. Phycol., 48, 1064–1078, doi:10.1111/j.1529-8817.2012.01224.x, 2012.

Heisler, N.: Acid-base regulation in fishes, in: Fish Physiology, vol. X, edited by: Hoar, W. S. and Randall D. J., 315–401, San Diego: Academic Press, 1984.

Hepburn, C. D., Pritchard, D. W., Cornwall, C. E., McLeod, R. J., Beardall, J., Raven, J. A., and Hurd, C. L.: Diversity of carbon use strategies in a kelp forest community: Implications for a high CO_2 ocean, Glob. Change Biol., 17, 2488–2497, doi:10.1111/j.1365-2486.2011.02411.x, 2011.

Hofmann, A. F., Peltzer, E. T., Walz, P. M., and Brewer, P. G.: Hypoxia by degrees: Establishing definitions for a changing ocean. Deep-Sea Res. Pt. I, 58, 1212–1226, doi:10.1016/j.dsr.2011.09.004, 2011a.

Hofmann, G. E., Smith, J. E., Johnson, K. S., Send, U., Levin, L. A., Micheli, F., Paytan, A., Price, N. N., Peterson B., Takeshita, Y., Matson, P. G., Crook, E. D., Kroeker, K. J., Gambi, M. C., Rivest, E. B., Frieder, C. A., Yu, P. C., and Martz, T. R.: High-frequency dynamics of ocean pH: A multi-ecosystem comparison, PLoSONE, 6, e28983, doi:10.1371/journal.pone.0028983, 2011b.

Jiang, Z.-P., Huang, J.-C., Dai, M., Kai, S. J., Hydes, D. J., Chou, W.-C., and Jan, S.: Short-term dynamics of oxygen and carbon in productive nearshore shallow water systems off Taiwan: Observations and modeling, Limnol. Oceanogr., 56, 1832–1849, 2011.

Kaplan, D. M., Largier, J. L., Navarrete, S., Guiñez, R., and Castilla, J. C.: Large diurnal temperature fluctuations in the nearshore water column, Estuar. Coast. Shelf S., 57, 385–398, 2003.

Keeling, R. F., Körtzinger, A., and Gruber, N.: Ocean deoxygenation in a warming world, Annu. Rev. Mar. Sci., 2, 199–229, doi:10.1146/annurev.marine.010908.163855, 2010.

Lentz, S. J. and Winant, C. J.: Subinertial currents on the Southern California shelf, J. Phys. Oceanogr., 16, 1737–1749, 1986.

Lerczak, J. A., Hendershott, M. C., and Winant, C. D.: Observations and modeling of coastal internal waves driven by a diurnal sea breeze, J. Geophys. Res., 106, 19715–19729, 2001.

Lluch-Cota, D. B., Wooster, W. S., and Hare, S. R.: Sea surface temperature variability in coastal areas of the northern Pacific related to the El Niño-Southern Oscillation and Pacific Decadal Oscillation, Geophys. Res. Lett., 28, 2029–2032, doi:10.1029/2000GL012429, 2001.

Martz, T. R., Connery, J. G., and Johnson, K. S.: Testing the Honeywell Durafet® for seawater pH applications, Limnol. Oceanogr.-Meth., 8, 172–184, 2010.

McClatchie, S., Goericke, R., Cosgrove, R., Auad, G., and Vetter, R.: Oxygen in the Southern California Bight: Multidecadal trends and implications for demersal fisheries, Geohpys. Res. Lett., 37, L19602, doi:10.1029/2010GL044497, 2010.

McPhee-Shaw, E. E., Siegel, D. A., Washburn, L., Brzezinski, M. A., Jones, J. L., Leydecker, A., and Melack, J.: Mechanisms for nutrient delivery to the inner shelf: Observations from the Santa Barbara Channel, Limnol. Oceanogr., 52, 1748–1766, 2007.

Mehrbach, C., Culberson, C. H., Hawley, J. E., and Pytkowicz, R. N: Measurement of the apparent dissociation constants of carbonic acid in seawater at atmospheric pressure, Limnol. Oceanogr., 18, 897–907, 1973.

Melzner, F., Thomsen, J., Koeve, W., Oschlies, A., Gutowska, M. A., Bange, H. W., Hansen, H. P., and Körtzinger, A.: Future ocean acidification will be amplified by hypoxia in coastal habitats, Mar. Biol., doi:10.1007/s00227-012-1954-1, in press, 2012.

Moore, T. S., Nuzzio, D. B., Di Toro, D. M., and Luther III, G. W.: Oxygen dynamics in a well mixed estuary, the lower Deleware Bay, USA, Mar. Chem., 117, 11–20, 2009.

Nam, S. and Send, U.: Direct evidence of deep-water intrusions onto the continental shelf via surging internal tides, J. Geophys. Res., 116, C05004, doi:10.1029/2010JC006692, 2011.

Nam, S. and Send, U.: Resonant diurnal oscillations and mean alongshore flows driven by sea/land breeze forcing in the coastal Southern California Bight, J. Phys. Oceanogr., in revision, 2012.

Nam, S., Kim, H.-J., and Send, U.: Amplification of hypoxic and acidic events by La Niña conditions on the continental shelf off California, Geophys. Res. Lett., 38, L22602, doi:10.1029/2011GL049549, 2011.

Narayan, N., Paul, A., Mulitza, S., and Schulz, M.: Trends in coastal upwelling intensity during the late 20th century, Ocean Sci., 6, 815–823, doi:10.5194/os-6-815-2010, 2010.

North, W. J., James, D. E., and Jones, L. G.: History of kelp beds (*Macrocystis*) in Orange and San Diego Counties, California, Hydrobiologia, 260/261, 277–283, 1993.

O'Donnell, M. J., Todgham, A. E., Sewell, M. A., Hammond, L. M., Ruggiero, K., Fangue, N. A., Zippay, M. L., and Hofmann, G. E.: Ocean acidification alters skeletogenesis and gene expression in larval sea urchins, Mar. Ecol.-Prog. Ser., 398, 157–171, 2010.

Parnell, P. E., Dayton, P. K., Lennert-Cody, C., Rasmussen, L. L., and Leichter, J. J.: Marine reserve design: Optimal size, habitats, species affinities, diversity, and ocean microclimate, Ecol. Appl., 16, 945–962, 2006.

Parnell, P. E., Miller, E. F., Lennert-Cody, C. E., Dayton, P. K., Carter, M. L., and Stebbins, T. D.: The response of giant kelp (*Macrocystis pyrifera*) in southern California to low-frequency climate forcing, Limnol. Oceanogr., 55, 2686–2702, 2010.

Pidgeon, E. J. and Winant, C. D.: Diurnal variability in currents and temperature on the continental shelf between central and southern California, J. Geophys. Res., 110, C03024, doi:10.1029/2004JC002321, 2005.

Pineda, J.: Circulation and larval distribution in internal tidal bore warm fronts, Limnol. Oceanogr., 44, 1400–1414, 1999.

Pringle, J. M. and Riser, K.: Remotely forced nearshore upwelling in Southern California, J. Geophys. Res., 108, 3131, doi:10.1029/2002JC001447, 2003.

Roleda, M. Y., Morris J. N., McGraw, C. M., and Hurd C. L.: Ocean acidification and seaweed reproduction: increased CO_2 ameliorates the negative effect of lowered pH on meiospore germination in the giant kelp *Macrocystis pyrifera* (Laminariales, Phaeophyceae), Glob. Change Biol., 18, 854–864, doi:10.1111/j.1365-2486.2011.02594.x, 2012.

Send, U. and Nam, S.: Relaxation from upwelling: the effect on dissolved oxygen on the continental shelf, J. Geophys. Res., 117, C04024, doi:10.1029/2011JC007517, 2012.

Stumpp, M., Trübenbach, K., Brennecke, D., Hu, M. Y., and Melzner F.: Resource allocation and extracellular acid-base status in the sea urchin *Strongylocentrotus droebachiensis* in response to CO_2 induced seawater acidification, Aquat. Toxicol. 110–111, 194–207, doi:10.1016/j.aquatox.2011.12.020, 2012.

Sunday, J. M., Crim, R. N., Harley, C. D. G., and Hart, M. W.: Quantifying rates of evolutionary adaptation in response to ocean acidification, PLoS ONE, 6, e22881, doi:10.1371/journal.pone.0022881, 2011.

Swanson, A. K. and Fox, C. H.: Altered kelp (Laminariales) phlorotannins and growth under elevated carbon dioxide and ultraviolet-B treatments can influence associated intertidal food webs, Glob. Change Biol., 13, 1696–1709, doi:10.1111/j.1365-2486.2007.01384.x, 2007.

Thomsen, J., Gutowska, M. A., Saphörster, J., Heinemann, A., Trübenbach, K., Fietzke, J., Hiebenthal, C., Eisenhauer, A., Körtzinger, A., Wahl, M., and Melzner, F.: Calcifying invertebrates succeed in a naturally CO_2-rich coastal habitat but are threatened by high levels of future acidification, Biogeosciences, 7, 3879–3891, doi:10.5194/bg-7-3879-2010, 2010.

van Heuven, S., Pierrot, D., Rae, J. W. B., Lewis, E., and Wallace, D. W. R.: MATLAB program developed for CO_2 system calculations, ORNL/CDIAC-105b, Carbon Dioxide Information Analysis Center, Oak Ridge National Laboratory, US Department of Energy, Oak Ridge, Tennessee, doi:10.3334/CDIAC/otg.CO2SYS_MATLAB_v1.1, 2011.

Vaquer-Sunyer, R. and Duarte, C. M.: Thresholds of hypoxia for marine biodiversity, P. Natl. Acad. Sci. USA, 105, 15452–15457, doi:10.1073/pnas.0803833105, 2008.

Winant, C. D.: Longshore coherence of currents on the Southern California Shelf during the summer, J. Phys. Oceanogr., 13, 55–64, 1983.

Yu, P. C., Matson, P. G., Martz, T. R., and Hofmann, G. E.: The ocean acidification seascape and its relationship to the performance of calcifying marine invertebrates: Laboratory experiments on the development of urchin larvae framed by environmentally-relevant pCO_2/pH, J. Exp. Mar. Biol. Ecol., 400, 288–295, doi:10.1016/j.jembe.2011.02.016, 2011.

Addendum

Frieder et al. (2012) analyzed data from 28 Sept. 2010 to 18 Oct. 2011. Additional SeapHOx deployments since this publication have been conducted (Table 2.3). The first deployment utilized two SeapHOx sensors at mooring A located at 7 and 17 m water depth (Fig. 2.11). Characterization of data matched qualitatively well with similar deployments presented in Frieder et al. (2012). The density difference between these two depths became larger over the duration of the deployment, which matches timing of seasonal upwelling. This corresponded with a decrease in $[O_2]$. pH data were not available for 17 m, but pH and $[O_2]$ at 7 m covaried. An intrusion of high-density seawater during March fueled primary production at the surface; $[O_2]$ and pH exceeded 350 μmol kg^{-1} and 8.3 units, respectively. This phenomenon is similar to that identified in Section 3.1.2 of Frieder et al. (2012). Two additional deployments were carried out at 17 m water depth at mooring A. The first was during June and July of 2012 (Fig. 2.12). pH data were not available for this deployment. $[O_2]$ and density during this time period were not as low as during February and March 2012. The second deployment was during March of 2013 (Fig. 2.13). Density, $[O_2]$ and pH ranges are similar to March 2012. Similarly, event-scale variability (days – weeks) was greater than short-term variability (semidiurnal and diurnal) as observed in Section 3.2.1 of Frieder et al. (2012). Lastly, a strong, positive relationship between $[O_2]$ and pH was well-maintained during these additional deployments, both at 7 m and 17 m water depth (Fig. 2.14). Altogether, from Sept. 2010 to March 2013 the time period of lowest $[O_2]$ and pH in the La Jolla Kelp Forest at the benthos was consistently during March each year.

This chapter, in part, is a reprint of the material as it appears in Biogeosciences. Frieder, Christina A., Nam, SungHyun, Martz, Todd R., Levin, Lisa A., 2012. The dissertation author was the primary investigator and author of this paper.

Table 2.3. List of SeapHOx deployments since Nov. 2011 and parameters measured.

Sensor ID	Deployment	Recovery	Mooring	Depth (m)	Temp	Salinity	Oxygen	pH
SP001	19 Nov 2011	23 Mar 2012	A	17	x	x	x	
SP002	17 Nov 2011	23 Mar 2012	A	7	x	x	x	x
SP002	29 May 2012	24 Jul 2012	A	17	x	x	x	
SP002	01 Apr 2013	30 Apr 2013	A	17	x	x	x	x

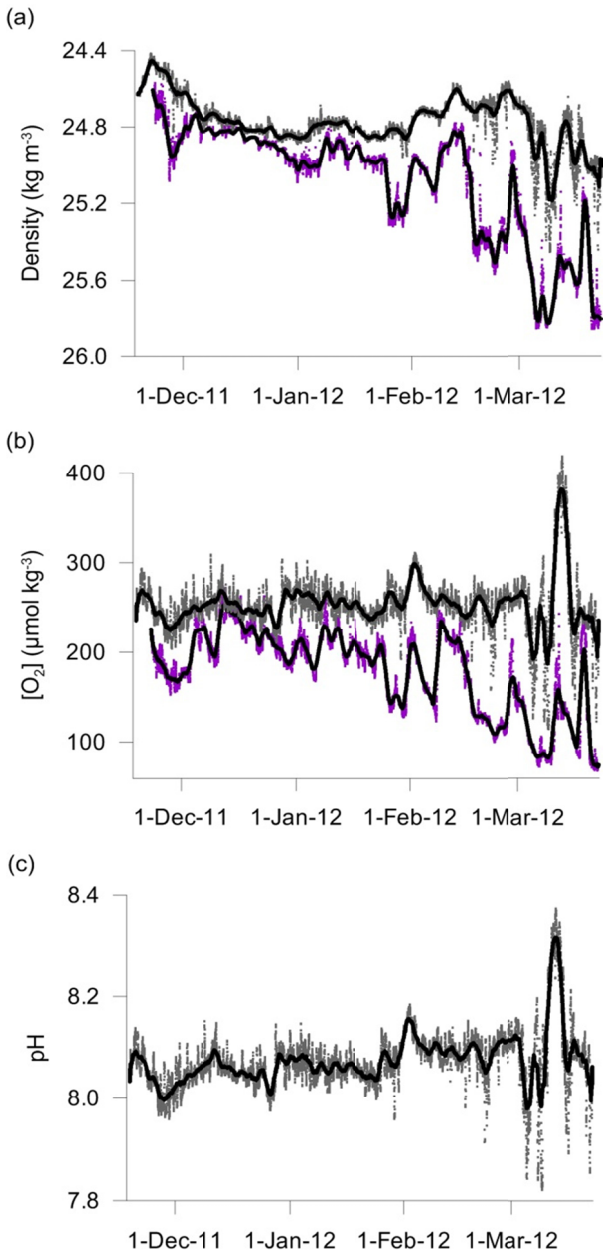

Figure 2.11. (a) Density, (b) dissolved oxygen ([O_2]) and (c) pH comparisons between 7 m (grey) and 17 m (purple) at mooring A. Black solid lines are 2-d smoothed data. Density scale is reversed.

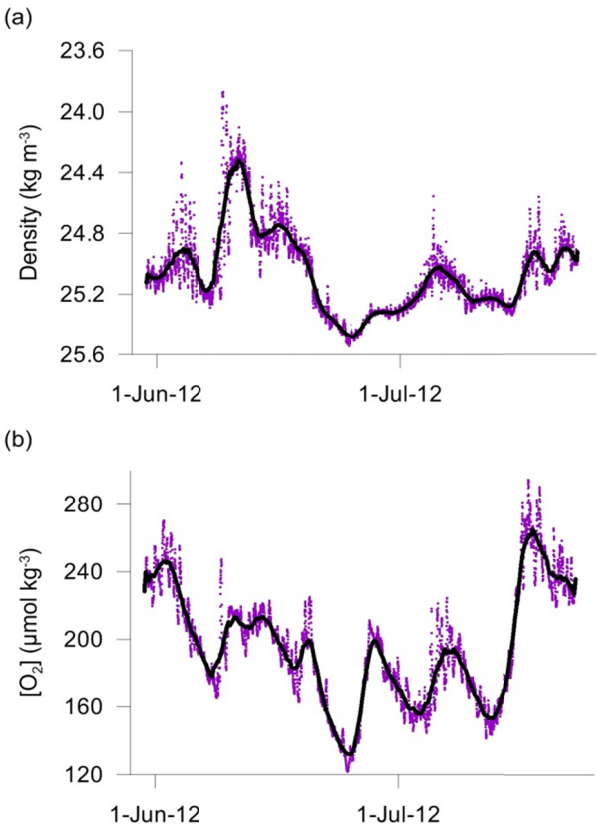

Figure 2.12. (a) Density and (b) dissolved oxygen ($[O_2]$) (pH data not available) at 17 m (purple) at mooring A. Black solid lines are 2-d smoothed data. Density scale is reversed.

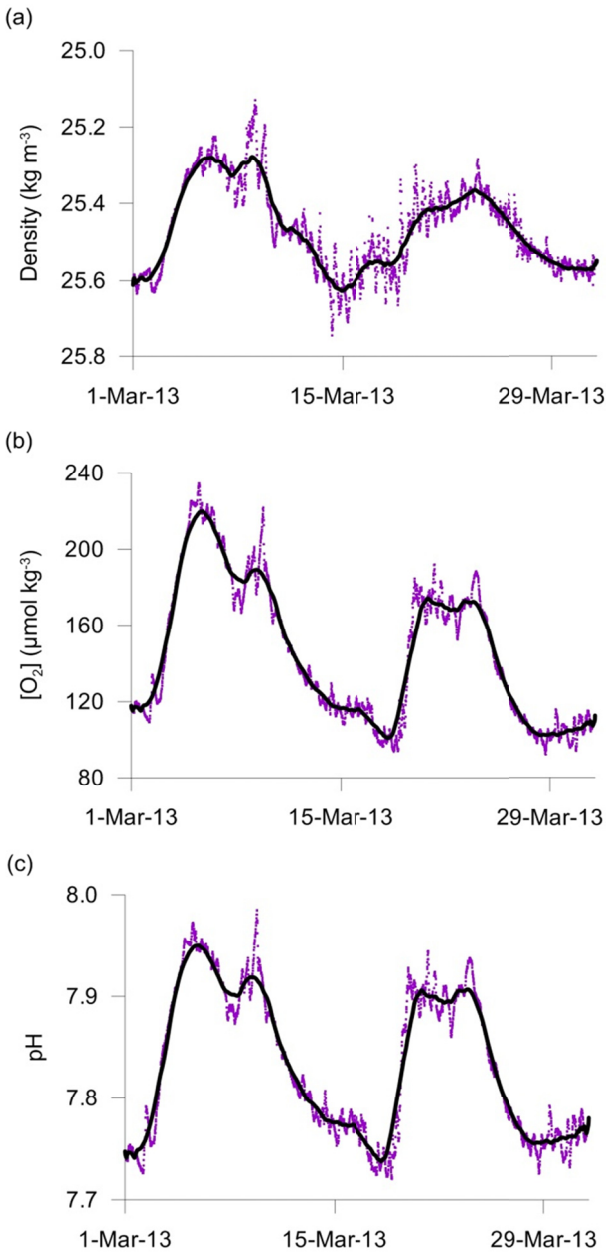

Figure 2.13. (a) Density, (b) dissolved oxygen ($[O_2]$) and (c) pH at 17 m (purple) at mooring A. Black solid lines are 2-d smoothed data. Density scale is reversed.

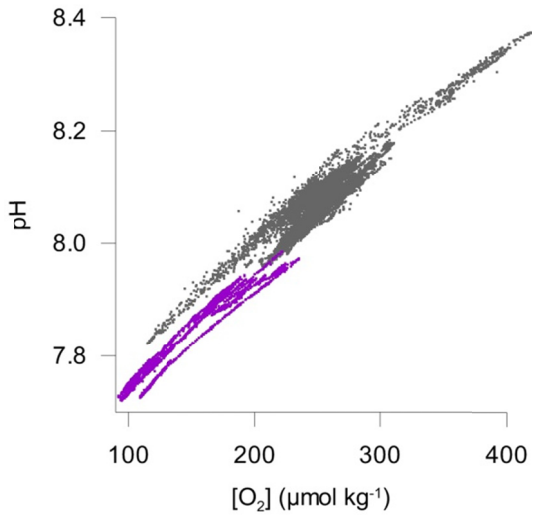

Figure 2.14 Scatter plot of dissolved oxygen ($[O_2]$) and pH at 7 m (grey) and 17 m (purple) water depth from all SeapHOx deployments since Frieder et al. 2012.

Chapter 3

Fertilization effects of reduced pH in temperate echinoids

Abstract

Some, but not all, species of echinoids experience reduced fertilization at pH values within the range of ocean acidification scenarios and present-day variability. In this study, I explored the effects of pH on the fertilization ratio, the fraction of eggs fertilized, in four species of temperate echinoids; three of the species were congeners of *Strongylocentrotus*, the fourth was the sand dollar, *Dendraster excentricus*. These species vary with extent of habitat overlap, depth distributions and relative phylogenetic relatedness. Fertilization ratios were determined across a range of sperm-egg ratios at ambient, > 7.95, and low pH, < 7.55. All four species had reduced fertilization, but only within species-specific sperm:egg ranges. In order to maintain 50% fertilization at low pH relative to ambient pH sperm-egg ratios needed to increase: 16 times greater for *S. franciscanus*, 2.7 times greater for *S. fragilis*, 1.5 times greater for *S. purpuratus*, and 1.5 times greater for *D. excentricus*. pH response curves were generated for *S. purpuratus* and *S. franciscanus* by measuring the fertilization ratio at nine pH levels at a sperm-egg ratio that was shown to be sensitive to pH reductions. *Strongylocentrotus purpuratus* maintained high fertilization across a broad range of pH but exhibited a threshold response below 7.44. *Strongylocentrotus franciscanus* had significant fertilization reductions at rather modest pH declines of 0.06 units from ambient pH 8.0, and this relationship between fertilization and pH was linear. Further experimentation revealed changing sire identity resulted in variable fertilization ratios under decreased pH in *S.*

pupuratus and *S. franciscanus*. Males with greater pH-tolerant gametes could become dominant sires with ocean acidification, representing a potential source of selection to pH stress. Fertilization in *S. franciscanus* was the most sensitive to pH, and natural pH conditions observed from its habitat during its reproductive season indicate there are time periods when fertilization success could be 79% relative to fertilization under ambient conditions. This information, in combination with ocean acidification predictions and an understanding of how sperm-egg ratios and thus population densities regulate the magnitude of the pH response could be incorporated into management practices of the *S. franciscanus* fishery. Lastly, impacts of reduced pH were species-specific even within closely related taxa with similar environmental histories, and complicate the validity of generalized extrapolations regarding winners and losers based on shared characteristics.

Introduction

Fertilization is a life event in which the fusion of gametes produces a new organism. Successful fertilization is vital for the persistence of a population, and in the marine environment, broadcast spawners release their gametes into the water column. The released gametes are exposed to the chemical and physical properties of the seawater, and known influences on fertilization success include temperature, turbulence, pollution and ecology (reviews and studies by Byrne, 2012; Levitan *et al.*, 1992; Marshall, 2006; Riffell and Zimmer, 2007). pH is an additional driver that has garnered recent attention due to concerns of pH reductions resulting from ocean acidification in shallow marine settings (Byrne, 2012; Kurihara, 2008). Of the Echinodermata, eight of the fifteen species studied to date exhibited reduced fertilization with decreased pH, but

with some of these detections occurring at extremely low pH values, *e.g.* 7.0 – 7.4, and low sperm-egg ratios (*e.g.*, Kurihara and Shirayama, 2004; Gonzales-Bernat *et al.*, 2013). Some of the observed robustness of fertilization to low pH may reflect species-specific adaptation to the fluctuating environmental conditions in shallow-water habitats. An emerging hypothesis is that fertilization sensitivity to reduced pH will be based on pH exposure histories; fertilization in species living in habitats where the pH is low, *e.g.* < 7.9, or highly variable may likely be more resistant to ocean acidification compared to that for species living in habitats where the pH is high, *e.g.* > 8.0, or relatively stable (Byrne, 2012; Dupont *et al.*, 2010).

Evidence from multiple studies suggests that fertilization in polar and temperate echinoderm species could be more sensitive to lowered pH compared to that for species from the tropics. Polar benthic habitats have stable pH conditions and exhibit low to moderate variation of < 0.12 units on the scale of hours to days (Matson *et al.*, 2011), while coral reef environments undergo large diel pH variations (Shaw *et al.*, 2012). Temperate systems, particularly along upwelling margins, exhibit precipitous changes in pH > 0.3 units on semidiurnal to seasonal timescales (Booth *et al.*, 2012; Frieder *et al.*, 2012; Nam *et al.*, 2011). Of five echinoid species studied from tropical intertidal and shallow subtitdal habitats two, the urchin *Heliocidaris erythrogramma* and the sand dollar *Arachnoides placenta*, are sensitive at a pH_{NBS} of 7.7 (Gonzalez-Bernat *et al.*, 2012; Havenhand *et al.*, 2008), while other studies on *H. erythrogramma* have found no effect down to pH_{NBS} of 7.6 (Byrne *et al.*, 2009, 2010a, 2010b). Fertilization in most echinoids from tropical environments may be robust to reductions in pH, and that sand dollars could be more sensitive. Echinoids from subtidal, temperate and polar habitats

have been reported more often to exhibit reduced fertilization at low pH. These species include *Sterechinus neumayeri* (effect observed at 7.50_{T}), *Strongylocentrotus franciscanus* (effect observed at 7.81_{NBS}), *Hemicentrotus puclherrimus* (effect observed at 6.83_{NBS}), *Echinometra mathaei* (effect observed at 7.1_{NBS}), and *Paracentrotus lividus* (effect observed at 7.6_{T}) (Ericson *et al.*, 2012; Kurihara and Shirayama, 2004; Moulin *et al.*, 2011; Reuter *et al.*, 2011a).

The underlying mechanisms responsible for reduced fertilization at lower pH remain elusive, but for broadcast spawners certain gamete properties can change with decreases in pH. Reduced pH decreases sperm motility in sea urchins (Havenhand *et al.*, 2008; Schlegel *et al.*, 2012), fish (Dey *et al.*, 2009; Ingermann *et al.*, 2002), and in sea cucumbers and corals (Morita *et al.*, 2010). Intracellular pH in sperm is directly dependent on extracellular pH, and decreasing intracellular pH narcotizes sperm and so could result in reduced sperm swimming and impaired fertilization success (Brokaw, 1990; Chia and Bickell, 1983; Christen *et al.*, 1983; Vacquier, 1986). pH could also affect properties of the egg. Low intracellular egg pH may prevent fertilization and subsequent development as well as slow the time that the fast block to polyspermy is established (Desrosiers *et al.*, 1996; Kurihara, 2008; Reuter *et al.*, 2011a). While reductions in pH may inhibit gamete performance, inter-individual variability in gamete performance may counteract these effects (Byrne and Przeslawski, 2013; Schlegel *et al.*, 2012). These authors propose the concept that ‘winners’ to ocean acidification occurs at the individual level and that acidification-resistant gametes will result in population-level selection for pH-tolerant gamete genotypes.

In studying the effects of pH on fertilization success, appropriate sperm-egg ratios that are species-specific should be utilized (Byrne, 2012; Levitan, 1993; Levitan *et al.*, 1991; Reuter *et al.*, 2011). Studying a range of sperm-egg ratios is also important because in the field population densities of adult urchins influence the degree of sperm limitation (Levitan, 2004). When testing pH effects at multiple sperm-egg ratios a fertilization kinetics model can be generated at which the probability of fertilization is a function of sperm-egg ratio (Vogel *et al.*, 1982). This experimental approach has been extensively used to characterize fertilization kinetics in echinoids (*e.g.*, Levitan, 1993; Levitan *et al.*, 1991; Vogel *et al.*, 1982). Changes in gamete performance are captured by the fertilization efficiency parameter, β/β_o, which can be estimated from the model. Such an approach has also been utilized to explore the effects of reduced pH on fertilization efficiency in the red sea urchin, *Strongylocentrotus franciscanus*, and revealed a 97% decrease in fertilization efficiency from pH_{NBS} 8.04 to 7.55 (Reuter *et al.*, 2011a; Reuter *et al.*, 2011b).

Given temporal and spatial pH variability and ocean acidification predictions along upwelling margins (*e.g.*, Hauri *et al.*, 2013), there are potentially temporal and spatial scales when reduced pH could elicit a negative fertilization response while increased pH could provide alleviation. This continuum of spatio-temporal variability could become increasingly important in the future as ocean acidification progresses. Few fertilization assays published to date employ more than two or three pH treatment levels, but the realization that pH varies with space and time requires that fertilization be studied over a broad range of pH in order to elicit linear and non-linear relationships and potential thresholds (Riebesell *et al.*, 2010). The ensuing response curves will improve

our ability to predict when and where the effects of a rapidly changing ocean climate will impact the sustainability of natural populations.

In this study, I compare the influence of pH on fertilization success in four species of echinoids found in temperate environments (Table 3.1). All species occur locally in the Southern California Bight but vary with respect to habitat overlap, phylogenetic relatedness and gametic traits. *Strongylocentrotus purpuratus* and *S. franciscanus*, the purple and red urchin, inhabit rocky reefs and kelp forests. *Strongylocentrotus purpuratus* occurs higher in the intertidal and extend to 160 m, while *S. franciscanus* is mostly subtidal to 90 m water depth (Morris *et al.*, 1980). Additionally, red and purple sea urchins are the basis for important fisheries, and while purple sea urchins make up a minor component of the fishery, they are also collected for scientific research (Rogers-Bennett, 2007). *Strongylocentrotus fragilis*, the pink urchin, is a deep-water sea urchin found in a low-pH, low-oxygen zone with peak abundances between 200 and 400 m water depth (Thompson *et al.*, 1987). *Dendraster excentricus*, the sand dollar, occurs in sandy bottom from within coastal inlets to the open coast and from intertidal to shallow subtidal (Merrill and Hobson, 1970). Predictions were that *S. fragilis* fertilization would be the most tolerant to low pH because natural populations occur in naturally low pH environments, and that *D. excentricus* fertilization would be the most sensitive to low pH because populations have a shallow depth distribution characterized by high wave energy resulting in high ambient pH conditions relative to the other species.

Fertilization experiments were carried out at ambient and low pH at multiple sperm-egg ratios. Fertilization kinetics curves were generated, and estimated fertilization efficiencies, β/β_o, were compared between pH treatments and across species. I

hypothesized that fertilization would only be sensitive to low pH at moderate and low sperm-egg ratios that were species-specific, since at high sperm densities any negative pH effect would likely be masked by high sperm-egg contact rates. I then developed response curves in *Strongylocentrotus purpuratus* and *S. franciscanus* across a broad range of pH at a sperm-egg ratio that was sensitive to pH change. Lastly, the mechanism by which pH influences fertilization success is thought to be a direct impact on sperm motility, but inter-individual variation to reduced pH among male gametes could influence fertilization success. By conducting experiments with pairwise crosses of eggs from a single female with sperm from multiple males, I quantified the variation in fertilization sensitivity to reduced pH as a function of sire identity. These studies revealed that *S. franciscanus* fertilization was the most sensitive to pH reductions, so pH data were collected from the natural habitat of *S. franciscanus* during its reproductive season to determine whether fertilization success could be influenced by present-day pH conditions.

Methods

Animals, gamete traits, and genetic relatedness

Three congeners of *Strongylocentrotus* and one sand dollar, *Dendraster excentricus*, were studied. *S. purpuratus* and *S. fragilis* are the most closely related, while *S. franciscanus* is the least related congener (Walters *et al.*, 2008). *Strongylocentrotus purpuratus*, the purple sea urchin, has the smallest egg diameter, 70 - 80 μm, and sperm velocity is 0.145 mm s^{-1} (Levitan, 1993). *Strongylocentrotus franciscanus*, the red sea urchin, has the largest egg diameter, 120 - 140 μm, and sperm velocity is 0.13 mm s^{-1}

(Levitan, 1993). *Strongylocentrotus fragilis*, the pink sea urchin, has a medium egg diameter, *ca.* 110 μm, and sperm traits are undocumented (Strathmann, 1987). *Dendraster excentricus* has an egg diameter of 125 μm, and sperm velocity is 0.195 mm s^{-1} (Podolsky, 2002).

Collecting animals and gametes, and fertilization assays

Strongylocentrotus purpuratus and *S. franciscanus* were collected at 15 m water depth by SCUBA from the La Jolla kelp forest where there is extensive overlap of adults (32.85 °N 117.29 °W). *Dendraster excentricus* was collected from 5 m water depth along sandy bottom offshore the Scripps Institution of Oceanography pier (32.87 °N 117.26 °W). *Strongylocentrotus fragilis* was collected from 200 m water depth with baited cages (32.88 °N 117.28 °W). Adults were maintained in flow-through aquaria at ambient sea surface temperature, 15 °C. All urchins were fed assorted macroalgae, and all specimens were used within a month of collection.

Spawning was induced by injecting 0.55 M KCl through the peristomal membrane. Oocytes were collected in dishes of filtered seawater (FSW, 0.22 μm). Number of adults used in each experiment ranged from 2 – 5 females and 3 – 5 males. Sperm were collected dry from the gonopores of males and placed in a small vial and kept on ice until use. A 0.1% dilution from dry sperm was made to verify sperm motility, and then preserved in formalin to count sperm densities with a hemacytometer in order to calculate the amount of diluted sperm required to attain desired sperm-egg ratios and sperm densities for each treatment. Oocytes from multiple females were mixed and egg densities determined by counting 8 x 20 μl aliquots. Eggs were added to experimental

beakers at a density of 5 eggs ml^{-1}, and incubated in experimental conditions for 10 min before sperm were added. Dry sperm was diluted immediately before addition to experimental beakers. Following sperm addition the seawater in each replicate was gently stirred. Fertilization proceeded for 20 min and was arrested by transferring the contents of each replicate to a 1% formalin solution. The fertilization ratio, defined as the proportion of eggs fertilized, was determined by counting the frequency of occurrence of a fertilization envelope in at least 100 eggs per replicate. All experiments were carried out in the Scripps experimental aquarium facility. Experiments on *Dendraster excentricus* were carried out during summer of 2012. All experiments on *Strongylocentrotus* spp. were carried out during the spring of 2013. 500 ml glass beakers were used, and there were three replicates per treatment level.

There were three types of experiments that followed the above protocol. The first experiment was conducted on all species. There were two treatments: pH and sperm-egg ratio. The two pH treatments were ambient pH, > 7.96, and low pH, < 7.53 (Table 3.2). The sperm-egg ratio levels varied among species and were based on preliminary experiments. There were eight *Strongylocentrotus purpuratus* sperm-egg ratios ranging from 1:1 to 2 x 10^4:1, eight *S. franciscanus* sperm-egg ratios ranging from 1:1 to 2 x 10^3:1, and eight *S. fragilis* sperm-egg ratios ranging from 10:1 to 10^3:1. Three *Dendraster excentricus* sperm-egg ratios were tested; these were 40:1, 400:1, and 4 x 10^3:1. The second experiment tested nine pH levels ranging from 7.26 to 8.00 on fertilization in *S. purpuratus* and *S. franciscanus*. A third experiment was conducted on *S. purpuratus* and *S. franciscanus* to determine the extent of sire-induced variability in fertilization success at low pH relative to ambient pH among pairwise crosses of eggs from a single female to

sperm from six males. The sperm-egg ratios used in the second and third experiment were 10^3:1 for *S. purpuratus*, and 2 x 10^3:1 for *S. franciscanus.* An attempt was made to conduct the second and third experiment on *S. fragilis* during June 2013, but too few individuals could be induced to spawn (less than 10% of adults), and fertilization did not occur from resulting gametes.

Manipulation of carbonate chemistry

pH levels for each experiment were manipulated by mixing different proportions of ambient and high total dissolved inorganic carbon (C_T) seawater. The high-C_T reservoir was attained by bubbling a 3% pCO_2 air mix into filtered seawater, and both reservoirs received flow-through filtered seawater. Discrete samples for determination of pH were taken for each treatment at the beginning of an experiment, and measured via a modified spectrophotometric method based on Dickson *et al.* (2007) using 1-cm cuvette cells and commercially available m-cresol dye with dye corrections based on Clayton and Byrne (1993). This method was calibrated with certified reference material from the Marine Physical Laboratory at Scripps Institution of Oceanography, and uncertainty of measurements was ± 0.03 pH units. All pH values reported unless otherwise noted in subscript are at in-situ temperature and on the total scale. Discrete samples were also taken for the determination of total alkalinity (A_T) and salinity. A_T for each treatment was determined using an open-cell, potentiometric titration with an accuracy of ± 2 μmol kg^{-1} (Dickson *et al.*, 2007). Salinity was calculated from density measured at 20°C on a Density Meter (Mettler Toledo DE45) with an accuracy of 0.05 salinity units. Salinity during the experiments ranged from 33.53 to 33.59. While only one discrete sample for

determination of pH and A_T was taken per treatment, an independent measure of pH was taken with the use of Honeywell Durafet III pH sensors to determine pH variance among replicates. The standard deviation among replicates was less than 0.02, and there was no significant drift in pH during the experiments. pCO_2 conditions were calculated from pH and A_T using the Matlab version of CO2SYS (van Heuven *et al.*, 2011) with dissociation constants from Mehrbach *et al.* (1973) as refitted by Dickson and Millero (1987). The average propagated uncertainties based on uncertainty in pH and A_T for pCO_2 was ± 85 µatm. Experiment water conditions are provided in Table 3.2. All experiments were conducted at 15 °C, and temperature was maintained by submerging replicate containers within a common water bath.

pH conditions in a natural habitat of *S. franciscanus*

Continuous pH data were collected 3 m above bottom at 17 m water depth in the south La Jolla Kelp Forest (32.81°N 117.29°W) during the spawning season of *S. franciscanus* from 1 – 31 March, 2013 to assess whether present-day pH variability could elicit decreases in fertilization success during natural spawning events. Details of instrumentation and deployment are provided in Frieder *et al.* (2012).

Data analysis and statistics

To determine the overall effect of pH and sperm-egg ratio on fertilization success, I used a two-way analysis of variance (ANOVA; fixed factors pH and sperm-egg ratio). Percentage data were square-root-arcsine transformed. Vogel's fertilization kinetics model was applied to the fertilization data to calculate fertilization rate as a function of

sperm-egg ratio, and to test whether pH resulted in decreased fertilization efficiency (Vogel *et al.*, 1982). This model assumes that sperm attach to the first egg they contact, regardless of whether fertilization occurs (the *Don Ottavio* model). It quantifies the fertilization ratio (φ) from the initial concentration of sperm (S_o, sperm μl^{-1}) and eggs (E_o, eggs μl^{-1}), sperm-egg contact time (t), constant rate of sperm-egg collision (β_o, $mm^3\ s^{-1}$), and the rate constant for fertilization (β, $mm^3\ s^{-1}$).

$$\varphi = 1 - exp\left[-\frac{\beta S_o}{\beta_o E_o}\left(1 - e^{-\beta o E o t}\right)\right] \qquad \text{(Eq. 1)}$$

The ratio of β/β_o can be interpreted as the fertilization efficiency and can be influenced by the fertilizable area of the egg, the proportion of sperm able to fertilize an egg, or the number of sperm contacts needed to allow for the penetration of a single spermatozoan. β/β_o for each pH treatment was estimated iteratively, along with 95% confidence intervals, using the Marquardt method of nonlinear regression in MATLAB. β/βo between pH treatments were considered significantly different if the 95% confidence intervals did not overlap. An index of gamete performance was calculated as the sperm density required to fertilize 50% of the eggs in each pH treatment (f_{50}). To determine the relationship between pH and fertilization success across a range of pH values, a simple linear regression was used. When thresholds were apparent a modified Michaelis-Menten equation was fit to fertilization data.

Results

Sperm-egg ratios sensitive to low pH and effects on fertilization efficiency

Fertilization success was reduced at low pH for all four species, but at different sperm-egg ratios (Table 3.3). Fertilization was significantly lower at sperm-egg ratios from $10^2 – 10^3$:1 in *Strongylocentrotus purpuratus*, 50 - 2000:1 in *S. franciscanus*, 2 x $10^3 – 10^5$:1 in *S. fragilis*, and 40 – 4 x 10^3:1 in *Dendraster excentricus* (Fig. 3.1). In order to maintain f_{50}, *S. purpuratus* required 1.5 times the sperm density (with constant egg density) with a pH decline from 7.96 to 7.37, *S. franiscanus* required 16 times the sperm density at pH decline from 7.99 to 7.50, and *S. fragilis* required 2.7 times the sperm density at pH decline from 7.99 to 7.50. *Dendraster excentricus* only required 1.5 times the sperm density from pH 8.06 to 7.53 to maintain f_{50}. Fertilization efficiency, β/β_o, was significantly lower at low pH for all three *Strongylocentrotus* spp., but not for *D. excentricus* (Fig. 3.2). At ambient pH, > 7.96, β/β_o was greatest for *S. purpuratus*, then *S. franciscanus*, and lowest in *S. fragilis* and *D. excentricus* indicating that these latter two species require higher sperm-egg ratios to attain fertilization success. *Strongylocentrotus franciscanus* exhibited the greatest reduction in β/β_o, 86%, at pH 7.50. This corresponds with the observation that *S. franciscanus* required the greatest increase in sperm densities in order to maintain f_{50}.

Shape of pH response curve and variability among male-female crosses

Both linear and non-linear responses of fertilization success to reduced pH were observed (Fig. 3.3). *Strongylocentrotus purpuratus* fertilization success exhibited a non-linear response to pH at a sperm-egg ratio of 1000:1. At pH values greater than 7.60 fertilization success was above 90%, from pH 7.60 to 7.44 fertilization began to slowly decrease, but a precipitous threshold existed below pH of 7.44. Applying a modified

Michaelis-Menten equation to the non-linear responses revealed an f_{50} at 7.27. In contrast, *S. franciscanus* fertilization success decreased from pH 8.00 to 7.36 at a sperm-egg ratio of 2000:1. The effect of pH on the fertilization ratio, φ, was well described by a negative linear relationship ($F_{1,7} = 204$, $p < 0.0001$, $r^2 = 0.97$).

$$\varphi = 0.602 * pH - 3.86 \qquad \text{(Eq. 2)}$$

Not all female by male crosses were sensitive to low pH for both species (Fig. 3.4). In *Strongylocentrotus purpuratus* only one of the pairwise crosses of eggs from a single female to sperm from six males exhibited a significant reduction in fertilization at a pH of 7.42 relative to ambient pH conditions. From the modified Michaelis-Menten fertilization pH curve a 6.5% reduction in fertilization success was expected; relative fertilization success at low pH relative to ambient ranged between -14% and +6% among individual sires. In *S. francicscanus*, two of the pairwise crosses exhibited a significant reduction in fertilization at a pH of 7.58. This pH value corresponds to an expected fertilization reduction of 30% based on Equation 2; relative fertilization success among the six males ranged between -3% and -12% relative to ambient.

Reduced output of *Strongylocentrotus franciscanus*

This study revealed a negative effect of reduced pH on fertilization success in *Strongylocentrotus franciscanus* at rather modest pH declines of 0.06 units from ambient pH of 8.0. The pH of the environment for *S. franciscanus* was observed to investigate whether present-day pH values could be limiting the potential reproductive output of natural populations. Fertilization success at a given in-situ pH was determined from the linear regression in Eq. 2 and plotted as a function of relative output from ambient pH 8.0

(Fig. 3.5). During March 2013, pH at depth was affected by alternating periods of a well-mixed water column and stratification, reflecting pH alternating from approximately 7.95 to 7.70 over week–long time periods. The corresponding fertilization success relative to ambient pH, 8.0, of *S. franciscanus* would have alternated between 0.79 and 0.93. This model assumes a constant sperm-egg ratio of 2000:1 at 15 °C. While sperm-egg ratios vary during spawning events, a value that represents sperm limitation can be justified as a first approximation since field experiments document that fertilization success for *S. franciscanus* varies between 0% and 82% (Levitan *et al.*, 1992).

Discussion

Fertilization in broadcast spawners has been considered rather robust to ocean acidification (Byrne, 2012), and sensitivity has usually been detected only at extremely low pH values (e.g. Kurihara and Shirayama, 2004). Still, a few species of echinoids from temperate and polar regions have exhibited reduced fertilization at rather modest pH reductions (Ericson *et al.*, 2012; Gonzalez-Bernat *et al.*, 2012; Moulin *et al.*, 2011; Reuter *et al.*, 2011a), particularly at sperm-egg ratios appropriate to the study species. Further exploration of the fertilization response of four echinoid species from temperate upwelling margins revealed that all species studied were sensitive to low pH, but only within a certain range of sperm-egg ratios (Table 3.3). Estimates from a fertilization kinetics model resulted in significant decreases in fertilization efficiency with declining pH for all *Strongylocentrotus* spp. but not for *Dendraster excentricus* (Fig. 3.2). Thus, a greater sperm density was required at low pH to attain fertilization rates comparable to those when gametes were exposed to ambient pH. Further experimentation to define the

nature of the response across a broad range of pH values revealed both a non-linear and linear relationship in *S. purpuratus* and *S. franciscanus*, respectively (Fig. 3.3). The *S. purpuratus* fertilization threshold response to pH was well below 7.6, suggesting fertilization in this species is rather robust to pH in the context of present-day variability regimes and regional acidification scenarios (Frieder *et al.*, 2012; Hauri *et al.*, 2013). Alternatively, *S. franciscanus* fertilization was sensitive to modest reductions of 0.06 pH units from 8.00, and these values are known to occur regularly within its present habitat during its reproductive season (Fig. 3.5).

The role of sperm-egg ratios in regulating the magnitude of the pH effect on fertilization is increasingly recognized. Sperm densities during natural spawning events may or may not be limiting; the degree to which sperm limitation occurs depends on the biotic and abiotic conditions under which spawning actually takes place (Levitan and Sewell, 1998; Yund, 2000). Broadcast spawners have evolved numerous mechanisms to prevent or to reduce sperm limitation. In sessile and sedentary invertebrates, these mechanisms include the release of sperm in viscous fluids to counteract dilution effects (Thomas, 1994), movement of adults towards other spawning individuals (Babcock *et al.*, 1992), spawning synchrony (Coma and Lasker, 1997), and extremely high levels of sperm production (Babcock *et al.*, 1994). Observation of natural spawning events in purple and red urchins in British Columbia, Canada, did not reveal spawning aggregation of sea urchins, but 30 to 44% of individuals spawned, and the majority spawning, 88%, were male (Levitan, 2002). Additional field observations of induced spawning events in *Strongylocentrotus franciscanus* revealed that 98% of females produced eggs that were sired by more than one male (Levitan, 2004). The extent of multiple-sired embryos could

decrease with ocean acidification as fertilization sensitivity to low pH varies among single female by male crosses (Fig. 3.4), resulting in a form of sexual selection that has only been recently considered (Foo *et al.*, 2012; Schlegel *et al.*, 2012).

Population density, especially male density, has also been shown to be a major determinant of sperm limitation (Levitan *et al.*, 1992). The reduction of population densities of *Strongylocentrotus franciscanus* by human exploitation could enhance sperm limitation during natural spawning events (Pfister and Bradbury, 1996), and would exacerbate reduced pH effects on fertilization success and result in Allee effects. Given the importance of sperm-egg ratios in regulating the magnitude of the pH effect and given the level of human exploitation of this species, there is a need for fishery management to consider the interplay of present-day pH conditions, ocean acidification and population densities. These factors could influence sustainable harvest levels. Even for present-day pH conditions there are time periods when fertilization in *S. franciscanus* could be 79% relative to fertilization at pH 8.0 (Eq. 2; Fig. 3.5).

Inter-individual variation in male gamete performance to reduced pH could provide population-level resilience to ocean acidification and decreased abundances from harvesting. Pairwise crosses among eggs from a single female and multiple males in both *Strongylocentrotus purpuratus* and *S. franciscanus* revealed a range of fertilization sensitivity to reduced pH, and some males of *S. purpuratus* had greater fertilization success at low pH than ambient pH. Sperm selection during fertilization plays a key role in the makeup of genotypes in subsequent generations (Levitan, 1996; 2008). With decreases in pH, the number of males producing high-quality gametes will decrease and

those males will contribute disproportionately to the next generation (Schlegel *et al.*, 2012).

To advance the field of marine fertilization ecology and its interaction with ocean acidification, research focus should be placed on the degree of sperm limitation of broadcast spawners during natural spawning events and how timing of spawning events coincides with environmental low pH conditions, or other abiotic and biotic conditions that could interact and modulate fertilization success at low pH. Additionally, future fertilization studies should explore the effects of reduced pH on *Strongylocentrotus droebachiensis*, which also has a productive fishery in the Northwest Atlantic and Northeast Pacific, and *S. intermedius* and *S. nudus*, which are fished commercially in the Northwest Pacific (Lawrence, 2007).

To assess the effects of climate change, one approach has been to define winners and losers based on unifying characteristics, such as calcifying versus non-calcifying taxa and the mineral form of calcium carbonate (Kroeker *et al.*, 2010). An objective of this study was to compare fertilization sensitivity to reduced pH in echinoids with varying overlap of phylogenetic relatedness, depth distributions, and natural-pH exposure histories. Differences among fertilization success in the species studied have revealed that not all congeners of *Strongylocentrotus* are sensitive to reduced pH, and in fact, members of this genus can exhibit different responses (Fig. 3.3). There was also no unifying theme of habitat or depth distribution in sensitivity among species that would have supported an exposure-history based hypothesis. While *S. fragilis* inhabits deeper waters with much lower in-situ pH conditions, fertilization effects of low pH were similar to fertilization effects in *S. purpuratus* and *Dendraster excentricus* (Fig. 3.1 and 3.2). This study

revealed that not all temperate echinoids seem to be sensitive to pH changes within the range of ocean acidification scenarios and present-day pH variability.

Acknowledgements

I thank A. Dickson for providing access to his laboratory facilities to run A_T and salinity samples. Specimen collections were assisted by P. Zerofski and E. Kelly. I thank L. Levin and J. Leichter for comments on earlier drafts of this manuscript, V. Vaquier and A. Hamdoun for insightful discussions, and J. Havenhand for sharing his insight into the importance of sperm-egg ratios on fertilization success in regulating pH responses at the Third Symposium on The Ocean in a High-CO_2 World. This research was supported by NSF-OCE Award No. 0927445. This chapter, in part, is currently being prepared for submission for publication of the material. Frieder, Christina A. The dissertation author was the primary investigator and author of this material.

References

Babcock, R. C., Mundy, C. N., Keesing, J. and Oliver, J. (1992). Predictable and unpredictable spawning events: In situ behavioural data from free-spawning coral reef invertebrates. *Invertebrate Reproduction & Development*, **22**, 213–227.

Babcock, R. C., Mundy, C. N. and Whitehead, D. (1994). Sperm diffusion models and in situ confirmation of long-distance fertilization in the free-spawning asteroid *Acanthaster planci*. *Biol. Bull.*, **186**, 17–28.

Booth, J. A. T., McPhee-Shaw, E. E., Chua, P., Kingsley, E., Denny, M., Phillips, R., Bograd, S. J., Zeidberg, L. D. and Gilly, W. F. (2012). Natural intrusions of hypoxic, low pH water into nearshore marine environments on the California coast. *Continental Shelf Research*, **45**, 108–115.

Brokaw, C. J. (1990). The sea urchin spermatozoon. *BioEssays*, **12**, 449–452.

Byrne, M. (2012). Global change ecotoxicology: Identification of early life history bottlenecks in marine invertebrates, variable species responses and variable experimental approaches. *Marine Environmental Research*, **76**, 3–15.

Byrne, M., Ho, M., Selvakumaraswamy, P., Nguyen, H. D., Dworjanyn, S. A. and Davis, A. R. (2009). Temperature, but not pH, compromises sea urchin fertilization and early development under near-future climate change scenarios. *Proceedings of the Royal Society B*, **276**, 1883–1888.

Byrne, M., Przeslwaski, R. (2013) Multistressor impacts of warming and acidification of the ocean on marine invertebrates' life histories. *Integrative and Comparative Biology*, 1-15.

Byrne, M., Soars, N., Selvakumaraswamy, P., Dworjanyn, S. A. and Davis, A. R. (2010a). Sea urchin fertilization in a warm, acidified and high pCO_2 ocean across a range of sperm densities. *Marine Environmental Research*, **69**, 234–239.

Byrne, M., Soars, N. A., Ho, M. A., Wong, E., McElroy, D., Selvakumaraswamy, P., Dworjanyn, S. A. and Davis, A. R. (2010b). Fertilization in a suite of coastal marine invertebrates from SE Australia is robust to near-future ocean warming and acidification. *Marine Biology*, **157**, 2061–2069.

Chia, F. S. and Bickell, L. R. (1983). Echinodermata. In *Reproductive Biology of Invertebrates, vol. 2* (ed. Adiyodi, K. G. and Adiyodi, R. G.), pp545–620. Wiley, New York.

Christen, R., Schackmann, R. W. and Shapiro, B. M. (1983). Metabolism of sea urchin sperm. Interrelationships between intracellular pH, ATPase activity, and mitochondrial respiration. *The Journal of Biological Chemistry*, **258**, 5392–9.

Clayton T. D. and Byrne R. H. (1993) Spectrophotometric seawater pH measurements: total hydrogen ion concentration scale calibration of m-cresol purple and at-sea results. *Deep-Sea Res.*, **40**, 2115–2129.

Coma, R. and Lasker, H. R. (1997). Small-scale heterogeneity of fertilization success in a broadcast spawning octocoral. *Journal of Experimental Marine Biology and Ecology* **214**, 107–120.

Desrosiers, R., Désilets, J. and Dubé, F. (1996). Early developmental events following fertilization in the giant scallop *Placopecten magellanicus*. *Canadian Journal of Fisheries and Aquatic Sciences*, **53**, 1382–1392.

Dey, S., Kharbuli, S. M., Chakraborty, R., Bhattacharyya, S. P. and Goswami, U. C. (2009). Toxic effect of environmental acid-stress on the sperm of a hill-stream fish *Devario aequipinnatus*: A scanning electron microscopic evaluation. *Microscopy Research and Technique*, **72**, 76–78.

Dickson, A. G. and Millero, F. J. (1987). A comparison of the equilibrium constants for the dissociation of carbonic acid in seawater media. *Deep-Sea Res.*, **34**, 1733–1743.

Dickson, A. G., Sabine, C. L. and Christian, J. R. (2007). *Guide to best practices for ocean CO_2 measurements*. Sidney, British Columbia: PICES Special Publication 3.

Dupont, S., Ortega-Martínez, O. and Thorndyke, M. (2010). Impact of near-future ocean acidification on echinoderms. *Ecotoxicology*, **19**, 449–62.

Ericson, J. A., Ho, M. A., Miskelly, A., King, C. K., Virtue, P., Tilbrook, B. and Byrne, M. (2012). Combined effects of two ocean change stressors, warming and acidification, on fertilization and early development of the Antarctic echinoid *Sterechinus neumayeri*. *Polar Biology*, **35**, 1027–1034.

Foo, S. A., Dworjanyn, S. A., Poore, A. G. B. and Byrne, M. (2012). Adaptive capacity of the habitat modifying sea urchin Centrostephanus rodgersii to ocean warming and ocean acidification: performance of early embryos. *PloS one*, **7**, e42497.

Frieder, C. A., Nam, S. H., Martz, T. R. and Levin, L. A. (2012). High temporal and spatial variability of dissolved oxygen and pH in a nearshore California kelp forest. *Biogeosciences*, **9**, 3917–3930.

Hauri, C., Gruber, N., Vogt, M., Doney, S. C., Feely, R. A., Lachkar, Z., Leinweber, A., McDonnell, A. M. P., Munnich, M. and Plattner, G.-K. (2013). Spatiotemporal

variability and long-term trends of ocean acidification in the California Current System. *Biogeosciences*, **10**, 193–216.

Havenhand, J. N., Buttler, F.-R., Thorndyke, M. C. and Williamson, J. E. (2008). Near-future levels of ocean acidification reduce fertilization success in a sea urchin. *Current Biology*, **18**, R651–R652.

Ingermann, R. L., Holcomb, M., Robinson, M. L. and Cloud, J. G. (2002). Carbon dioxide and pH affect sperm motility of white sturgeon (*Acipenser transmontanus*). *J. Exp. Biol.*, **205**, 2885–2890.

Kroeker, K. J., Kordas, R. L., Crim, R. N. and Singh, G. G. (2010). Meta-analysis reveals negative yet variable effects of ocean acidification on marine organisms. *Ecology Letters*, **13**, 1419–34.

Kurihara, H. (2008). Effects of CO_2-driven ocean acidification on the early developmental stages of invertebrates. *Marine Ecology Progress Series*, **373**, 275–284.

Kurihara, H. and Shirayama, Y. (2004). Effects of increased atmospheric CO_2 on sea urchin early development. *Marine Ecology Progress Series*, **274**, 161–169.

Lawrence, J. M. ed. (2007). *Edible Sea Urchins: Biology and Ecology*. Elsevier.

Levitan, D. R. (1993). The importance of sperm limitation to the evolution of egg size in marine invertebrates. *The American Naturalist*, **141**, 517–536.

Levitan, D. R. (2002). Density-dependent selection, on gamete traits in three congeneric sea urchins. *Ecology*, **83**, 464–479.

Levitan, D. R. (2004). Density-dependent sexual selection in external fertilizers: variances in male and female fertilization success along the continuum from sperm limitation to sexual conflict in the sea urchin *Strongylocentrotus franciscanus*. *The American Naturalist*, **164**, 298–309.

Levitan, D. R. and Sewell, M. A. (1998). Fertilization success in free-spawning marine invertebrates: Review of the evidence and fisheries implications. *Canadian Special Publication of Fisheries and Aquatic Sciences*, **125**, 159–164.

Levitan, D. R., Sewell, M. A. and Chia, F.-S. (1991). Kinetics of fertilization in the sea urchin *Strongylocentrotus franciscanus*: Interaction of gamete dilution, age, and contact time. *Biological Bulletin*, **181**, 371–378.

Levitan, D. R., Sewell, M. A. and Chia, F.-S. (1992). How distribution and abundance influence fertilization success in the sea urchin *Strongylocentrotus franciscanus*. *Ecology*, **73**, 248–254.

Marshall, D. J. (2006). Reliably estimating the effect of toxicants on fertilization success in marine broadcast spawners. *Marine Pollution Bulletin*, **52**, 734–738.

Matson, P. G., Martz, T. R. and Hofmann, G. E. (2011). High-frequency observations of pH under Antarctic sea ice in the southern Ross Sea. *Antarctic Science*, **23**, 607–613.

Meehl, G. A., Stocker, T. F., Collins, W. D., Friedlingstein, P., Gaye, A. T., Gregory, J. M., Kitoh, A., Knutti, R., Murphy, J. M., Noda, A., et al. (2007). Global climate projections. In *Climate Change 2007: The Physical Science Basis. Contribution of Working Group I to the Fourth Assessment Report of the Intergovernmental Panel on Climate Change* (ed. Solomon, S., Qin, D., Manning, M., Chen, Z., Marquis, M., Averyt, K. B., Tignor, M., and Miller, H. L.), Canbridge, UK and New York, NY, USA.

Mehrbach, C., Culberson, C. H., Hawley, J. E. and Pytkowicz, R. N. (1973). Measurement of the apparent dissociation constants of carbonic acid in seawater at atmospheric pressure. *Limnol. Oceanogr.*, **18**, 897–907.

Merrill, R. J. and Hobson, E. S. (1970). Field observations of *Dendraster excentricus*, a sand dollar of western North America. *American Midland Naturalist*, **83**, 595–624.

Morita, M., Suwa, R., Iguchi, A., Nakamura, M., Shimada, K., Sakai, K. and Suzuki, A. (2010). Ocean acidification reduces sperm flagellar motility in broadcast spawning reef invertebrates. *Zygote*, **18**, 103–107.

Morris, R., Abbott, D. and Haderlie, E. (1980). *Intertidal Invertebrates of California*. Stanford: Stanford University Press.

Moulin, L., Catarino, A. I., Claessens, T. and Dubois, P. (2011). Effects of seawater acidification on early development of the intertidal sea urchin *Paracentrotus lividus* (Lamarck 1816). *Marine Pollution Bulletin*, **62**, 48–54.

Nam, S., Kim, H.-J. and Send, U. (2011). Amplification of hypoxic and acidic events by La Niña conditions on the continental shelf off California. *Geophysical Research Letters*, **38**, L22602.

Pfister, C. A. and Bradbury, A. (1996). Harvesting red sea urchins: Recent effects and future predictions. *Ecological Applications*, **6**, 298–310.

Podolsky, R. D. (2002). Fertilization ecology of egg coats: Physical versus chemical contributions to fertilization success of free-spawned eggs. *J. Exp. Biol.*, **205**, 1657–1668.

Reuter, K. E., Lotterhos, K. E., Crim, R. N., Thompson, C. A. and Harley, C. D. G. (2011a). Elevated pCO_2 increases sperm limitation and risk of polyspermy in the red sea urchin *Strongylocentrotus franciscanus*. *Global Change Biology*, **17**, 163–171.

Reuter, K. E., Lotterhos, K. E., Crim, R. N., Thompson, C. A. and Harley, C. D. G. (2011b). Corrigendum for: Elevated pCO_2 increases sperm limitation and risk of polyspermy in the red sea urchin *Strongylocentrotus franciscanus*. *Global Change Biology*, **17**, 2512–2512.

Riebesell, U., Fabry, V. J., Hansson, L. and Gattuso, J.-P. (2010). *Guide to best practices for ocean acidification research and data reporting*. Luxembourg: Publications Office of the European Union.

Ries, J. B., Cohen, A. L. and McCorkle, D. C. (2009). Marine calcifiers exhibit mixed responses to CO_2-induced ocean acidification. *Geology*, **37**, 1131–1134.

Riffell, J. A. and Zimmer, R. K. (2007). Sex and flow: the consequences of fluid shear for sperm-egg interactions. *The Journal of Experimental Biology*, **210**, 3644–60.

Rogers-Bennett, L. (2007). The ecology of *Strongylocentrotus franciscanus* and *Strongylocentrotus purpuratus*. In *Edible Sea Urchins: Biology and Ecology* (ed. Lawrence, J. M.), pp393–425. Elsevier.

Schlegel P., Havenhand J. N., Gillings M. R., Williamson J. E. (2012) Individual variability in reproductive success determines winners and losers under ocean acidification: a case study with sea urchins. *PloS one*, **7**, e53118.

Shaw E. C., McNeil B. I. and Tilbrook B. (2012) Impacts of ocean acidification in naturally variable coral reef flat ecosystems. *Journal of Geophysical Research*, **117**, C03038.

Shirayama, Y. and Thornton, H. (2005). Effect of increased atmospheric CO_2 on shallow water marine benthos. *Journal of Geophysical Research*, **110**, C09S08.

Strathmann, M. F. (1987). *Reproduction and development of marine invertebrates of the northern Pacific coast: data and methods for the study of eggs, embryos, and larvae*. Seattle: University of Washington Press.

Thomas, F. (1994). Physical properties of gametes in three sea urchin species. *J. Exp. Biol.*, **194**, 263–284.

Thompson, B. E., Jones, G. F., Laughlin, J. D. and Tsukada, D. T. (1987). Distribution, abundance, and size composition of echinoids from basin slopes off southern California. *Bulletin of Southern California Academy of Sciences*, **86**, 113–125.

Vacquier, V. D. (1986). Activation of sea urchin spermatozoa during fertilization. *Trends in Biochemical Sciences*, **11**, 77–81.

van Heuven, S. D., Pierrot, J. W. B., Lewis, R. E. and Wallace, D. W. R. (2011). *MATLAB Program Developed for CO_2 System Calculations, ORNL/CDIAC-105b*. Oak Ridge, Tennessee: Carbon Dioxide Information Analysis Center, Oak Ridge National Laboratory, U.S. Department of Energy.

Vogel, H., Czihak, G., Chang, P. and Wolf, W. (1982). Fertilization kinetics of sea urchin eggs. *Mathemetical Biosciences*, **58**, 189–216.

Walters, J., Binkley, E., Haygood, R. and Romano, L. A. (2008). Evolutionary analysis of the cis-regulatory region of the spicule matrix gene SM50 in strongylocentrotid sea urchins. *Developmental Biology*, **315**, 567–78.

Yund, P. (2000). How severe is sperm limitation in natural populations of marine free-spawners? *Trends in Ecology and Evolution*, **15**, 10–13.

Table 3.1. Study species and corresponding habitat type and depth distributions.

Species	Habitat Type	Depth Range (m)*
Strongylocentrotus purpuratus	nearshore rocky reef	intertidal - 160
Strongylocentrotus franciscanus	nearshore rocky reef	subtidal - 90
Strongylocentrotus fragilis	outer-shelf to offshore basins and slopes	150 – 480
Dendraster excentricus	coastal inlet to open coast	1 - 15

*Presented ranges represent common depth distributions, and individuals of each species can be found beyond depth ranges presented here.

Table 3.2. pH treatment levels used during each experiment. Experiment 1 tested at which sperm-egg ratios was fertilization sensitive to low pH. Experiment 2 developed fertilization response curves across a range of 9 pH values. Experiment 3 determined the variation in fertilization at ambient and low pH among one female by six male crosses. pH is reported on the total scale, A_T, total alkalinity in μmol kg^{-1}, pCO_2 in μatm calculated using CO2SYS software. Purp = *Strongylocentrotus purpuratus*; Red = *S. franciscanus*; Pink = *S. fragilis*; Sand = *Dendraster excentricus*. * A_T samples were not available for Experiment 1 on *D. excentricus*, so pCO_2 was calculated with average A_T and salinity from all experiments.

Species	Expt.	pH	A_T	pCO_2
Purple	1	7.96	2236	495
Purple	1	7.37	2239	2120
Red	1	7.99	2236	450
Red	1	7.5	2239	1578
Pink	1	7.99	2236	455
Pink	1	7.5	2241	1552
Sand	1	8.06	*	378
Sand	1	7.53	*	1456
Purple	2	7.95	2241	501
Purple	2	7.88	2240	607
Purple	2	7.8	2237	736
Purple	2	7.72	2238	920
Purple	2	7.62	2238	1156
Purple	2	7.54	2239	1427
Purple	2	7.46	2238	1729
Purple	2	7.38	2236	2081
Purple	2	7.26	2237	2801
Red	2	8	2235	442
Red	2	7.94	2235	526
Red	2	7.84	2235	669
Red	2	7.78	2236	781
Red	2	7.69	2236	992
Red	2	7.61	2235	1203
Red	2	7.54	2235	1410
Red	2	7.44	2241	1797
Red	2	7.36	2237	2212
Purple	3	8.02	2236	418
Purple	3	7.42	2238	1913
Red	3	8.02	2238	424
Red	3	7.58	2238	1286

Table 3.3. ANOVA *F* ratios for analyses of effects of pH and sperm-egg ratios on fertilization ratios and root-mean-square error (RMSE) of fertilization kinetics model for ambient pH and low pH. *F*-ratio values in bold indicate *P* values < 0.0001. *df* degrees of freedom

Species	pH (*df*)	Sperm:egg (*df*)	pH*Sperm:egg (*df*)	Ambient pH RMSE	Low pH RMSE
S. purpuratus	**286** (1,32)	**776** (7,32)	**51** (7,32)	0.104	0.161
S. franciscanus	**351** (1,32)	**167** (7,32)	**25** (7,32)	0.062	0.036
S. fragilis	**30** (1,32)	**166** (7,32)	**7.5** (7,32)	0.063	0.049
D. excentricus	**39** (1,12)	**164** (3,12)	1.1 (2,12)	0.126	0.056

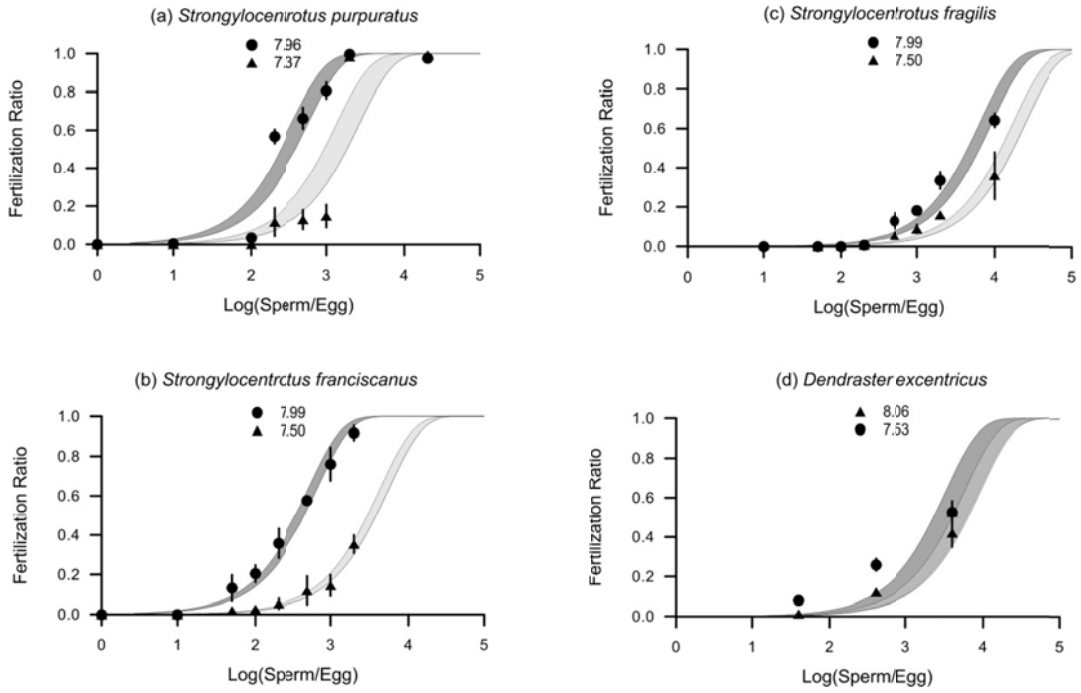

Figure 3.1. Fertilization success as a function of sperm-egg ratio in ambient pH (circles) and low pH (triangles) conditions in (a) *Strongylocentrotus purpuratus*, (b) *S. franciscanus,* (c) *S. fragilis* and (d) *Dendraster excentricus*. Error bars represent the standard deviation of three replicates. Ninety-five percent confidence intervals on fertilization curve per pH treatment indicated by shaded region for ambient pH (dark grey) and low pH (light grey). Root-mean-square error values for fit of data to each model are provided in Table 3.

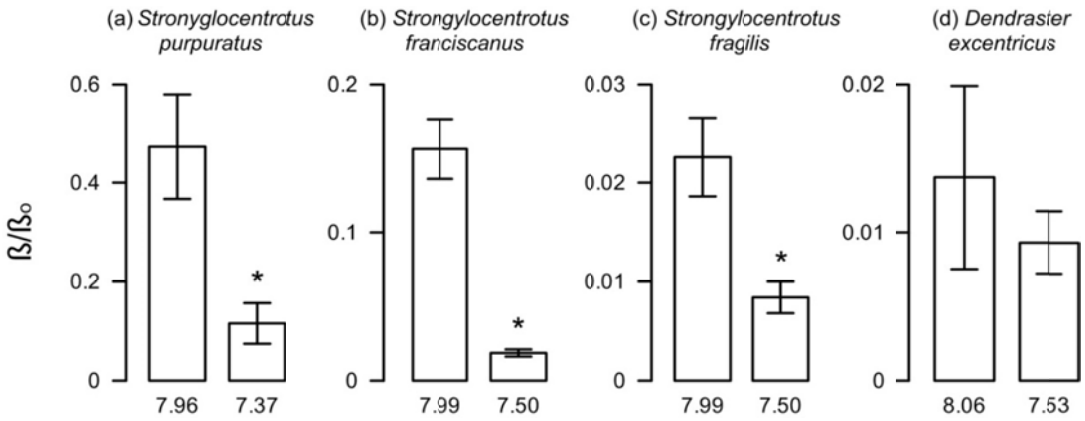

Figure 3.2. Estimation of fertilization efficiency, β/β_o, from the fertilization kinetics model at ambient and low pH in (a) *Strongylocentrotus purpuratus*, (b) *S. franciscanus*, (c) *S. fragilis* and (d) *Dendraster excentricus*. Bars represent the mean and error bars represent 95% confidence intervals on the parameter. Asterisks indicate β/β_o values that are significantly lower at low pH relative to ambient pH per species.

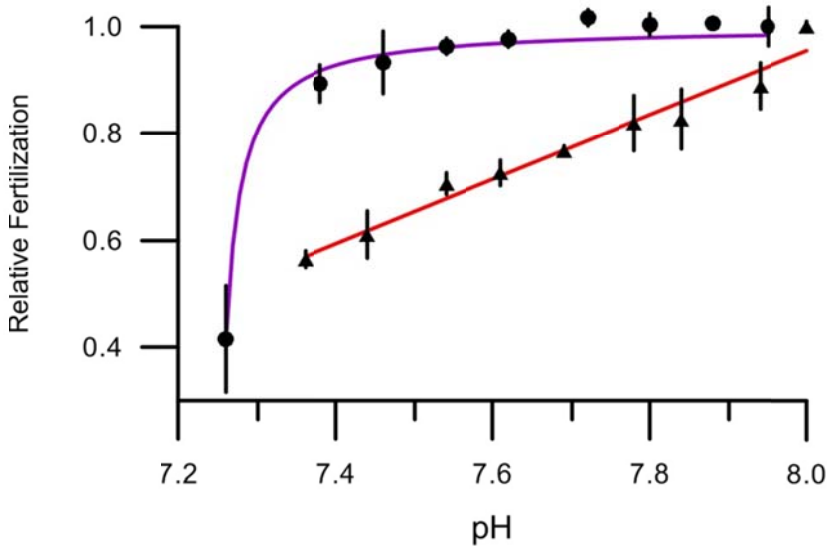

Figure 3.3. Fertilization response curve to pH for *Strongylocentrotus purpuratus* (purple line) and *S. franciscanus* (red line). Sperm density used was 5 sperm μl^{-1} and 10 sperm μl^{-1} for *S. purpuratus* and *S. franciscanus*, respectively. Each point represents the mean and standard deviation of three replicates. Relationship between fertilization success and pH in *S. franciscanus* was linear (red line), and non-linear in *S. purpuratus* (purple line).

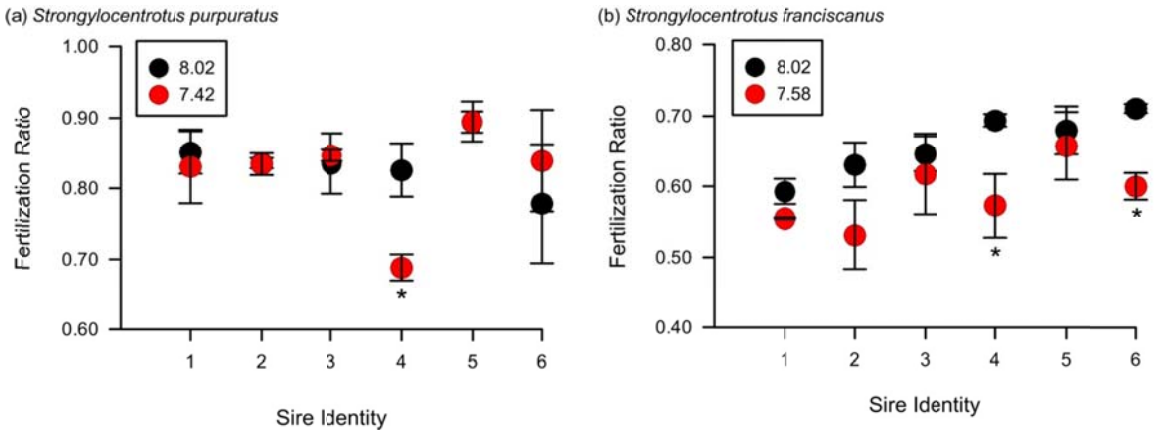

Figure 3.4. Fertilization ratio at ambient pH (black circles) and low pH (red circles) in (a) *Strongylocentrotus purpuratus* and (b) *S. franciscanus* for six males individually crossed with one female. Each point represents the mean ± 1SD. Asterisks indicate differences in fertilization at low pH from ambient pH following significant 2-way ANOVA tests (Tukey HSD, $p < 0.05$).

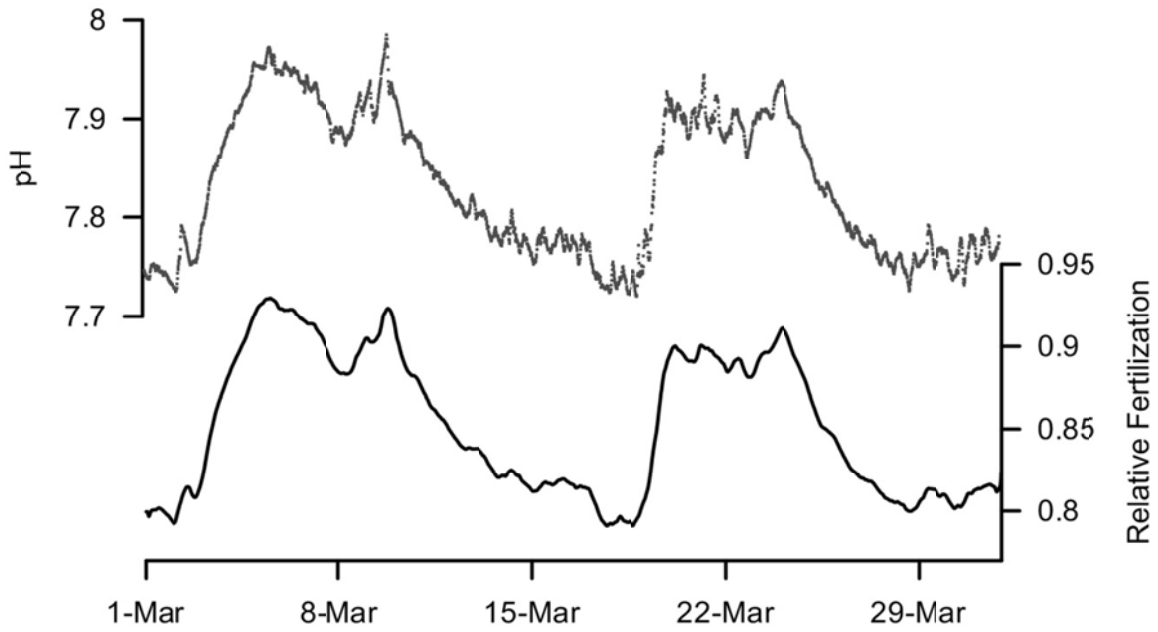

Figure 3.5. pH observations (light grey hatches) made in the south La Jolla Kelp Forest throughout March 2013 at 17 m water depth. Details of deployment and instrumentation are provided in Frieder et al. (2012). Model of relative fertilization in *Strongylocentrotus franciscanus* from ambient pH of 8.00 to in-situ pH conditions observed during spawning season. Relative fertilization was calculated from observed pH values and Eq. 2. Tick marks on x-axis are weekly.

CHAPTER 4

An in-situ test of sea urchin larval responses to reduced pH

Abstract

Adults of the urchins *Paracentrotus lividus* and *Arbacia lixula* are absent from naturally enriched CO_2 venting regions but live in surrounding waters. While limited tolerance of the adult stage to low pH at CO_2 vents has been well established, evidence for limited tolerance of the larval stage is based on laboratory-controlled experiments. Here we test whether sea urchin plutei are smaller at reduced pH. An in-situ larval culturing technique was used to expose laboratory-spawned echinoid larvae to natural gradients in pH induced by CO_2 venting off the coast of Ischia, Italy. During the first experiment, *A. lixula* embryos were reared at nine moorings ranging in mean pH from 6.83 to 8.04 as unhatched blastulas for two days, and developed into 4-arm echinoplutei. Length of the larvae did not vary with pH. Small-scale patchiness from site-to-site resulted in greater variability in larval sizes than reduced pH from the venting, and suggests that other unknown environmental conditions and natural cycles could be influencing larval performance even in the face of extreme reductions in pH. In a second experiment, *P. lividus* larvae were reared in the laboratory for ten days and then exposed to CO_2 venting for three days at six moorings ranging in mean pH from 6.85 to 8.04. At pH values $\leq$ 7.48 larvae were smaller relative to when they were initially outplanted, and there was increasing variance in the lengths of the plutei skeletal body rods with decreasing pH. We suggest that this could be a result of budding, the release of blastula-like particles, in a fraction of the larval population at the extreme low pH moorings,

although this was not observed directly. This field-based study at CO_2 vents reveals that larvae of these two species are tolerant of pH levels predicted for near-future pH scenarios (*e.g.*, ocean acidification scenarios of 7.7 units by 2100). Still, at extreme low pH values in the region of high CO_2 venting activity, where adults are absent, shrinking of *P. lividus* plutei would likely limit their ability to successfully recruit to venting regions.

Introduction

All benthic invertebrate larval studies investigating the impacts of ocean acidification conducted thus far have been under controlled laboratory conditions (reviewed in Kurihara, 2008; Dupont *et al.*, 2010; Byrne, 2012), because manipulation of pH in situ has proven to be logistically challenging (sensu Barry, 2005; Kline *et al.*, 2012). The use of natural CO_2 flux from volcanic vents, which lower the pH of the surrounding seawater, can serve as a model system to study the impacts of ocean acidification on marine organisms. The advantages of in-situ studies is that they incorporate natural environmental variability associated with light, temperature, currents and food cycles that is difficult to mimic in laboratory experiments (Barry *et al.*, 2010). Natural cycles in carbonate chemistry, that are mostly absent from laboratory studies, can also be incorporated into in-situ studies (Kline *et al.*, 2012). For example, CO_2 vents incorporate natural variability associated with tidal and diel cycles, but at vents magnitude of variability in carbonate chemistry often exceeds present-day variability regimes due to small-scale circulation features that replenish acidified waters over varying time scales (Kerrison *et al.*, 2011).

Such CO_2 vents occur off the coast of Italy where seawater is being acidified by gas containing 90-95% CO_2 (Tedesco, 1996; Hall-Spencer *et al.*, 2008). The vents occur on the north and south sides of Castello Aragonese at depths from 0.5 to 3 m. The waters have ambient seawater temperature and lack toxic compounds such as sulfur (Tedesco, 1996; Hall-Spencer *et al.*, 2008). These vents represent an in-situ model system to investigate effects of ocean acidification on benthic ecosystems and selected organisms (*e.g.*, Martin *et al.*, 2008; Rodolfo-Metalpa *et al.*, 2010; Cigliano *et al.*, 2010; Kroeker *et al.*, 2011, 2012, 2013). No larval studies have been conducted at these vents to date.

Adult echinoids, *Paracentrotus lividus* and *Arbacia lixula*, are among the more common benthic macro-invertebrates on sublittoral rocks outside of the vent areas, but their abundance and feeding behavior is significantly reduced in the venting region (Hall-Spencer *et al.*, 2008; Kroeker *et al.*, 2013). Differential sensitivity between the species has been observed at another venting site in the Mediterranean; adults of *A. lixula* were more tolerant to CO_2 venting than *P. lividus* adults due to species-specific differences in homeostatic ability in response to high CO_2 (Calosi *et al.*, 2013). Given that adult urchins are absent from extreme low pH zones (Hall-Spencer *et al.*, 2008; Kroeker *et al.*, 2013), the population bottleneck could be a reflection of not only limited adult tolerance to extreme low pH but also limited larval tolerance. Both sea urchin species have echinopluteus larval types.

CO_2-induced acidification experiments have revealed many sublethal effects on echinopluteus larvae. In general, development is slower and the pluteus arms grow slower at reduced pH (Kurihara, 2008; Dupont *et al.*, 2010; Ross *et al.*, 2011; Byrne, 2012). Laboratory studies on *Paracentrotus lividus* early life stages reveal that this species is

relatively robust to near-future ocean acidification (*e.g.*, pH_T 7.7, as projected for 2100). In one study, fertilization and larval survival were robust down to pH_T value of 7.0 (Martin *et al.*, 2011), while another study observed reduced fertilization at pH_T 7.6 (Moulin *et al.*, 2011). The effect of low pH on larval size was similar in both studies; in the two experiments size reductions occurred between 7.2 and 7.5 pH_T units. In comparison to other echinoids, size effects occurred at lower pH values compared to those of other species (Moulin *et al.*, 2011). For *Arbacia lixula*, developmental rates were sensitive to decreasing pH, but this effect was modulated by temperature (Gianguzza *et al.*, 2013). At lower temperature, 20 °C, reduced pH (7.9_{NBS}) resulted in faster development to the pluteus stage, at 24 °C there was no effect of decreased pH, and at 26 °C development to the pluteus stage was slower at reduced pH.

The objective of this study was to test the hypothesis that the sizes of larval sea urchin arms are smaller and more variable at reduced pH with the use of field experiments where CO_2 conditions are naturally elevated and natural environmental cycles are incorporated. A field-based larval culturing technique was used to expose laboratory-spawned larvae of *Arbacia lixula* and *Paracentrotus lividus* to natural gradients in pH. During the first experiment, *A. lixula* larvae were exposed in situ to reduced pH prior to skeletogenesis as un-hatched blastulas. They remained in the field for two days, and developed into 4-arm echinoplutei. In order to investigate the sensitivity of 'older' urchin larvae to changes in pH, a second experiment cultured *P. lividus* larvae in the laboratory for ten days before they were exposed to reduced pH in situ for three days. Older larvae have been considered less sensitive to reduced pH than earlier stages (Moulin *et al.*, 2011), and this experiment could represent larvae advected from

unacidified regions. As an indication of larval success, we measured the length of various skeletal components of larvae and tested whether the mean and variance in these measurements varied with pH. This study provides the first test of effects of reduced pH on sea urchin larvae in situ, and will help to further evaluate and predict the sensitivity of echinopluteus to ocean acidification.

Methods

Study Site

CO_2 venting of volcanic origin occurs at two distinct areas on the north and south side of Castello Aragonese off the north-eastern coast of the island of Ischia (40.733 °N 13.964 °E). The vent area and venting rates have been described by Hall-Spencer *et al.* (2008). Moorings were placed along gradients of CO_2 venting (Fig. 4.1), and consisted of a 1- to 2-m long line with a subsurface buoy attached to a cement block. Larval homes, as detailed in 'In-situ Larval Culturing,' were attached to the mooring line.

Species Collection, Spawning and Larval Culturing

The echinoids *Arbacia lixula* (Linneus, 1758) and *Paracentrotus lividus* (Lamarck, 1816) are the most common sea urchin species in the coastal rocky and seagrass habitat off the Italian coast (Tortonese, 1965), and both play a critical ecological role as grazers in these habitats (Bulleri *et al.*, 1999). In early September 2009, adult specimens of *P. lividus* and *A. lixula* were collected in shallow waters (< 2 m) from rocky substrate in Ischia (Naples), Italy (40.75 °N 13.95 °E). The collection site was a few miles west off the vent area. The urchins were transported to the laboratory where they

were maintained in flow-through aquaria and induced to spawn within one hour of collection. Adult sea urchins were injected with 1-2 ml of 0.5 M potassium chloride through the peristomal membrane. After urchins spawned, unfertilized eggs (mean diameter 75 ± 0.75 µm) were placed in 0.22-µm filtered seawater containing a diluted sperm mixture. Gametes of three females and three males were used for the *A. lixula* experiment, and gametes of one female and one male were used for the *P. lividus* experiment. Twenty minutes post-fertilization, excess sperm was removed from culture via reverse filtration, and embryos were kept in 4 L of 0.22-µm filtered seawater and maintained at 19 °C. For Expt. I, *A. lixula* embryos were cultured in the laboratory for 12 h before being transferred to the field. For Expt. II, *P. lividus* embryos were cultured in the laboratory for ten days to the 4-arm pluteus stage before transfer to the field. Cultures were kept at 19 ºC and received a 12:12 h light-dark cycle. When the larvae completed gut formation in the laboratory they were fed live *Isochrysis* sp. daily. Seawater of the laboratory cultures was exchanged daily.

In-situ Larval Culturing

Larvae were cultured in situ at each mooring with the use of larval 'homes.' A larval home was 200 ml and consisted of a 14-cm long by 3.8-cm diameter pipe coupler made of poly-vinyl chloride (PVC) with an open 35-µm nitex mesh cap on either end. The homes were attached to the mooring line with zip-ties at 2-3 m below the sea surface. Larvae were loaded into homes at densities of 10 larvae ml^{-1}. For Expt. I, *Arbacia lixula* larvae were transferred to the field as un-hatched blastulas and exposed to venting for two days from Sept. 12-14, 2009. Nine moorings were utilized in this study. For Expt. 2, *P.*

lividus were transferred to the field as 10-day old plutei and exposed to venting for three days from Sept. 11-14, 2009. Six moorings were utilized during this experiment. At the end of the experiments, remaining larvae in homes were taken back to the laboratory and were transferred from their homes to 50-ml vials and preserved in 2.5% seawater buffered formalin.

Environmental Monitoring

pH, total dissolved inorganic carbon (C_T), total alkalinity (A_T), temperature and salinity conditions were monitored directly next to the larval cultures at each mooring throughout the experiment. pH was determined daily via a modified spectrophotometric method (Dickson *et al.*, 2007). Two samples per mooring were taken in the morning in 25-ml glass scintillation vials and samples were poisoned with a saturated mercuric chloride solution. Samples were transferred to the laboratory and analyzed within a week on a Varian Cary 1E UV/Visible spectrophotometer with a 1-cm path-length cell and commercially available m-cresol dye with dye corrections based on Clayton & Byrne (1993). This method was calibrated with certified reference material from the Marine Physical Laboratory at Scripps Institution of Oceanography, and uncertainty of measurements was ± 0.03 pH units. pH values are reported at the in-situ temperature and on the total pH scale. At the beginning and end of the experiments, A_T, C_T and salinity samples were taken with a 500-ml clean borosilicate glass bottle with a ground glass neck and stopper, poisoned with a saturated mercuric chloride solution and transferred to the laboratory for analysis. A_T measurements were determined using open-cell, potentiometric titration with an accuracy of ± 2 μmol kg^{-1} (Dickson *et al.*, 2007). C_T

measurements were determined by acid extraction and coulometric detection of CO_2 with an accuracy of ± 2 μmol kg^{-1} (Dickson *et al.*, 2007). pH, pCO_2 and saturation state of calcite, Ω_c, were calculated from a combination of A_T, C_T or pH measurements using the Matlab version of CO2SYS (van Heuven *et al.*, 2011) and thermodynamic carbonate dissociation constants (Mehrbach *et al.*, 1973; Dickson & Millero, 1987). The average propagated uncertainties based on uncertainty in pH, A_T, and C_T for pCO_2 and Ω_c were ± 46 μatm and ± 0.03, respectively. Salinity samples were run on an AUTOSAL Model 8400 Series salinometer. Temperature was monitored every 15 minutes at each mooring with the use of a HOBO Onset temperature logger with an accuracy of ± 0.5 °C.

Response Measurements

To determine the lengths of various morphometric measurements larvae were photographed under a compound microscope. Larvae were pipetted onto a flat microscope slide, and a cover slip, with modeling-clay feet on the corners, was placed over them. Two digital photographs were taken of each larva. The first photograph focused on the postoral arms and body and the second photograph focused on the anterolateral arms. Three morphological measurements were obtained from each larva: postoral rod length (PRL), anterolateral rod length (ARL), and body rod length (BRL) (Fig. 4.2). Images were analyzed using ImageJ v1.40f (NIH). Results are expressed in terms of length (μm). In Expt. II, initial lengths were averaged from 20 individuals that were preserved in 2.5% buffered formalin at the initiation of the field experiment, ten days post-fertilization.

Statistical Analysis

The morphometric lengths of 4 – 34 larvae from each mooring were averaged and the variances were calculated. Untransformed morphometric data did not violate assumptions of normality and homogeneity of variances. The effects of pH on mean larval size and variance were analyzed with a simple linear regression testing whether the slope was significantly different from zero ($\alpha = 0.05$). To test whether there was an increase in larval size from the beginning to the end of Expt. II, we used analysis of variance (ANOVA) to compare the BRL, PRL and ARL at the end of the experiment with lengths of the BRL, PRL and ARL at the beginning of the experiment. Post-hoc Tukey HSD tests ($\alpha = 0.05$) were used to identify significant effects revealed during ANOVA.

Results

Environmental Conditions

Field environmental conditions measured at each mooring are given in Table 4.1. There was little variation in A_T (range = 22 μmol kg^{-1}, N = 28). Mean temperature was 25 °C for both experiments. Salinity ranged from 38.0 to 38.1. In Expt. I, pH ranged from 6.83 to 8.04 across nine moorings (Fig. 4.3a). In Expt. II, pH ranged from 6.85 to 8.04 across six moorings (Fig. 4.3b). pH variability at a mooring increased with decreasing pH. For both experiments, Ω_c was supersaturated at all moorings except the two lowest pH moorings.

Experiment I - *Arbacia lixula*

Arbacia lixula larvae were exposed to in-situ CO_2 venting for two days as unhatched blastulas and developed into 4-arm plutei. At the end of the experiment the BRL, PRL, ARL and sum of the three measurements did not vary with pH (Fig. 4.4a-d; $p > 0.05$). There was also no significant relationship between the variance of each morphometric term and pH (Figure 4.4e-h; $p > 0.05$). Results were qualitatively similar when morphometric terms were regressed with pCO_2 and Ω_c.

Experiment II - *Paracentrotus lividus*

Paracentrotus lividus larvae were exposed to in-situ CO_2 venting for three days as 10-d old larvae. At the end of the experiment there was no significant effect of pH on any of the morphometric measurements (Fig. 4.5a-d; $p > 0.05$), but length of the BRL, PRL and ARL were shorter at the end of the experiment at the two lowest pH moorings, 6.85 and 7.48, relative to when they were first outplanted. The BRL did not get longer at any of the moorings but shrank at two moorings with lowest pH, 7.48 and 6.85 ($F_{6,106} = 18.3$, $p < 0.0001$). The ARL was longer at the end of the experiment at all but two moorings; the ARL shrank at pH 6.85 and 7.48 ($F_{6,106} = 75$, $p < 0.0001$). The PRL was larger at the end of the experiment at all but two moorings; the PRL shrank at pH 6.85 and 7.48 ($F_{6,106} = 85$, $p < 0.0001$). The sum of the larval components was greater at the end of the experiment at all but two moorings; the sum was lower at pH 6.85 and 7.48 ($F_{6,106} = 87$, $p < 0.0001$). There was a significant effect of pH on the variance of the BRL (Fig. 4.5e; $F_{1,4} = 7.972$, $p = 0.048$). Variance in BRL increased with decreasing pH, but there was no significant effect of pH on the variance of the PRL or ARL (Fig. 4.5f-h; $p > 0.05$).

Discussion

Naturally enriched CO_2 field sites provide unique opportunities to conduct ocean acidification experiments in natural settings. CO_2 vents in the Mediterranean can reveal the effects of reduced pH, increased pCO_2, on benthic marine ecosystems and processes (Barry *et al.*, 2010). The lack of adult echinoids from extreme low pH regions was further explored in this study by examining effects of low pH at CO_2 vents on early life stages. In the *Arbacia lixula* experiment (Expt. I) the length of larval arms did not vary across a broad range of pH from 6.83 to 8.04 (Fig. 4.4). This finding differs from those of laboratory-controlled experiments. Observations are typically a decrease in echinopluteus larval arm lengths with reduced pH (reviewed in Kurihara, 2008; Dupont *et al.*, 2010; Ross *et al.*, 2011). Shorter arms have a suite of implications for dispersing larvae. The arms of echinoplutei are lined with ciliated bands that are utilized for food capture and swimming (Strathmann, 1971), swimming ability and stability depend on body size and shape (Pennington & Strathmann, 1990; Strathmann & Grünbaum, 2006), and shorter arms reduce feeding capacity (Sewell *et al.*, 2004). In-situ experiments provide an independent approach to laboratory studies to study the effects of reduced pH. The lack of a relationship between pH and larval size highlights the role that uncontrollable natural processes may be playing in modulating responses to pH. This observation suggests that findings from laboratory-based experiments overestimate sensitivity. On the other hand, the realism of in-situ studies leads to variation in response variables from undetectable natural processes (Barry *et al.*, 2010). Increased variability in a response measurement can reduce inferential power of the in-situ experiment.

The lengths of the ARL, BRL and PRL of 'old' larvae of *Paracentrotus lividus* (Expt. II) also did not vary with pH, but the lengths of these components shrank at extreme low pH, ≤ 7.48, during the experiment (Fig. 4.5). Budding, the constriction and release of a blastula-like particle, may have caused the observed shrinkage in *P. lividus* 10-d old plutei. Budding has been observed in > 50% of larval cultures of *Strongylocentrotus purpuratus* when exposed to an elevated pCO_2 level of 700 μatm, although the released buds did not develop into viable clones (Chan *et al.*, 2013). Budding takes place at the posterior end of echinoids (Eaves & Palmer, 2003), and has not been reported to date in *A. lixula* but may occur in *P. lividus* (Runnström & Immers, 1970). The mechanisms by which reduced pH and elevated pCO_2 induce larval budding and cloning are unknown, but could provide ecological benefits for mitigating elevated mortality in response to acute exposure to low pH. Furthermore, there was an increase in variance with decreasing pH for the length of the body rod (BRL) in *P. lividus*. Decreased BRL lengths along with increased BRL variance suggest a subset of the larval population was undergoing budding.

The dramatic decrease in pluteus arm lengths and body rod length in *Paracentrotus lividus* indicates that this larval stage has limited pH tolerance. Given that the adult stage is absent from CO_2 venting regions and that extreme low pH results in poor larval performance, the lack of adults could be attributed to a population bottleneck at the larval stage. The area of venting is small, and movement of later life stages would be possible if physiological tolerance of extreme low pH was not an issue, so it is likely that sensitivity of all life stages results in their absence from venting regions. For *A.*

lixula there was no evidence that extreme low pH limited their ability to successfully develop and ultimately settle.

There are many advantages to conducting experiments in field-based settings, mainly associated with incorporation of natural environmental cycles and food sources. There are also associated disadvantages. For example, a common weakness of studies using natural CO_2 vent sites is the geographically limited opportunity for replication (Havenhand *et al.*, 2010). In this study, regression models were employed. Other researchers have grouped sites (moorings in this case) into categorical pH bins with each bin represented by sites with similar average pH conditions. Data were then analyzed with analysis of variance models (e.g., Hall-Spencer *et al.*, 2008; Cigliano *et al.*, 2010; Kroeker *et al.*, 2013). Regression analysis has been suggested as more useful in field-based studies because it allows identification of the functional relationship between the treatment variable (e.g. pH) and the response variable (*e.g.*, larval size); knowledge of these relationships are extremely valuable for modelers, and allows prediction of a response at interpolated values (Havenhand *et al.*, 2010). Additionally, a regression-based experimental design can reveal the need for non-linear models that reveal response thresholds. Another limitation of CO_2 vents is the large degree of temporal pH variability among treatments (Kerrison *et al.*, 2011). Large changes in pH can occur over rapid periods of less than a day. There is still uncertainty as to what aspects of environmental pH (e.g. mean ambient pH, extreme low pH events, rates of pH reduction) result in biological sensitivity. We interpreted larval responses in our experiments as a function of mean pH, although increased pH variance increased with decreasing pH (Fig. 4.3).

In conclusion, our results provide a unique in-situ test of sea urchin larval sensitivity to reduced pH. In-situ field experimental designs incorporate natural cycles and variability of light, temperature, and food, while these conditions are rigorously controlled in laboratory settings. While laboratory studies aim to limit variability among replicates, this study highlights the importance of small-scale patchiness which in natural settings resulted in variable larval performance regardless of pH conditions. Favorable, but presently unknown, natural processes that increase larval performance could become increasingly important in mitigating larval sensitivity to reduce pH in future oceans.

Acknowledgements

I would like to thank the Stazione Zoologica Anton Dohrn of Napoli and the staff of the benthic ecology group for their logistical support. Captain Vincenzo Rando, Francesco Mattera and Bruno Iacono supported the work at sea. This research was generously supported by NSF-OCE Award No. 0927445, and the Michael M. Mullin graduate research fellowship. This publication was also developed under a Science to Achieve Results (STAR) Fellowship Assistance Agreement No. FP916973 awarded by the U.S. Environmental Protection Agency (EPA). It has not been formally reviewed by EPA. The views expressed in this publication are solely those of the authors. This chapter, in part, is currently being prepared for submission for publication of the material. Frieder, Christina A.; Gambi, M. Cristina; Levin, Lisa A. The dissertation author was the primary investigator and author of this material.

References

Barry JP (2005) Utility of deep sea CO_2 release experiments in understanding the biology of a high-CO_2 ocean: Effects of hypercapnia on deep sea meiofauna. *Journal of Geophysical Research*, **110**, C09S12.

Barry JP, Hall-Spencer JM, Tyrell T (2010) In situ perturbation experiments: natural venting sites, spatial/temporal gradients in ocean pH, manipulative in situ pCO_2 perturbations. In: *Guide to best practices for ocean acidification research and data reporting* (eds: Riebesell U, Fabry VJ, Hansson L, Gattuso J-P), pp123–136. Luxembourg, Publications Office of the European Union.

Bulleri F, Benedetti-Cecchi L, Cinelli F (1999) Grazing by the sea urchins *Arbacia lixula* L. and *Paracentrotus lividus* Lam. in the Northwest Mediterranean. *Journal of Experimental Marine Biology and Ecology*, **241**, 81–95.

Byrne M (2012) Global change ecotoxicology: Identification of early life history bottlenecks in marine invertebrates, variable species responses and variable experimental approaches. *Marine Environmental Research*, **76**, 3–15.

Calosi P, Rastrick SPS, Graziano M, *et al.* (2013) Distribution of sea urchins living near shallow water CO_2 vents is dependent upon species acid-base and ion-regulatory abilities. *Marine Pollution Bulletin*, **In Press**.

Chan KYK, Grünbaum D, Arnberg M, Thorndyke M, Dupont ST (2013) Ocean acidification induces budding in larval sea urchins. *Marine Biology*, **160**, 2129–2135.

Cigliano M, Gambi MC, Rodolfo-Metalpa R, Patti FP, Hall-Spencer JM (2010) Effects of ocean acidification on invertebrate settlement at volcanic CO_2 vents. *Marine Biology*, **157**, 2489–2502.

Clayton TD, Byrne RH (1993) Spectrophotometric seawater pH measurements: total hydrogen ion concentration scale calibration of m-cresol purple and at-sea results. *Deep-Sea Res.*, **40**, 2115–2129.

Dickson AG, Millero FJ (1987) A comparison of the equilibrium constants for the dissociation of carbonic acid in seawater media. *Deep-Sea Res.*, **34**, 1733–1743.

Dickson AG, Sabine CL, Christian JR (2007) *Guide to best practices for ocean CO_2 measurements*. Sidney, British Columbia, PICES Special Publication 3.

Dupont S, Ortega-Martínez O, Thorndyke M (2010) Impact of near-future ocean acidification on echinoderms. *Ecotoxicology*, **19**, 449–62.

Eaves AA, Palmer AR (2003) Reproduction: Widespread cloning in echinoderm larvae. *Nature*, **425**, 146.

Hall-Spencer JM, Rodolfo-Metalpa R, Martin S, *et al.* (2008) Volcanic carbon dioxide vents show ecosystem effects of ocean acidification. *Nature*, **454**, 96–99.

Havenhand JN, Dupont ST, Quinn GP (2010) Designing ocean acidificaiton experiments to maximize inference. In: *Guide to best practices for ocean acidification research and data reporting* (eds: Riebesell U, Fabry VJ, Hansson L, Gattuso J-P), pp67–80. Luxembourg, Publications Office of the European Union.

Van Heuven SD, Pierrot JWB, Lewis RE, Wallace DWR (2011) *MATLAB Program Developed for CO_2 System Calculations, ORNL/CDIAC-105b*. Oak Ridge, Tennessee, Carbon Dioxide Information Analysis Center, Oak Ridge National Laboratory, U.S. Department of Energy.

Kerrison P, Hall-Spencer JM, Suggett DJ, Hepburn LJ, Steinke M (2011) Assessment of pH variability at a coastal CO_2 vent for ocean acidification studies. *Estuarine, Coastal and Shelf Science*, **94**, 129–137.

Kline DI, Teneva L, Schneider K, *et al.* (2012) A short-term in situ CO_2 enrichment experiment on Heron Island (GBR). *Scientific Reports*, **2**.

Kroeker KJ, Gambi MC, Micheli F (2013) Community dynamics and ecosystem simplification in a high-CO_2 ocean. *Proceedings of the National Academy of Sciences*, **110**, 12721–12726.

Kroeker KJ, Micheli F, Gambi MC (2012) Ocean acidification causes ecosystem shifts via altered competitive interactions. *Nature Climate Change*, **3**, 156–159.

Kroeker KJ, Micheli F, Gambi MC, Martz TR (2011) Divergent ecosystem responses within a benthic marine community to ocean acidification. *Proceedings of the National Academy of Sciences*, **108**, 14515–20.

Kurihara H (2008) Effects of CO_2-driven ocean acidification on the early developmental stages of invertebrates. *Marine Ecology Progress Series*, **373**, 275–284.

Martin S, Richier S, Pedrotti M-L, *et al.* (2011) Early development and molecular plasticity in the Mediterranean sea urchin *Paracentrotus lividus* exposed to CO_2-driven acidification. *The Journal of Experimental Biology*, **214**, 1357–68.

Martin S, Rodolfo-Metalpa R, Ransome E, Rowley S, Buia M-C, Gattuso J-P, Hall-Spencer J (2008) Effects of naturally acidified seawater on seagrass calcareous epibionts. *Biology Letters*, **4**, 689–92.

Mehrbach C, Culberson CH, Hawley JE, Pytkowicz RN (1973) Measurement of the apparent dissociation constants of carbonic acid in seawater at atmospheric pressure. *Limnology and Oceanography*, **18**, 897–907.

Moulin L, Catarino AI, Claessens T, Dubois P (2011) Effects of seawater acidification on early development of the intertidal sea urchin *Paracentrotus lividus* (Lamarck 1816). *Marine Pollution Bulletin*, **62**, 48–54.

Pennington JT, Strathmann RR (1990) Consequences of the calcite skeletons of planktonic echinoderml larvae for orientation, swimming, and shape. *Biological Bulletin*, **179**, 121–133.

Rodolfo-Metalpa R, Lombardi C, Cocito S, Hall-Spencer JM, Gambi MC (2010) Effects of ocean acidification and high temperatures on the bryozoan *Myriapora truncata* at natural CO_2 vents. *Marine Ecology*, **31**, 447–456.

Ross PM, Parker L, O'Connor WA, Bailey EA (2011) The impact of ocean acidification on reproduction, early development and settlement of marine organisms. *Water*, **3**, 1005–1030.

Runnström J, Immers J (1970) Heteromorphic budding in lithium-treated sea urchin embryos. *Experimental Cell Research*, **62**, 228–238.

Sewell MA, Cameron MJ, McArdle BH (2004) Developmental plasticity in larval development in the echinometrid sea urchin *Evechinus chloroticus* with varying food ration. *Journal of Experimental Marine Biology and Ecology*, **309**, 219–237.

Strathmann RR (1971) The feeding behavior of planktotrophic echinoderm larvae: Mechanisms, regulation, and rates of suspension feeding. *Journal of Experimental Marine Biology and Ecology*, **6**, 109–160.

Strathmann RR, Grünbaum D (2006) Good eaters, poor swimmers: Compromises in larval form. *Integrative and Comparative Biology*, **46**, 312–22.

Tedesco D (1996) Chemical and isotopic investigations of fumarolic gases from Ischia island (southern Italy): Evidences of magmatic and crustal contribution. *Journal of Volcanology and Geothermal Research*, **74**, 233–242.

Tortonese E (1965) *Echinodermata, Fauna d'Italia* (Calderini, Ed.). Bologna, Italy.

Table 4.1. Seawater carbonate chemistry and environmental conditions (mean ± SD) by mooring for each experiment at Ischia, Italy. Mooring identification corresponds to Fig. 4.1. Temperature is in degrees Celsius and was measured every 15 minutes. Salinity, total alkalinity (A_T) and total dissolved inorganic carbon (C_T) were measured at the beginning and end of each experiment (n = 2). Any deviation in sample size is denoted in parentheses. A_T and C_T are in μmol kg^{-1}. pH is mean pH on the total scale and was measured daily using the spectrophotemtric method or calculated from C_T and A_T. pH sample size is in parentheses. The saturation state of calcite, Ω_c, and pCO_2 (μatm) were calculated from C_T and A_T at 25.5 ºC and a salinity of 38.

	Mooring	pH	Temp	Salinity	A_T	C_T	Ω_c	pCO_2
Expt. I	A	8.04 ± 0.02 (3)	25.6 ± 0.45	38.1 ± 0.03	2564 (1)	2240 (1)	5.54 (1)	490 (1)
	B	8.00 ± 0.03 (5)	25.4 ± 0.45	38.1 ± 0.04	2570 ± 7.0	2254 ± 1	5.15 ± 0.22	550 ± 37
	C	7.97 ± 0.13 (5)	25.6 ± 0.50	38.1 (1)	2561 ± 0.5	2255 ± 28	5.26 ± 0.41	532 ± 64
	D	7.85 ± 0.03 (5)	25.0 ± 0.29	38.1 (1)	2566 ± 2.6	2353 ± 9	3.88 ± 0.17	830 ± 49
	E	7.69 ± 0.30 (5)	25.5 ± 0.41	38.1 ± 0.05	2565 ± 1.3	2372 ± 67	3.61 ± 0.96	958 ± 387
	F	7.59 ± 0.31 (5)	25.2 ± 0.31	38.1 ± 0.05	2572 ± 1.0	2506 ± 152	2.19 ± 1.57	2443 ± 1995
	G	7.47 ± 0.29 (5)	25.4 ± 0.50	38.1 ± 0.05	2567 ± 5.1	2573 ± 97	1.41 ± 0.70	3302 ±1802
	H	7.12 ± 0.30 (5)	25.3 ± 0.48	38.1 ± 0.05	2571 ± 1.8	2968 ± 84	0.99 ± 0.49	4914 ± 2623
	I	6.83 ± 0.42 (5)	25.6 ± 0.63	38.1 ± 0.04	2578 ± 6.1	2654 ± 108	0.30 ± 0.06	15099 ± 2997
Expt. II	A	8.04 ± 0.04 (7)	25.4 ± 0.45	38.1 ± 0.04	2564 (1)	2240 (1)	5.54 (1)	490 (1)
	B	7.98 ± 0.04 (7)	25.6 ± 0.43	38.1 ± 0.03	2570 ± 7.0	2254 ± 1	5.15 ± 0.22	550 ± 37
	C	7.75 ± 0.27 (7)	25.5 ± 0.40	38.1 ± 0.05	2565 ± 1.3	2372 ± 67	3.61 ± 0.96	958 ± 387
	D	7.59 ± 0.27 (7)	25.2 ± 0.31	38.1 ± 0.05	2572 ± 1.0	2506 ± 152	2.19 ± 1.57	2443 ± 1995
	E	7.48 ± 0.24 (7)	25.4 ± 0.48	38.1 ± 0.05	2578 ± 6.1	2654 ± 108	0.99 ± 0.49	4914 ± 2623
	F	6.85 ± 0.34 (7)	25.6 ± 0.62	38.1 ± 0.04	2571 ± 1.8	2968 ± 84	0.30 ± 0.06	15099 ± 2997

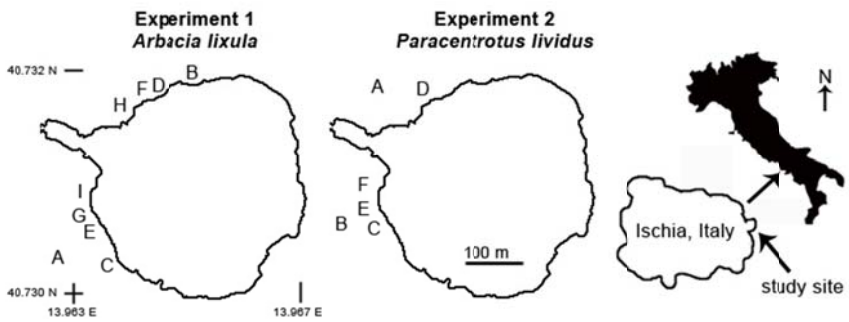

Figure 4.1. Map of CO_2 vent study site at the Castello Aragonese off Ischia (Naples). Ischia is located on the west side of Italy in the Tyrrhenian Sea. The Castello Aragonese is situated off the north-eastern coast of the island of Ischia (indicated by arrow). Venting occurs on the north and south side of the island. Mooring locations are indicated by letters; highest to lowest mean pH are alphabetized.

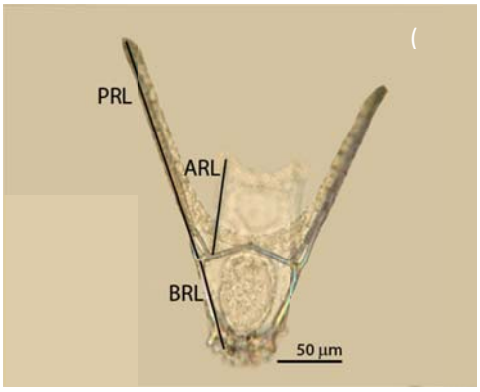

Figure 4.2. General morphology of a 3-day old, 4-arm pluteus larva of *Arbacia lixula* exposed to ambient pH in situ and morphometric parameters measured: postoral rod length (PRL), anterolateral rod length (ARL), and body rod length (BRL).

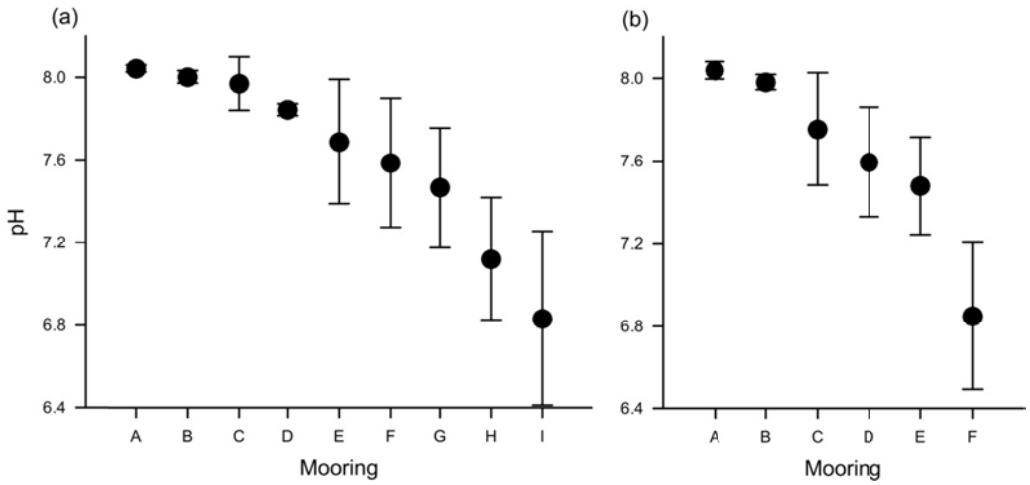

Figure 4.3. Mean pH (± 1 SD) at each mooring for (a) Experiment I on *Arbacia lixula* (n = 5 discrete samples for pH determination per mooring), and (b) Experiment II on *Paracentrotus lividus* (n = 7 discrete samples for pH determination per mooring).

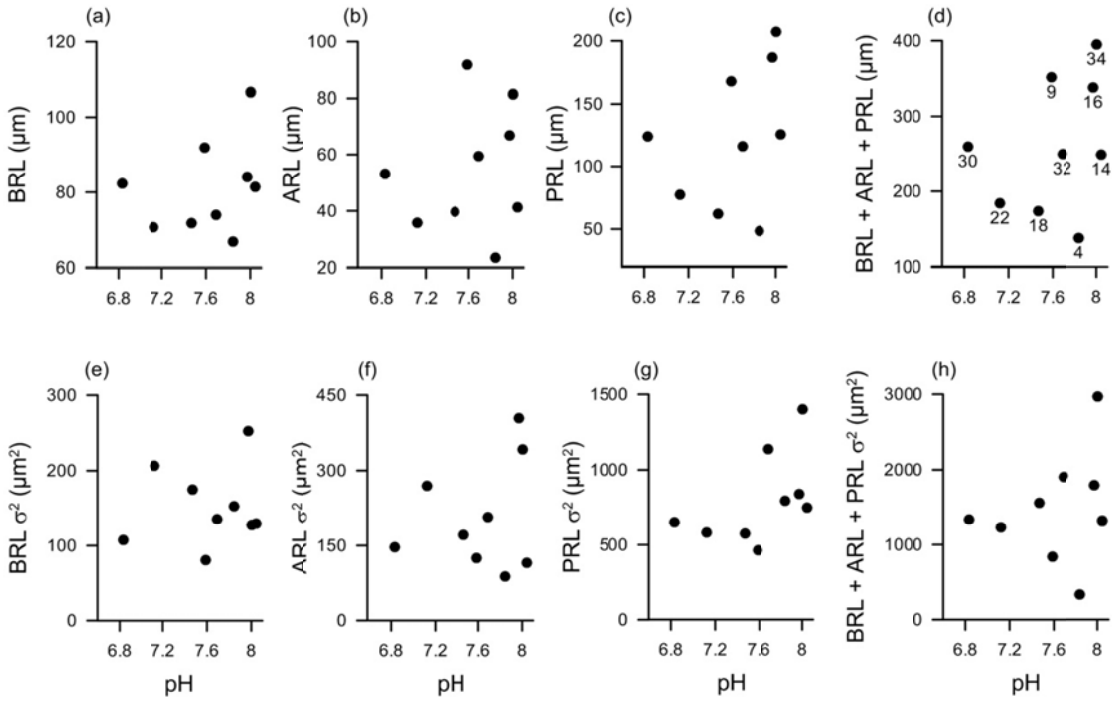

Figure 4.4. Scatterplots of pH and length of *Arbacia lixula* echinopluteus morphometric measurements for (a, e) BRL, (b, f) ARL, (c, g) PRL and (d, h) the sum of BRL, ARL and PRL. Length plotted as the mean of multiple larvae (a - d), and the variance of multiple larvae from each mooring in (e - h). The number of larvae used to calculate the population mean and variance from each mooring is denoted in (d) as labels next to points. All relationships were non-significant ($p > 0.05$). BRL = body rod length; ARL = anterolateral rod length; PRL = postoral rod length.

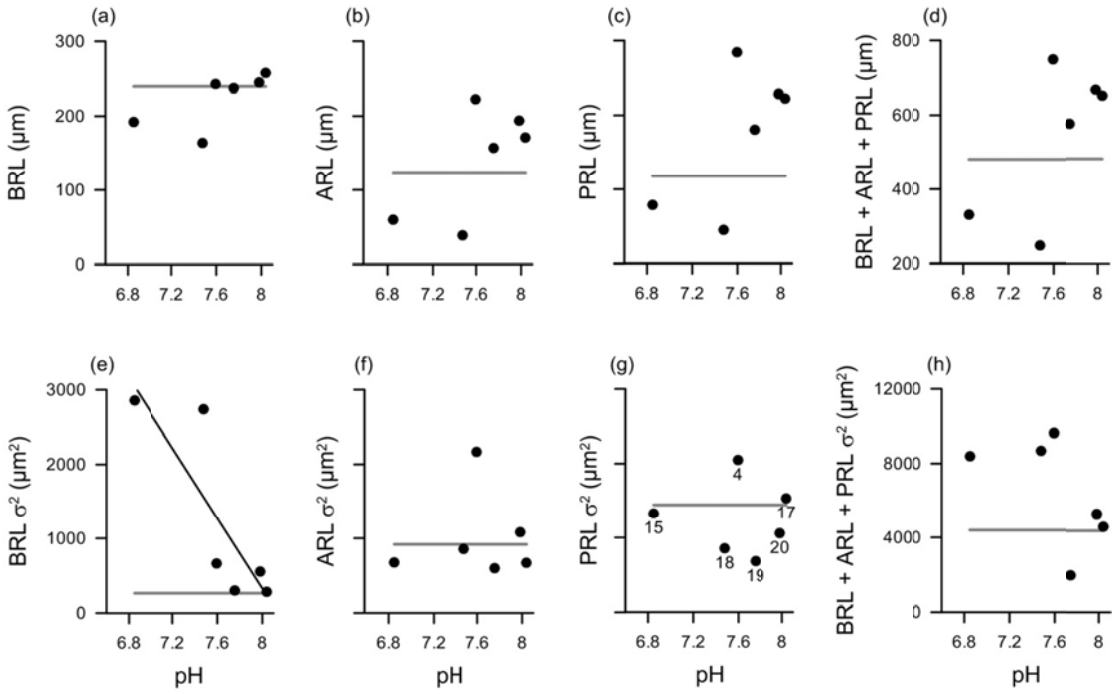

Figure 4.5. Scatterplots of pH and length of *Paracentrotus lividus* echinopluteus morphometric measurements for (a, e) BRL, (b, f) ARL, (c, g) PRL and (d, h) the sum of BRL, ARL and PRL. Length plotted as the mean of multiple larvae (a - d), and the variance of multiple larvae from each mooring in (e - h). The number of larvae to calculate the population mean and variance from each mooring is denoted in (g) as labels next to points. Solid black line in (e) is significant ($F_{1,4} = 7.972$, $p = 0.048$). Solid horizontal grey lines in (a - d) represents the average length or variance of each measurement for 25 larvae at 10-d post-fertilization directly before in-situ exposure to CO_2 venting. BRL = body rod length; ARL = anterolateral rod length; PRL = postoral rod length.

CHAPTER 5

Evaluating ocean acidification consequences under natural oxygen and periodicity regimes: Mussel development on upwelling margins

Abstract

Natural variation and changing climate on upwelling margins subject meroplanktonic organisms to broad ranges of pH and oxygen ($[O_2]$) levels. Semidiurnal fluctuations and upwelling events create excursions of 0.1 – 0.3 pH units and 50 - 100 μmol O_2 kg^{-1}. Here we explore in controlled laboratory experiments the interactive effects of pH, $[O_2]$, and semidiurnal pH fluctuations on the survivorship, development and size of early life stages of two mytilid mussels, *Mytilus californianus* and *M. galloprovincialis*. Survivorship of larvae was unaffected by low pH, low $[O_2]$ or semidiurnal fluctuations for both mytilid species. Low (stable) pH at ~7.5 resulted in delayed transition from the trochophore to veliger stage, but this effect of low pH was absent when incorporating semidiurnal fluctuations in both species. Larval shells were smaller in low pH (< 7.6); this effect was absent when semidiurnal fluctuations of 0.3 units were incorporated at low pH for *M. galloprovincialis* but not for *M. californianus.* There was no effect on larval size of low $[O_2]$ alone or in combination with pH. Larvae of the two mytilid species exhibited similar magnitudes of size reduction with reduced pH, and variation in the size response increased with decreasing pH. Early life stages of mytilid mussels appear largely tolerant to a broad range of $[O_2]$ experienced in their environment. The results of this study reveal that the incorporation of pH fluctuations characteristic of coastal settings into experimental studies of ocean acidification impacts

on biological systems reduce the apparent negative consequences of declining pH. Furthermore, quantifying changes in variation of a response to pH stress can reveal early signs of perturbation to populations and potential resilience capacity.

Introduction

A strong positive correlation exists between pH and dissolved oxygen ($[O_2]$) along upwelling margins. During upwelling events, the inner-shelf is exposed to deep seawater depleted in $[O_2]$ and enriched in pCO_2 from remineralization of organic matter (Feely *et al.*, 2008). In addition to upwelling, the inner-shelf undergoes multiple scales of environmental variability resulting in high-frequency (largely semidiurnal and diurnal) excursions of $[O_2]$ and pH (Booth *et al.*, 2012; Frieder *et al.*, 2012). Understanding how interactions among low $[O_2]$, low pH and environmental variability affect biological processes is important to interpret the effects of pH changes related to ocean acidification. High-frequency variability in pH could temper low pH conditions, while low $[O_2]$ coupled with low pH could exacerbate effects of low pH alone. Furthermore, long-term secular reductions in pH and $[O_2]$ could increase the extent of affected areas along upwelling margins. Reductions in sub-surface $[O_2]$ have been observed globally (Keeling *et al.*, 2010) especially in subtropical and tropical waters (Stramma *et al.*, 2008), and along upwelling margins (Whitney *et al.*, 2007; Chan *et al.*, 2008; Bograd *et al.*, 2008; Crawford & Peña, 2013). A decrease in pH has also been observed globally (Bates *et al.*, 2012), as well as along upwelling margins (Feely *et al.*, 2008), and is predicted to continue decreasing within the California Current due to ocean acidification (Hauri *et al.*, 2013).

Many benthic invertebrates disperse as free-living larvae that drift among the plankton. During this dispersive stage, larvae are highly susceptible to environmental stressors (Pechenik, 1999). Declining pH, [O_2], fluctuating environments, and their interactions could influence larval survival, development, growth and behavior. Of these stressors, low pH and high pCO_2 effects on planktonic invertebrate larvae have been the most extensively investigated. Studies have revealed that most calcifying larvae are sensitive to reduced seawater pH (Kurihara, 2008; Byrne, 2012) associated with increased pCO_2, decreased [CO_3^{2-}], and decreased $CaCO_3$ saturation state (Ω). For calcifying veligers, developmental success and growth rates seem to be directly affected by the availability of carbonate ions (Gazeau *et al.*, 2011), and suggest that the mechanisms used by these organisms to regulate calcification rates cannot compensate for low [CO_3^{2-}] under low pH conditions.

Our understanding of the effects of pH on biological responses result largely from experiments that maintain stable pH conditions and do not incorporate or investigate the role of high-frequency semidiurnal or diurnal variability that dominate within many inner-shelf habitats (Hofmann *et al.*, 2011). One study to date has investigated periodicity in pH variability by employing diel fluctuations in pCO_2 that are typical on shallow tropical reefs and demonstrated that growth and survivorship of coral recruits benefitted from the cyclic pH fluctuations (Dufault *et al.*, 2012). A few studies have explored the effects of early exposure to low pH on later phases of development. Early exposure to low pH has been shown to determine the shell size of bay scallop, *Argopecten irradians*, and the Olympia oyster, *Ostrea lurida*, at later stages of development (Hettinger *et al.*, 2012; White *et al.*, 2013). Another study investigated the

timing and duration of pCO_2 exposure on bivalve larvae and juvenile survival. Exposure to pCO_2 of 390 µatm at the start of larval development in *A. irradians* prolonged exposure to higher pCO_2 of 730 µatm later in development before significant declines in survival occurred (Gobler & Talmage 2013).

Clues into the extent that high-frequency pH variability could modify biological responses may be found from studies that have investigated the effects of temperature fluctuations on larval growth. For example, daily fluctuations of 5°C resulted in increased hatchling and survival rates relative to constant temperature in the mud-crab *Rhithropanopeus harrissii* (Costlow and Bookhout, 1971). Veligers of *Crepidula fornicata* reared in cyclic daily temperatures with a range of 5°C exhibited growth rates that were the same as growth under temperatures corresponding to the mean of the cycle, but when cyclic temperatures incorporated thermal limits the shells were malformed (Lucas and Costlow, 1979). It is thought that varying temperature results in the production and activation of a variety of cellular functions that operate optimally over different temperature ranges (Hochachka & Somero, 2001), or results in complementary functions such as increased food intake at high temperatures and decreasing rates of energy expenditure at lower temperatures (Sastry, 1979). Correspondingly, we hypothesize that varying pH in controlled-laboratory experiments that reflect local environmental fluctuations should optimize the functional capacity of a larva within a certain pH range.

The effects of hypoxia on planktonic larvae have been less well studied than those of pH. Experiments exposing marine animals to hypoxic conditions have revealed tolerance levels that are taxon-specific (Vaquer-Sunyer & Duarte, 2008). Of the mytilids,

Mytilus californianus pediveligers exposed to $[O_2] < 0.5$ ml l^{-1} for 6 days did not exhibit increased mortality relative to pediveligers cultured at ambient $[O_2]$ (Eerkes-Medrano *et al.*, 2013), while *Mytilus edulis* veligers had a median mortality time of 15 hours when exposed to the same conditions (Wang & Widdows, 1991). Differences in hypoxia tolerance also vary as a function of larval size; smaller and younger larvae are more sensitive than larger and older larvae (Widdows *et al.*, 1989; Wang & Widdows, 1991). The small energy reserves and high costs of maintaining anaerobic metabolism for smaller larvae are considered to be responsible for this differential oxygen sensitivity (Gabbott, 1976). To our knowledge, no studies to date have investigated the interactive effects of low pH and low $[O_2]$ on planktonic larvae. Low pH and low $[O_2]$ are likely to act as synergistic stressors in limiting species performance (Pörtner, 2012). An organism responds to low oxygen by metabolic down-regulation, and hypoxia combined with hypercapnia could emphasize metabolic depression, reduce functional flexibility, and have consequences for growth and reproduction (Pörtner *et al.*, 2005). For planktonic larvae, we might expect to observe an enhanced effect of delayed development and slowed growth in response to the combined stressors of low pH and $[O_2]$. In the inner-shelf along upwelling margins on the Oregon coast, off Monterey, and sometimes along the San Diego coast, $[O_2]$ can rapidly reach 62 – 143 μmol kg^{-1}, or 1.4 – 3.3 ml l^{-1} (Booth *et al.*, 2012; Frieder *et al.*, 2012). These levels are likely not inhibitory for mytilid larvae as indicated by previous experimental studies (Eerkes-Medrano *et al.*, 2013), but could become relevant when low $[O_2]$ is combined with low pH.

The objectives of this study were to investigate the interactive effects of (1) low pH and low $[O_2]$, and (2) semidiurnal pH fluctuations relative to stable pH on the

survivorship, development, and size of the early life stages of mytilid mussels. Laboratory-controlled experiments were designed to determine whether incorporation of cyclic semidiurnal fluctuations of pH would influence larvae at ambient pH or alleviate negative effects of low pH. We also tested the carry-over effect of early low-pH exposure on larval performance later in development. Lastly, experiments were conducted to explore the relative sensitivity of larvae to low pH versus low [O_2], and determine if there is an interactive effect when the two drivers are combined. Values of oxygen chosen for the experiments reflect present-day observations from shallow, nearshore settings in the Southern California Bight during well-oxygenated ambient conditions, *ca.* 200 - 250 μmol kg^{-1}, and upwelling events, *ca.* 80 - 100 μmol kg^{-1} (Frieder *et al.*, 2012). Experimental values of pH reflect present-day observations, *ca.* 7.90 – 8.00, and region-specific acidification scenarios, *ca.* 7.50 – 7.70 (Hauri *et al.*, 2013), and pH fluctuations were based on the dominant periodicity, semidiurnal, with an amplitude of 0.3 units (Fig. 5.1).

We adopted *Mytilus californianus* and *M. galloprovincialis* larvae as model species because they have been shown to be sensitive to low pH (Kurihara *et al.*, 2008; Gaylord *et al.*, 2011), larval development patterns are similar between the two species, adults coexist but dominate in different environments, and peak spawning periods are different for the two species (Carson *et al.*, 2010). Estimates of planktonic larval durations from the literature range between 9 and 45 days for *M. californianus*, and 14 days and 3 months for *M. galloprovincialis* (see Carson *et al*., 2010 for a summary). Recent field surveys have observed larvae of *Mytilus* spp. distributed close to shore (< 5 km), and below the surface Eckman layer (> 10 m) (Shanks and Shearman 2009). We

hypothesized there would be no effect of the single or combined drivers of pH and [O_2] on survivorship rates as previous studies have indicated pH effects on mytilid larvae are non-lethal (Byrne, 2012). Low [O_2] and low pH were hypothesized to result in delayed development from the trochophore to veliger stage as well as smaller veliger shells, and that when low pH and [O_2] occurred together developmental and growth would be even slower. Semidiurnal pH fluctuations were hypothesized to increase developmental rates and result in larger larvae relative to those reared under stable pH. We also hypothesized that larvae temporarily exposed to low pH during the first two days of development would exhibit smaller shell size later in development since early shell formation has been shown to be critical in determining larval size (Kurihara *et al.*, 2008). We expected similar responses for both species but that the sensitivity to low pH would be greater in *M. californianus* versus *M. galloprovincialis* because *M. californianus* reproduces in fall when seasonal pH and oxygen is higher than in spring when *M. galloprovincialis* reproduces (Nam *et al.*, 2011). These seasonal spawning differences could result in different pH exposure histories and sensitivity of larval tolerances.

Methods

Larval Cultures and Experimental Conditions

Three separate larval culturing experiments were carried out for eight days on *Mytilus californianus* and *M. galloprovincialis* to elucidate the effect of (A) low pH, fluctuations in pH and early exposure to low pH, (B) low pH combined with low [O_2], and (C) low pH versus low [O_2] on larval survivorship, development, and size (Table 5.1). Adult *Mytilus californianus* were collected from the Scripps Institution of

Oceanography pier at 32.867° N 117.257° W, and adult *M. galloprovincialis* were collected from San Diego Bay at 32.725° N 117.203° W. Gametes from at least four females and four males were used per experiment. Within two-hours of fertilization 10 larvae ml^{-1} in Expt. A and 50 larvae ml^{-1} in Expt. B and C were transferred to the experimental culturing vessels at the beginning of the experiment. Larvae were cultured in 4 L polycarbonate buckets nested within a 7.5 L bucket. This nested bucket design allowed for a flow-through seawater system while keeping larvae contained within the inner bucket. Culturing buckets were treated as replicates, and there were 2 or 3 per treatment for each experiment (Table 5.1). Larvae were cultured for eight days, fed *ad libitum* daily starting on day 2 a pre-mixed diet of 50,000 cells ml^{-1} during Expt. A and 100,000 cells ml^{-1} during Expt. B and C of *Isochrysis* sp., *Pavlova* sp., *Thalassiosira weissflogii*, and *Tetraselmis* sp., and maintained on a 12h:12h light:dark cycle. Additional adult spawning and larval culturing methods are provided in supplementary material.

Culturing experiments

Expt. A was designed to explore whether fluctuations in pH altered effects of low pH conditions. For *M. californianus* Expt. A, there were four treatments: ambient pH, ambient variable pH with semidiurnal fluctuations, low pH, and low variable pH with semidiurnal fluctuations (Table 5.1; Fig. 5.2). Semidiurnal ranges were 0.23 and 0.30 in the ambient and low variable pH treatments, respectively. For *M. galloprovincialis* Expt. A, there were four treatments: ambient pH, low pH, low variable pH with semidiurnal fluctuations and the fourth treatment exposed larvae to low pH of 7.56 for two days post-fertilization and then pH was elevated to ambient pH of 7.98 for the rest of the

experiment (Table 5.1; Fig. 5.2). Semidiurnal range in pH in the low fluctuating pH treatment was 0.30 units. pH data were continuously collected from one replicate per treatment and confirm the stability of the amplitude and timing of the semidiurnal fluctuations applied to the variable pH treatments (Fig. 5.2). Discrete pH readings from replicate containers that did not have continuous sensors were in good agreement (Fig. 5.S1). The average offset among replicates was 0.02 and 0.03 units in the *M. californianus* and *M. galloprovincialis* experiments, respectively.

To test for interactive effects of low pH and low [O_2] on larval responses Expt. B was designed with two treatments: ambient pH with ambient [O_2], and low pH with low [O_2], termed low pHOx (Table 5.1). pH and [O_2] data were continuously collected from one replicate per treatment and confirm the stability of conditions along with discrete samples of pH and [O_2] (Fig. 5.3). Discrete samples revealed that the average offset of replicates from average conditions was 0.01 pH units and 3 μmol O_2 kg^{-1} (Fig. 5.S1).

To compare how larvae respond to low pH versus low [O_2] associated with major upwelling events, Expt. C was designed with two treatments: low pH with ambient [O_2] and low [O_2] with ambient pH (Table 5.1). pH and [O_2] data were continuously collected from one replicate per treatment at a time and were transferred among replicates daily to confirm the stability of conditions (Fig. 5.3). Discrete samples revealed that the average offset of replicates from average conditions was 0.02 pH units and 3 μmol O_2 kg^{-1} (Fig. 5.S1).

Control of seawater pH and [O_2]

Two separate methods were utilized to manipulate seawater conditions. To maintain desired pH conditions and incorporate fluctuations in Expt. A we designed a feedback system in which target values were designated by the user and a Honeywell Durafet III pH sensor continuously monitored the pH of one replicate per treatment. Based upon the target value and the pH feedback, the culturing containers received either high-pH or low-pH equilibrated seawater controlled by a solenoid valve. High-pH seawater was achieved by circulating seawater through a Liqui-Cel® gas membrane contactor receiving a specialty air mix of 300 ppm CO_2. Low-pH seawater was achieved by aerating the seawater with a specialty air mix containing 20,000 ppm CO_2. The high-pH and low-pH seawater sources received continuous flow of 0.35-µm filtered seawater; one reservoir each of high-pH and low-pH seawater provided seawater to all culturing containers. To study [O_2] and pH effects in Expt. B and C, [O_2] and pH conditions were maintained by circulating treatment seawater in a 7.5 L header tank for each replicate through a gas membrane contactor (Liqui-Cel Part No. G501) that received a user-specified specialty air mixture of N_2, O_2 and CO_2 (Bockmon *et al.*, 2013). The larval cultures received treated seawater from the header tank at a rate of 60 ml min^{-1}. Experimental [O_2] and pH conditions were monitored with an Aanderaa optode and Honeywell Durafet III pH sensor that were transferred daily among replicates. While a tight relationship between [O_2] and pH in nearshore upwelling-influenced environments results in conditions where they fluctuate in unison, the systems utilized during this study were unable to mimic the effects of stable [O_2] versus fluctuating [O_2] and so oxygen variation could not be incorporated as experimental treatments.

Discrete samples were taken daily from all replicates during each experiment for spectrophotometric determination of pH, and when [O_2] was manipulated samples were taken for Winkler titration. At the beginning and end of each experiment discrete samples were also taken for determination of total alkalinity (A_T) and salinity. pH samples were determined spectrophotometrically via a modified method based on Dickson et al. (2007) using 1-cm cuvette cells and commercially available m-cresol dye with dye corrections based on Clayton and Byrne (1993). This method was calibrated with certified reference material from the Marine Physical Laboratory at Scripps Institution of Oceanography, and uncertainty of measurements was ± 0.03 pH units. pH values are reported at the in situ temperature and on the total pH scale. [O_2] measurements were made with a modified Winkler method (Dickson 1996) with an accuracy of ± 2 μmol kg^{-1}. A_T measurements were determined using an open-cell, potentiometric titration with an accuracy of ± 2 μmol kg^{-1} (Dickson *et al.*, 2007). Salinity was calculated from density measured at 20°C on a Density Meter (Mettler Toledo DE45) with an accuracy of 0.05 salinity units. pCO_2, aragonite saturation state (Ω_{arag}) and [CO_3^{2-}] were calculated from average A_T and pH using the Matlab version of CO2SYS (van Heuven *et al.*, 2011) with dissociation constants from Mehrbach et al. (1973) as refit by Dickson and Millero (1987). The average propagated uncertainties based on uncertainty in pH and A_T for pCO_2, Ω_{arag} and [CO_3^{2-}] were ± 72 μatm, ± 0.09 and ± 5.7 μmol kg^{-1}, respectively. Temperature was monitored every five minutes in all replicates by HOBO Pendant® temperature data loggers with an accuracy of ± 0.5 °C.

Response Metrics

Larval survivorship, developmental stage, and size were measured 2, 4, 6 and 8 days post-fertilization. Five replicate water samples of ~50 larvae were sampled from each replicate culturing container and preserved in 1% buffered formalin. Culture densities were quantified by counting the number of larvae in each aliquot and averaging across the aliquots for a single replicate value. Survivorship was calculated as the density of larvae remaining in each replicate container relative to the initial density. To examine treatment effects on development, the proportion of veligers on day 2 was used as a metric to quantify rate of larval transition from the trochophore to veliger stage. It was calculated as the density of veligers divided by the total density of larvae from each replicate. To examine treatment effects on larval shell size, veliger larvae from each replicate were oriented in lateral position on a microscope slide with an elevated cover slip, and photographed with a digital camera fitted to a compound microscope. Images were analyzed using ImageJ (NIH) to determine shell length for 30 veliger larvae from each experimental culturing bucket. Shell length was measured as the anterior to posterior dimension of the shell parallel to the hinge line and is referred to as larval size. The size effect was calculated as the mean of results on a given day in low pH as a percentage of the ambient pH treatment within the same experiment.

Statistical analyses

To test for differences among treatments in the size response of larvae, two metrics were calculated from the sample distribution of 30 larvae per replicate, the average and the coefficient of variation (CV). The CV is the ratio of the standard deviation to the mean and is a normalized measured of dispersion. A Shapiro-Wilks test

for departure from normality and Bartlett's test for homogeneity of variance revealed that the data fulfilled assumptions of normality and homogeneity of variance, so untransformed morphometric data were used in the analyses. Survivorship and development data were square-root-arcsine-transformed. A repeated-measures analysis of variance (ANOVA) was used to test for significant differences in survivorship and size among treatment, day and the interaction of treatment and day. For repeated-measures ANOVA tests, data met assumptions of sphericity as determined by the Mauchly Criterion Sphericity test. An ANOVA was used to test for significant effects of treatment on the proportion of veligers on day 2. Post-hoc Tukey HSD tests ($\alpha = 0.05$) were used to further explore significant differences among treatments for each response measurement. An analysis of covariance (ANCOVA) was used to test for differences in the relationship between pH and size between species; size was the dependent variable, species was a categorical independent variable, and pH was treated as the covariate. pH treatments with stable conditions were only included in the ANCOVA test. Statistical analyses were carried out in JMP 9.0 (SAS Institute Inc., 2010).

Results

Expt. A - Effect of low pH, variable pH and early exposure to low pH

Effects of pH treatment on larval survival, development, and veliger size differed across the response measurements and between species (Table 5.S1). There was no effect of low pH or low variable pH relative to ambient pH on survivorship in either mytilid species (Repeated-Measures ANOVA, $F_{2,6} = 4.296$, $p = 0.070$ for *M. californianus* and $F_{3,8} = 2.097$, $p = 0.180$ for *M. galloprovincialis*). Development,

measured as the proportion of veligers on day 2, was altered (Fig. 5.4, ANOVA, $F_{3,8}$ = 12.027, p = 0.003 for *M. californianus* and $F_{3,8}$ = 6.711, p = 0.014 for *M. galloprovincialis*). Post-hoc contrasts revealed that larvae exposed to low pH conditions had a lower proportion of veligers on day 2 relative to larvae exposed to ambient pH conditions in both mytilid species indicating a developmental delay at low pH (Tukey HSD, $p < 0.05$). In contrast, larvae reared at low pH with semidiurnal fluctuations did not have a lower proportion of veligers for both mytilid species (Tukey HSD, $p < 0.05$), potential evidence for amelioration of the negative effects of low pH by incorporation of high-frequency pH fluctuations.

The effect of low pH and variable low pH on veliger size differed between species. There was a significant decline in size in *M. californianus* veligers (Fig. 5.5, Repeated-Measures ANOVA, $F_{2,6}$ = 36.8, $p < 0.001$) reared in low pH and variable low pH relative to larvae reared in ambient pH (Tukey HSD, $p < 0.05$). There was no effect of low pH or variable low pH on the size of *M. galloprovincialis* veligers (Repeated-Measures ANOVA, $F_{3,8}$ = 3.659, p = 0.063), but there was significant pH treatment by day interaction ($F_{9,24}$ = 4.358, p = 0.002). Veliger size was smaller on day 2 in low pH and variable low pH relative to ambient pH, but by day 8 only low pH veligers were smaller than ambient pH veligers (Tukey HSD, $p < 0.05$). Day 8 larvae in the variable low pH treatment had recovered to ambient size. The variation in size as measured by the coefficient of variation was greater at low pH relative to ambient pH in both mytilid species (Table 5.S1; Tukey HSD, $p < 0.05$). When incorporating semidiurnal fluctuations at low pH, variation in size was not greater than it was at ambient pH in *M. galloprovincialis*. This contrasts with *M. californianus* in which variation in size at low

pH with semidiurnal fluctuations was greater than ambient pH. We note that the mean pH conditions for low and variable low pH treatments were the same in the *M. californianus* experiment (7.51), but the variable low pH treatment had a slightly higher mean pH (7.54) than the stable low pH treatment (7.48) in the *M. galloprovincialis* experiment.

In *Mytilus californianus* Expt. A there was a fourth treatment in which pH fluctuated twice per day at ambient pH conditions. Due to a sensor malfunction treatment conditions were only controlled from the beginning of the experiment through day 2. On day 2, larvae reared in ambient variable pH did not exhibit differential survival, development or veliger size compared to larvae reared in stable ambient pH conditions (Table 5.S1; Fig. 5.4).

In *Mytilus galloprovincialis* Expt. A there was a fourth treatment that tested the effects of early, 2-day exposure to low pH followed by return to ambient condition on larval responses throughout the 8-day experiment (Table 5.S1). There was no effect of early low pH exposure of 7.56 on survivorship, development, or size relative to larvae exposed to ambient pH conditions (Fig. 5.4 & 5.5; Table 5.S1).

Expt. B & C - Effect of low pHOx and low [O_2] versus low pH

There were no effects of low pHOx versus ambient pH and [O_2] on larval survival, development, and veliger size for both species (Table 5.S2). pH employed during this experiment was higher than during Expt. A, and could account for the difference in observed sensitivity between experiments. Effects of low [O_2] versus low pH on larval survival, development, and veliger size differed across the response

measurements and between species (Table 5.S3). Larvae exposed to low [O_2] and those exposed to low pH in both mytilid species exhibited similar survivorship (Repeated-Measures ANOVA, $F_{1,4} = 4.961$, $p = 0.090$ for *M. californianus* and $F_{1,2} = 4.227$, $p = 0.176$ for *M. galloprovincialis*), and development on day 2 (ANOVA, $F_{1,4} = 0.990$, $p = 0.376$ for *M. californianus* and $F_{1,2} = 13.87$, $p = 0.065$ for *M. galloprovincialis*). There was no effect of low pH at 7.59 or low [O_2] on veliger size in *M. galloprovincialis* (Fig. 5.5, Repeated-Measures ANOVA, $F_{1,2} = 1.146$, $p = 0.396$), but *M. californianus* veligers were smaller when exposed to low pH of 7.64 at ambient [O_2] than in low [O_2] at ambient pH (Repeated-Measures ANOVA, $F_{1,4} = 20.3$, $p = 0.011$). (Tukey HSD, $p < 0.05$). There was no change in the coefficient of variation in size at low pHOx, or low [O_2] versus low pH (Table 5.S2 and 5.S3).

Species Comparison

The effect of low pH on shell size, as a percentage of size at ambient pH across experiments and between species, was 2 - 10% (Fig. 5.6). There was a linear relationship between size effect and pH (MS = 23.915, $F_{1,5} = 13.79$, $p = 0.014$, $r^2 = 0.73$).

$$\text{Size Effect} = -220 + 29.3 * \text{pH} \qquad \text{(Eq. 1)}$$

Both slopes (ANCOVA, MS = 2.010, $F_{1,4} = 1.21$, $p = 0.334$) and intercepts (ANCOVA, MS = 0.291, $F_{1,5} = 0.05$, $p = 0.840$) generated for each species are not significantly different indicating that shell size of *Mytilus californianus* larvae was not more or less sensitive to pH reduction than for *M. galloprovincialis* larvae.

Discussion

Interactive effects of multiple drivers

The susceptibility of planktonic larvae to environmental stress is well recognized. Studies on the role of pH as a single stressor have become plentiful. Although decreased larval performance at low pH is not universal (e.g. Dupont *et al.*, 2010), heavily calcified forms tend to exhibit reduced size, growth rates and calcification (Kurihara, 2008; Byrne, 2012). While these effects continue to be documented across calcifying taxa and with increasing mechanistic detail (e.g. Waldbusser *et al.*, 2013), the performance of larvae in the field reflects an integration of many environmental factors, not just pH. These additional factors include the role of low [O_2] and natural environmental fluctuations, both of which are prominent features along upwelling margins. Investigating the effects of multiple drivers on biological systems alone and in combination will help elucidate the potential threat of each in the context of changing ocean climates.

Where natural fluctuations in pH occur, the effects of ocean acidification when reaching pH values of 7.5 – 7.6 could be alleviated. Decreased mytilid developmental rates at low pH were alleviated with high-frequency pH excursions (Fig. 5.4). The transition from a trochophore to a veliger represents a critical time period in development when a specialized group of ectodermal cells initiate calcification and the shell is formed (Hayakaze & Tanabe, 1999; Wilt, 2005). This earlier stage of development could be the most sensitive stage to pH as seen in other studies (e.g., Gobler & Talmage 2013). The precise cause of delayed development at low pH remains elusive, but incorporating excursions to higher pH conditions can alleviate this stress. These results suggest that in the field when pH is low larvae exposed to higher pH for even a few hours as a late trochophore would develop into veligers more quickly. The scale of environmental

fluctuation within the larval ambit can therefore influence its performance. In order to know the pH and [O_2] levels and fluctuations that larvae experience in their environment, the cross-shore and depth distribution of larvae must be known. Field surveys have demonstrated that veligers of intertidal bivalve species are found close to shore, from just outside the surf zone to only a few kilometers offshore (*e.g.*, Shanks and Shearman, 2009; Shanks and Brink, 2005). Larval traps and plankton tows have revealed that larvae are nearly absent from surface waters (Shanks and Shearman, 2009), or that larval distributions as a function of depth (4, 8.5, 14 m) are inconsistent over time (Rilov *et al.*, 2008). These field surveys support our experimental use of pH and [O_2] conditions recorded at 7 and 17 m water depth along the inner-shelf outside of the surf zone.

While developmental rates of each *Mytilus* species exhibited similar responses to semidiurnal variability, the effect of variability on shell size relative to stable low pH differed between species. Shell length throughout development has shown to be determined at time of first shell formation (Kurihara *et al.*, 2008; White *et al.*, 2013). This observation was corroborated in both species, and *Mytilus californianus* larvae that were reared in low variable pH also exhibited reduced shell size throughout the experiment. However, while *M. galloprovincialis* larvae at low variable pH exhibited reduced shell size on day 2 (when the shell is first formed), they also exhibited greater shell growth throughout the experiment and by day 8 had equivalent shell size to larvae reared at ambient pH (Fig. 5.5). While pH fluctuations at low pH have altered developmental and shell size responses relative to stable low pH, fluctuations at ambient pH did not reveal any benefits for survivorship, developmental rates or veliger size in *M. californianus*. From a biological performance perspective, environmental pH

fluctuations have greater influence at low pH as opposed to ambient pH and thus will become increasingly important in future ocean environments. Environments where such fluctuations are prominent features include estuaries, kelp forests, coral reefs, the inner-shelf along upwelling margins, intertidal pools, and fjords (Wootton *et al.*, 2008; Thomsen *et al.*, 2010; Hofmann *et al.*, 2011).

The observed present-day [O_2] conditions along the San Diego inner-shelf encompass a range of values that did not influence mytilid larval survivorship, development or veliger size. The range tested did not incorporate hypoxic conditions, which have not been observed within 20 m water depth in the region under study. There are other coastal locations along the biogeographic range of *Mytilus californianus* that have been observed to experience lower [O_2] excursions than utilized in this study (Chan *et al.*, 2008; Booth *et al.*, 2012). Still, previous investigations into lethal effects of [O_2] as low as 0.5 ml l^{-1} on *Mytilus californianus* larvae reveal remarkable tolerance (Eerkes-Medrano *et al.*, 2013), suggesting that [O_2] is not a strong influence on larval performance.

Functional consequences of smaller larval populations with greater variance

Results of these experiments reveal a negative linear effect of pH on size of mussel larvae (Fig. 5.6). This finding corroborates results of other studies (Kurihara *et al.*, 2008; Gaylord *et al.*, 2011). Reduced larval size at settlement has been demonstrated for not only pH effects but as a product of low maternal investment, food availability in the plankton, water temperature, other environmental conditions encountered in the plankton, and duration of the planktonic phase (Pechenik, 1999). There are functional

consequences of settling at a smaller size. Larger settlers may have greater post-settlement growth than smaller settlers because they begin sessile life with more nutritional reserves (Moran & Emlet 2001), and they may also have the capacity to filter a larger volume of food than smaller settlers. Smaller individuals may be more susceptible to predation, particularly if they have thinner, weaker shells as shown by Gaylord et al. (2011). Juvenile whelks which prefer 1-2 mm mussels over other prey (Gosselin & Chia, 1996) may prey more successfully on mussels exposed to low pH during early development.

Decreasing pH not only decreased mean size of larvae but also increased the variance, therefore changing the observed shape of the distribution of shell sizes (Fig. 5.7). Increased variance in a population in response to a stressor can represent the first steps in the evolution of a population to a changing environment (Orlando & Guillette, 2001), and a population's resilience could be dependent on increased phenotypic variance. *Mytilus galloprovincialis* had an increase in size variance of 76% at low pH relative to ambient pH and *M. californianus* had an increase of 49% during Expt. A. This leads to the possibility that *M. galloprovincialis* will have greater resilience to reductions in pH than *M. californianus*.

Species Comparison

Although we hypothesized that *Mytilus californianus* would be more sensitive to reductions in pH than *M. galloprovincialis*, there was no difference in the effect of pH on size between the species across a range of low pH values from 7.48 – 7.70 as revealed by ANCOVA. While similarity in size reduction with pH reduction between species

indicates that generalizations could be made for this genus, differences in their response to semidiurnal fluctuations at low pH suggest that each species has a differential capacity for adaptation. Not only did the size of *M. galloprovincialis* larvae benefit from semidiurnal fluctuations at low pH, but the variation in the size response was also reduced (Fig. 5.7). In combination, these size response metrics suggest that *M. galloprovincialis* larval populations might better cope with ocean acidification than *M. californianus*, particularly due to the role of high-frequency pH variability in modulating responses.

It has been recognized that intertidal mussels are not obvious candidates to exhibit vulnerability to ocean acidification (Gaylord et al. 2011; Thomsen et al. 2010). Even though adult mussels are found in environments that can experience low pH and low [O_2] from upwelling events (e.g. Feely *et al.*, 2008) or tidepool isolation (e.g. Wootton *et al.*, 2008), the pH conditions that elicit larval sensitivities are predicted to occur with increasing frequency by 2050 (Hauri *et al.*, 2013). The result may be that populations of planktonic larvae inhabiting differing spatial and temporal pH gradients will differ in performance. This further supports the need to consider the role of environmental variability in modulating biological responses. Further implementation of multistressor studies will provide much needed information on the relative effects and interactions of changing ocean climate parameters for biological performance.

Acknowledgements

We thank A. G. Dickson and T. R. Martz for providing access to their laboratory facilities to run A_T, salinity, and $[O_2]$ samples. The experimental system used in Expt. A was developed in partnership with Brian Cregger at Safe Harbor Associates LLC. We thank J. Leichter, D. Holway, and A. G. Dickson for comments on an earlier draft of this manuscript. This research was supported by NSF-OCE Award Nos. 0927445 and 1041062, and under NOAA Grants NA10OAR4170060 and NA08OAR4170669, California Sea Grant College Program Project R/CC-02EPD, R/CC-04, and R/OPCENV-09, through NOAA'S National Sea Grant College Program, U.S. Dept. of Commerce; and was supported in part by the California Natural Resources Agency. The statements, findings, conclusions and recommendations are those of the authors and do necessarily reflect the views of California Sea Grant, state agencies, NOAA or the U.S. Dept. of Commerce. The manuscript was also developed under a Science to Achieve Results Fellowship Assistance Agreement No. FP916973 awarded to CAF by the US Environmental Protection Agency (EPA). It has not been formally reviewed by the EPA. This chapter, in full, has been submitted for publication of the material as it may appear in Global Change Biology, 2013, Frieder, Christina A.; Gonzalez, Jennifer P.; Bockmon, Emily A.; Navarro, Michael O.; Levin, Lisa A. The dissertation author was the primary investigator and author of this material

References

Bates NR, Best MHP, Neely K, Garley R, Dickson AG, Johnson RJ (2012) Detecting anthropogenic carbon dioxide uptake and ocean acidification in the North Atlantic Ocean. *Biogeosciences*, **9**, 2509–2522.

Bockmon EE, Frieder CA, Navarro MO, White-Kershek LA, Dickson AG (2013) Controlled experimental aquarium system for multi-stressor investigation: Carbonate chemistry, oxygen saturation, and temperature. *Biogeosciences Discussions*, **10**, 3431–3453.

Bograd SJ, Castro CG, Di Lorenzo E, Palacios DM, Bailey H, Gilly W, Chavez FP (2008) Oxygen declines and the shoaling of the hypoxic boundary in the California Current. *Geophysical Research Letters*, **35**, L12607.

Booth JAT, McPhee-Shaw EE, Chua P, *et al.* (2012) Natural intrusions of hypoxic, low pH water into nearshore marine environments on the California coast. *Continental Shelf Research*, **45**, 108–115.

Byrne M (2012) Global change ecotoxicology: Identification of early life history bottlenecks in marine invertebrates, variable species responses and variable experimental approaches. *Marine Environmental Research*, **76**, 3–15.

Carson HS, López-Duarte PC, Rasmussen L, Wang D, Levin LA (2010) Reproductive timing alters population connectivity in marine metapopulations. *Current Biology*, **20**, 1926–31.

Chan F, Barth JA, Lubchenco J, Kirincich A, Weeks H, Peterson WT, Menge BA (2008) Emergence of anoxia in the California current large marine ecosystem. *Science*, **319**, 920.

Clayton TD, Byrne RH (1993) Spectrophotometric seawater pH measurements: total hydrogen ion concentration scale calibration of m-cresol purple and at-sea results. *Deep Sea Research Part I: Oceanographic Research Papers*, **40**, 2115–2129.

Costlow JDJ, Bookhout CG (1971) The effect of cyclic temperatures on larval development in the mud-crab *Rhithropanopeus harrisii*. In: *Fourth European Marine Biology Symposium* (eds: Crisp DJ), pp211–220. Cambridge University Press.

Crawford WR, Peña MA (2013) Declining oxygen on the British Columbia continental shelf. *Atmosphere-Ocean*, **51**, 88–103.

Dickson AG (1996) Determination of dissolved oxygen in sea water by Winkler titration. In: *WOCE Operations Manual, Volume 3: The Observational Programme, Section 3.1: WOCE Hydrographic Programme. Part 3.1.3: WHP Operations and Methods* (eds: World Ocean Circulation Experiment), pp 1-13. Woods Hole, Massachusetts, USA.

Dickson AG, Millero FJ (1987) A comparison of the equilibrium constants for the dissociation of carbonic acid in seawater media. *Deep-Sea Res.*, **34**, 1733–1743.

Dickson AG, Sabine CL, Christian JR (2007) *Guide to best practices for ocean CO_2 measurements*. Sidney, British Columbia, PICES Special Publication 3.

Dufault AM, Cumbo VR, Fan T-Y, Edmunds PJ (2012) Effects of diurnally oscillating pCO_2 on the calcification and survival of coral recruits. *Proceedings of the Royal Society B*, **279**, 2951–8.

Dupont S, Lundve B, Thorndyke M (2010) Near future ocean acidification increases growth rate of the lecithotrophic larvae and juveniles of the sea star *Crossaster papposus*. *Journal of Experimental Zoology*, **314**, 382–9.

Eerkes-Medrano D, Menge BA, Sislak C, Langdon CJ (2013) Contrasting effects of hypoxic conditions on survivorship of planktonic larvae of rocky intertidal invertebrates. *Marine Ecology Progress Series*, **478**, 139–151.

Feely RA, Sabine CL, Hernandez-Ayon JM, Ianson D, Hales B (2008) Evidence for upwelling of corrosive "acidified" water onto the continental shelf. *Science*, **320**, 1490–2.

Frieder CA, Nam SH, Martz TR, Levin LA (2012) High temporal and spatial variability of dissolved oxygen and pH in a nearshore California kelp forest. *Biogeosciences*, **9**, 3917–3930.

Gabbott PA (1976) Energy Metabolism. In: *Marine Mussels: Their Ecology and Physiology* (eds: Bayne BL), pp293–355. Cambridge, Cambridge University Press.

Gaylord B, Hill TM, Sanford E, *et al.* (2011) Functional impacts of ocean acidification in an ecologically critical foundation species. *The Journal of Experimental Biology*, **214**, 2586–94.

Gazeau F, Gattuso J-P, Greaves M, Elderfield H, Peene J, Heip CHR, Middelburg JJ (2011) Effect of carbonate chemistry alteration on the early embryonic development of the Pacific oyster (*Crassostrea gigas*). *PloS ONE*, **6**, e23010.

Gobler CJ, Talmage SC (2013) Short- and long-term consequences of larval stage exposure to constantly and ephemerally elevated carbon dioxide for marine bivalve populations. *Biogeosciences*, **10**, 2241–2253.

Gosselin LA, Chia F-S (1996) Prey selection by inexperienced predators: do early juvenile snails maximize net energy gains on their first attack? *Journal of Experimental Marine Biology and Ecology*, **199**, 45–58.

Hauri C, Gruber N, Vogt M, *et al.* (2013) Spatiotemporal variability and long-term trends of ocean acidification in the California Current System. *Biogeosciences*, **10**, 193–216.

Hayakaze E, Tanabe K (1999) Early larval shell development in mytilid bivalve *Mytilus galloprovincialis*. *Venus*, **58**, 119–127.

Hettinger A, Sanford E, Hill TM, *et al.* (2012) Persistent carry-over effects of planktonic exposure to ocean acidification in the Olympia oyster. *Ecology*, **93**, 2758 – 68.

van Heuven SD, Pierrot JWB, Lewis RE, Wallace DWR (2011) *MATLAB Program Developed for CO2 System Calculations, ORNL/CDIAC-105b*. Oak Ridge, Tennessee, Carbon Dioxide Information Analysis Center, Oak Ridge National Laboratory, U.S. Department of Energy.

Hochachka PW, Somero GN (2001) *Biochemical Adaptation : Mechanism and Process in Physiological Evolution*. Oxford University Press.

Hofmann GE, Smith JE, Johnson KS, *et al.* (2011) High-frequency dynamics of ocean pH: a multi-ecosystem comparison. *PloS ONE*, **6**, e28983.

Keeling RF, Körtzinger A, Gruber N (2010) Ocean deoxygenation in a warming world. *Annual Review of Marine Science*, **2**, 199–229.

Kurihara H (2008) Effects of CO_2-driven ocean acidification on the early developmental stages of invertebrates. *Marine Ecology Progress Series*, **373**, 275–284.

Kurihara H, Asai T, Kato S, Ishimatsu A (2008) Effects of elevated pCO_2 on early development in the mussel *Mytilus galloprovincialis*. *Aquatic Biology*, **4**, 225–233.

Lucas JS, Costlow JD (1979) Effects of various temperature cycles on the larval development of the gastropod mollusc *Crepidula fornicata*. *Marine Biology*, **51**, 111–117.

Mehrbach C, Culberson CH, Hawley JE, Pytkowicz RN (1973) Measurement of the apparent dissociation constants of carbonic acid in seawater at atmospheric pressure. *Limnol. Oceanogr.*, **18**, 897–907.

Moran AL, Emlet RB (2001) Offspring size and performance in variable environments: Field studies on a marine snail. *Ecology*, **82**, 1597–1612.

Nam S, Kim H-J, Send U (2011) Amplification of hypoxic and acidic events by La Niña conditions on the continental shelf off California. *Geophysical Research Letters*, **38**.

Orlando EF, Guillette LJ (2001) A re-examination of variaiton associated with environmentally stressed organisms. *Human Reproduction Update*, **7**, 265–272.

Pechenik JA (1999) On the advantages and disadvantages of larval stages in benthic marine invertebrate life cycles. *Marine Ecology Progress Series*, **177**, 269–297.

Peterson G, Allen CR, Holling CS (1998) Ecological resilience, biodiversity, and scale. *Ecosystems*, **1**, 6–18.

Pörtner HO (2012) Integrating climate-related stressor effects on marine organisms: Unifying principles linking molecule to ecosystem-level changes. *Marine Ecology Progress Series*, **470**, 273–290.

Pörtner HO, Langenbuch M (2005) Synergistic effects of temperature extremes, hypoxia, and increases in CO_2 on marine animals: From Earth history to global change. *Journal of Geophysical Research*, **110**, C09S10.

Rilov G, Dudas SE, Menge BA, Grantham BA, Lubchenco J, Schiel DR (2008) The surf zone: a semi-permeable barrier to onshore recruitment of invertebrate larvae? *Journal of Experimental Marine Biology and Ecology*, **361**, 59–74.

Sastry AN (1979) Metabolic adaptation of *Cancer irroratus* developmental stages to cyclic temperatures. *Marine Biology*, **51**, 243–250.

Shanks AL, Brink L (2005) Upwelling, downwelling, and cross-shelf transport of bivalve larvae: Test of a hypothesis. *Marine Ecology Progress Series*, **302**, 1–12.

Shanks AL, Shearman RK (2009) Paradigm lost? Cross-shelf distributions of intertidal invertebrate larvae are unaffected by upwelling or downwelling. *Marine Ecology Progress Series*, **385**, 189–204.

Stramma L, Johnson GC, Sprintall J, Mohrholz V (2008) Expanding oxygen-minimum zones in the tropical oceans. *Science*, **320**, 655–8.

Thomsen J, Gutowska MA, Saphörster J, *et al.* (2010) Calcifying invertebrates succeed in a naturally CO_2-rich coastal habitat but are threatened by high levels of future acidification. *Biogeosciences*, **7**, 3879–3891.

Vaquer-Sunyer R, Duarte CM (2008) Thresholds of hypoxia for marine biodiversity. *Proceedings of the National Academy of Sciences*, **105**, 15452–7.

Waldbusser GG, Brunner EL, Haley BA, Hales B, Langdon CJ, Prahl FG (2013) A developmental and energetic basis linking larval oyster shell formation to acidification sensitivity. *Geophysical Research Letters*, **40**, 2171-2176.

Wang W, Widdows J (1991) Physiological responses of mussel larvae *Mytilus edulis* to environmental hypoxia and anoxia. *Marine Ecology Progress Series*, **70**, 223–236.

White MM, McCorkle DC, Mullineaux LS, Cohen AL (2013) Early Exposure of Bay Scallops (*Argopecten irradians*) to high CO_2 causes a decrease in larval shell growth. *PloS ONE*, **8**, e61065.

Whitney FA, Freeland HJ, Robert M (2007) Persistently declining oxygen levels in the interior waters of the eastern subarctic Pacific. *Progress in Oceanography*, **75**, 179–199.

Widdows J, Newell RIE, Mann R (1989) Effects of hypoxia and anoxia on survival, energy metabolism, and feeding of oyster larvae (*Crassostrea virginica*, Gmelin). *Biological Bulletin*, **177**, 154–166.

Wilt FH (2005) Development biology meets material science: morphogenesis of biomineralized structures. *Developmental Biology*, **280**, 15–25.

Wootton JT, Pfister CA, Forester JD (2008) Dynamic patterns and ecological impacts of declining ocean pH in a high-resolution multi-year dataset. *Proceedings of the National Academy of Sciences*, **105**, 18848–18853.

Table 5.1. Experimental details and seawater properties for Experiment A, B and C used to raise mussel larvae of *Mytilus californianus* and *M. galloprovincialis* for 8 days. Experiments were conducted between April 2012 and April 2013. There were 2 or 3 replicated containers per treatment (Reps). Mean pH ± manipulated range is reported on the total scale and is calculated from discrete samples taken daily from each replicate. Discrete $[O_2]$ ($\mu mol\ kg^{-1}$) measurements were made daily or every other day in Expt. B and C. Temperature (°C) was measured every 15 minutes with a temperature logger. Discrete samples were taken for salinity and total alkalinity (A_T; $\mu mol\ kg^{-1}$) at the beginning and end of each experiment. pCO_2 (μatm), saturation state of aragonite (Ω_{arag}), and $[CO_3^{2-}]$ ($\mu mol\ kg^{-1}$) were calculated using CO2SYS.

Species	Experiment	Treatment (Reps)	pH	$[O_2]$	Temperature	Salinity	A_T	pCO_2	Ω_{arag}	$[CO_3^{2-}]$
M. californianus	A	Ambient pH (3)	8.04	-	16.5	33.53	2235	399	2.40	155
		Ambient Variable pH (3) ^	7.97 ± 0.12	-	16.5	-	-	482 ± 155	2.10 ± 0.50	136 ± 32
		Low pH (3)	7.51	-	16.5	33.53	2241	1542	0.81	52
		Low Variable pH (3)	7.51 ± 0.15	-	16.5	33.53	2240	1542 ± 574	0.81 ± 0.27	52 ± 17
	B	Ambient pH & O_2 (3)	7.90	223	15.9	33.49	2228	576	1.78	115
		Low pHOx (3)	7.68	104	15.8	33.49	2227	1006	1.13	73
	C	Low pH (3)	7.64	230	16.3	33.55	2233	1116	1.06	68
		Low O_2 (3)	8.00	101	16.1	33.54	2232	443	2.19	142
M. galloprovincialis	A	Ambient pH (3)	7.95	-	15.7	33.65	2213	501	1.95	126
		Low pH (3)	7.48	-	15.7	33.64	2222	1637	0.73	47
		Low Variable pH (3)	7.54 ± 0.15	-	15.7	33.65	2239	1426 ± 533	0.84 ± 0.28	54 ± 18
		Early pH Exposure (3)	7.56 → 7.98	-	15.7	33.64	2222	1348 → 465	0.87 → 2.07	56 → 134
	B	Ambient pH & O_2 (2)	7.91	231	17.2	33.64	2250	567	1.93	124
		Low pHOx (2)	7.61	86	17.2	33.65	2252	1216	1.04	67
	C	Low pH (2)	7.59	234	16.9	33.60	2240	1269	0.98	63
		Low O_2 (2)	7.95	87	17.1	33.62	2241	509	2.07	134

^ Treatment only carried out through day 2 due to a sensor malfunction; pCO_2, Ω_{arag}, and $[CO_3^{2-}]$ calculated from mean A_T and mean salinity for the experiment.

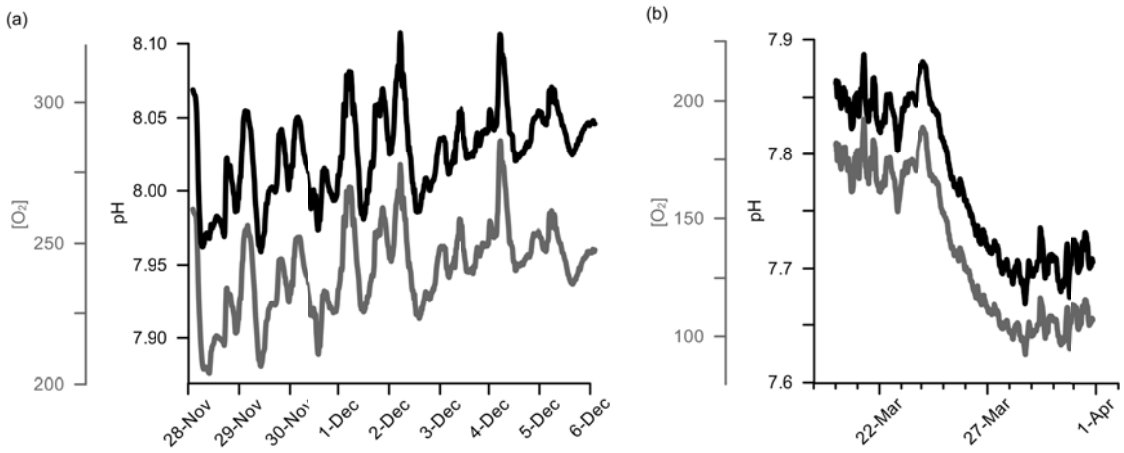

Figure 5.1. pH (black lines) and [O_2] (µmol kg^{-1}; grey lines) measurements made in south La Jolla Kelp Forest, 32.81°N 117.29°W, to illustrate (a) semidiurnal pH and [O_2] fluctuations at 7 m water depth along with the positive correlation between the two, and (b) an upwelling event observed at 17 m water depth when pH and [O_2] were as low as 7.7 and 100 µmol kg^{-1}, respectively. Details of deployment and instrumentation are provided in Frieder et al. (2012). Tick marks on x-axes are daily.

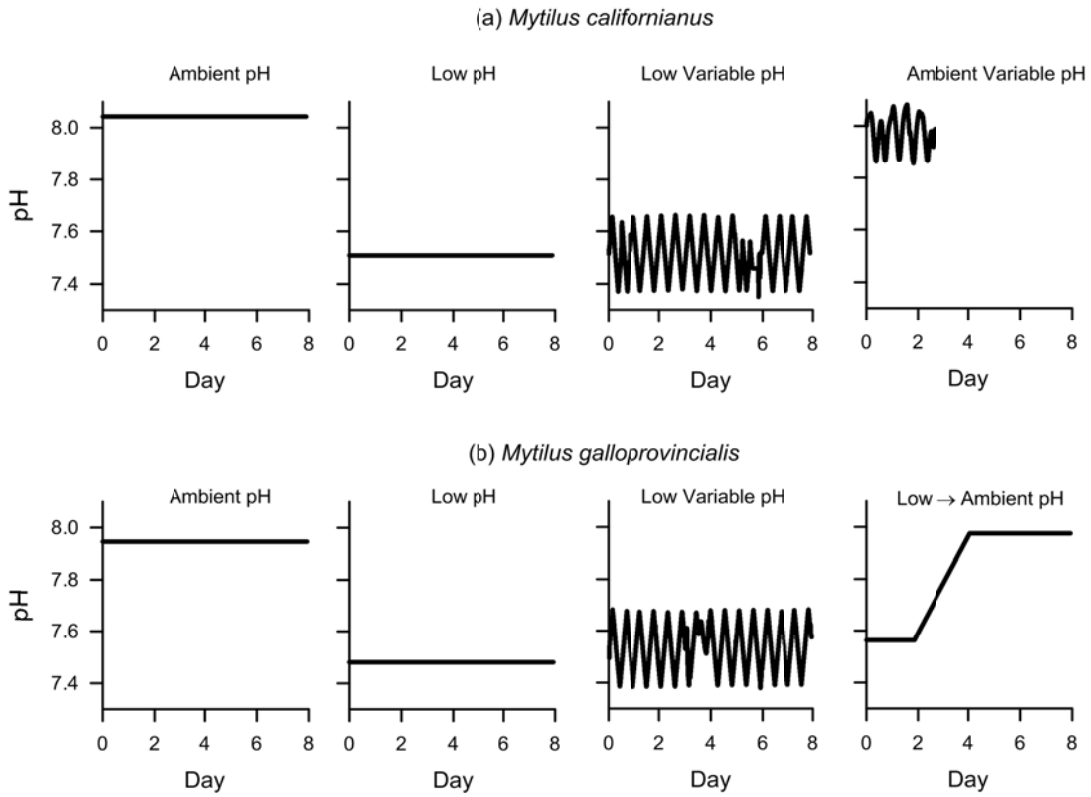

Figure 5.2. Environmental pH conditions in each treatment during Experiment A performed on (a) *Mytilus californianus* larvae and (b) *M. galloprovincialis* larvae for 8 days. pH for each treatment was measured continuously from one rep for each treatment. Variable treatments had a pH range of 0.23 and 0.30 for high and low pH, respectively. During the *M. californianus* Expt. A, the ambient variable pH treatments was carried out for the first 2 days only due to a sensor malfunction. Deviations among replicates within a treatment are illustrated in Figure S1.

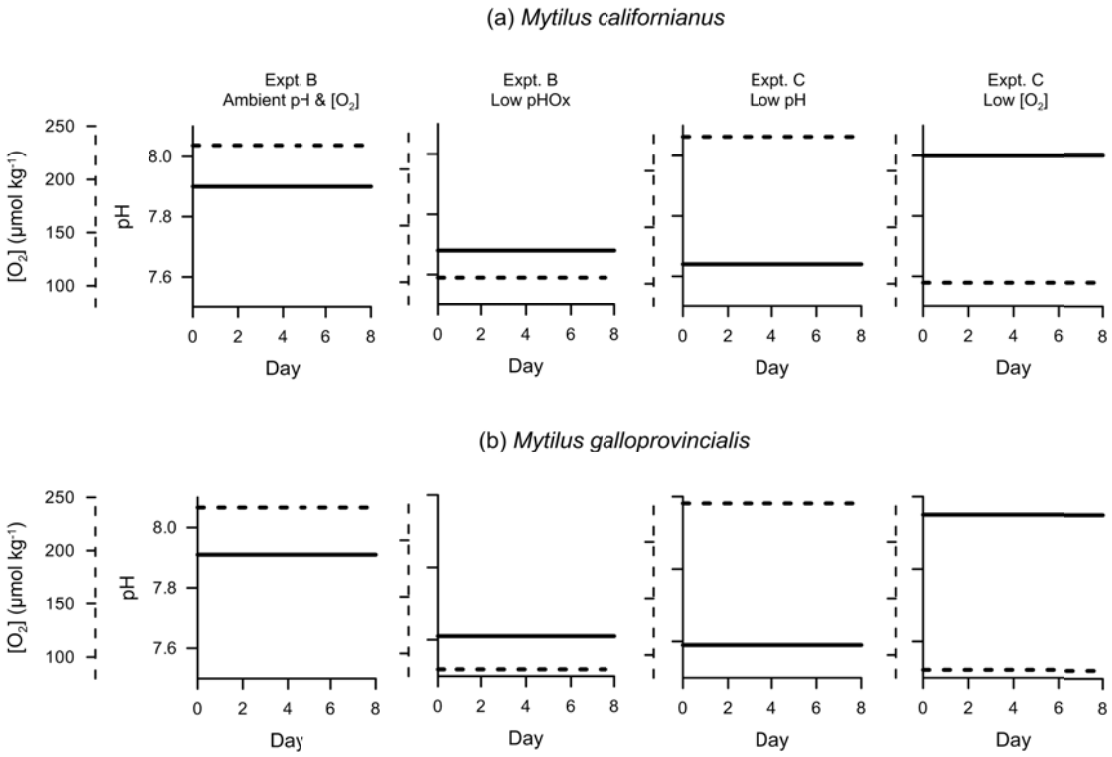

Figure 5.3. Environmental pH (solid line) and [O_2] (µmol kg^{-1}; dashed line) conditions during Experiment B and C performed on (a) *Mytilus californianus* larvae and (b) *M. galloprovincialis* larvae for 8 days. pH and [O_2] for each treatment were measured continuously from one rep for each treatment. Deviations among replicates within a treatment are illustrated in Figure S1.

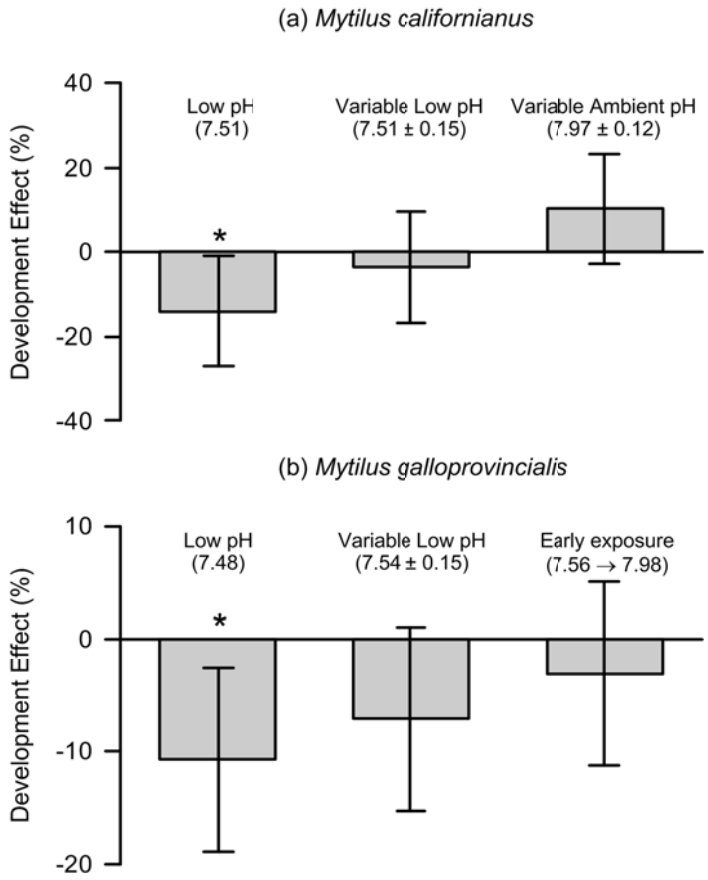

Figure 5.4. The effect of pH conditions on early development rate of mussel larvae during Expt. A for (a) *Mytilus californianus* and (b) *M. galloprovincialis*. Data show means of the proportion of veligers in pH treatments as a percentage of stable ambient pH on day 2. Asterisks indicate significant differences between ambient pH and the corresponding treatment (Tukey HSD, $\alpha = 0.05$).

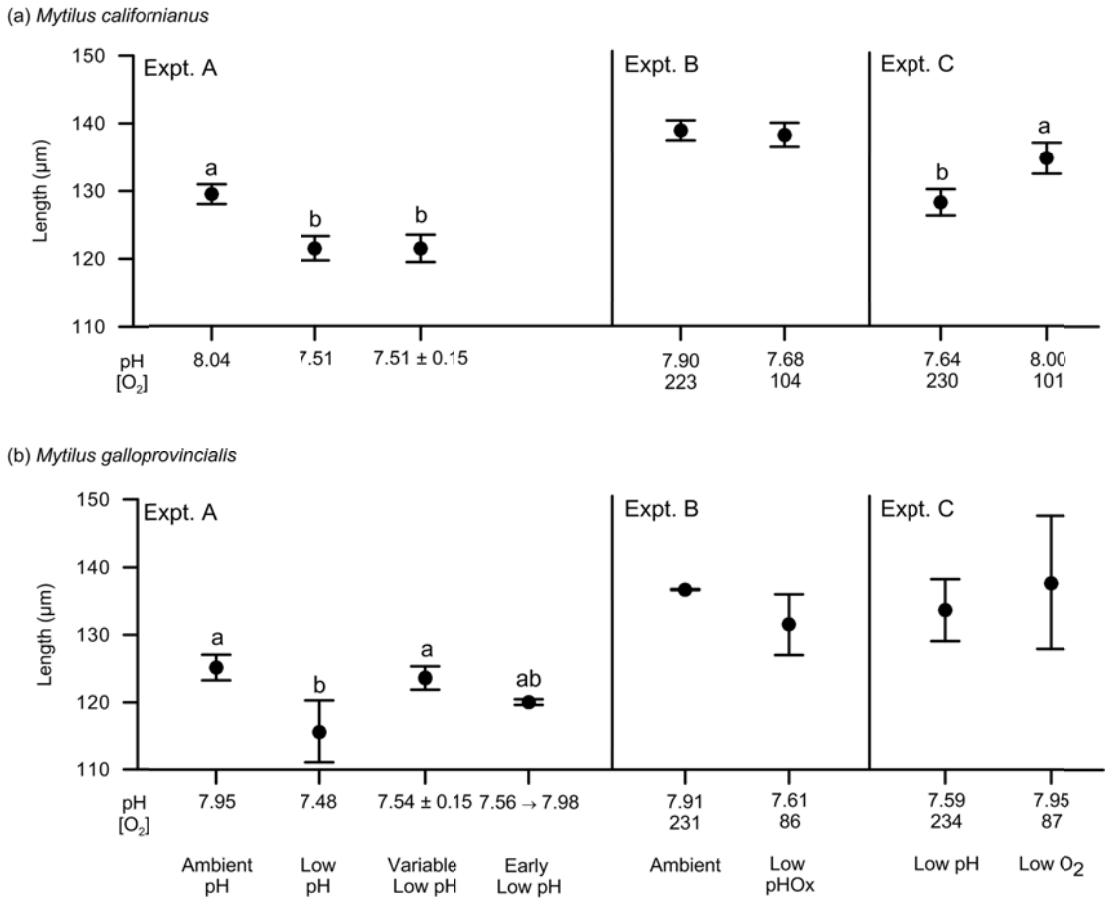

Figure 5.5. Mean length of veliger shell (µm ± SD) on day 8 for (a) *Mytilus californianus* and (b) *M. galloprovincialis* exposed to low pH and fluctuating pH during Expt. A, low pHOx during Expt. B, and low pH versus low $[O_2]$ during Expt. C. Different letters (a, b) denote significant differences (Tukey HSD, $p < 0.05$) between and among treatments within an experiment. Mean pH and $[O_2]$ (µmol kg^{-1}) of each treatment indicated below x-axis.

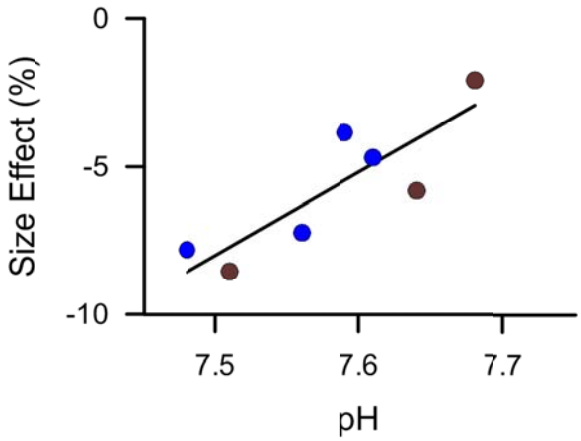

Figure 5.6. Effect of pH on size in *Mytilus californianus* (brown circles) and *M. galloprovincialis* (blue circles). Data show means of results in low-pH treatments from all experiments as a percentage of corresponding ambient pH treatment. Linear fit selected based on ANCOVA.

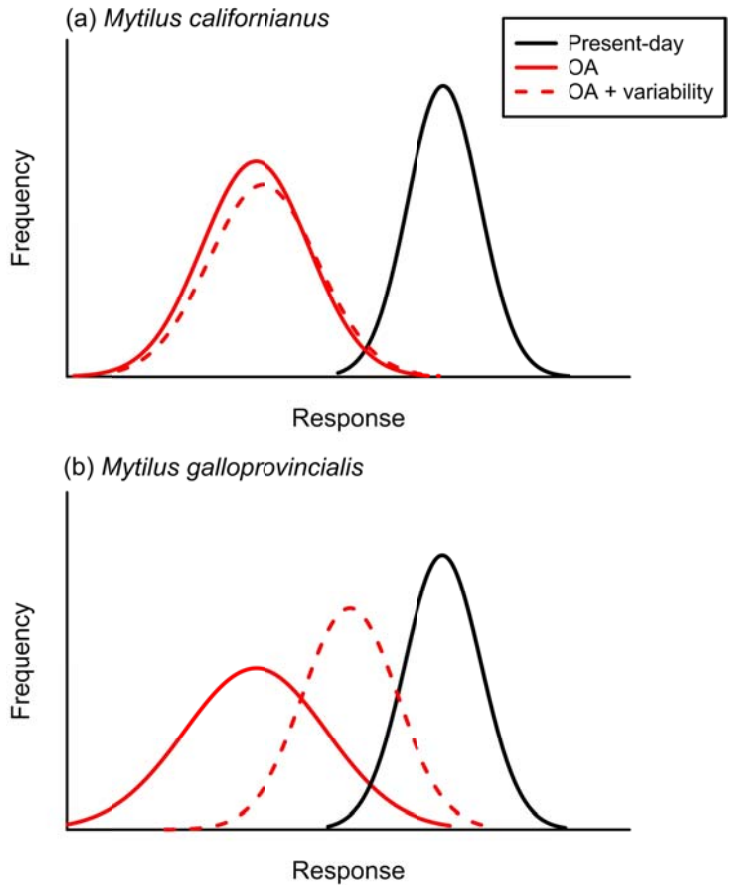

Figure 5.7. The frequency of theoretical veliger size distributions exposed to present-day pH (solid black line), reduced pH representative of OA conditions (solid red line), and reduced pH that incorporates cyclical fluctuations (dashed red line). (a) In *Mytilus californianus* the mean is lower and the variance has increased in both reduced pH and reduced pH that also incorporates semidiurnal fluctuations. (b) In *Mytilus galloprovincialis* the mean is lower and the variance has increased at reduced pH, but these changes in the size distribution are ameliorated when incorporating pH fluctuations at reduced pH.

Supplementary Information – Additional methods, 3 Tables, 1 Figure

Adult Spawning and Larval Culturing

Adult mussels were maintained in ambient temperature in aerated, flow-through seawater aquaria until use. Epibionts were scraped from shells and adult mussels were alternated every 20 minutes between a hot (22°C) and cold (12°C) temperature bath to induce spawning. Spawning occurred within six hours and females and males were separated. An approximate equal proportion of eggs from females were transferred through 125-µm mesh to 0.2-µm filtered seawater at a temperature of 18°C and ambient pH (~8.0) and oxygen (~100%) conditions. A dilution of sperm from males was added to the egg mixture for twenty minutes and then reverse filtered three times to remove excess sperm. Larvae were cultured in 4 L polycarbonate buckets. These vessels contained two holes covered with 55-µm mesh, and were nested within a 7.5 L bucket. The inner bucket received continuous flow of 5-µm filtered seawater and the turnover time of the water in the nested buckets was two hours. This nested bucket design allowed for a flow-through seawater system while keeping larvae contained within the inner bucket. Continuous water flow through the culturing containers was maintained with a multi-channel peristaltic pump at 60 ml min^{-1}. Larvae were gently stirred with a rotating paddle at 7 rpm.

Table 5.S1. Analysis of variance (ANOVA) and repeated-measures ANOVA (RM) results on the effects of pH and variable pH on (a, e) larval survivorship, (b, f) the proportion of veligers on day 2, (c, g) mean veliger size, and (d, h) coefficient of variation in shell size on *Mytilus californianus* and *M. galloprovincialis* during Expt. A. Treatments during the *M. californianus* experiment were ambient pH, low pH, and variable low pH. A fourth treatment of variable ambient pH was included in ANOVA test on the proportion of veligers on day 2 but not included in RM tests because this treatment was not carried out for the full experiment. Treatments during the *M. galloprovincialis* experiment were ambient pH, low pH, variable low pH, and early-exposure to low pH.

Source	df	MS	F-ratio	P
Mytilus californianus – Expt. A				
(a) Survivorship (RM)				
Treatment	2	0.125	4.30	0.070
Replicates in Treatments	6	0.029		
Day	3	0.468	82.06	< 0.0001
Day x Treatment	6	0.006	1.08	0.412
Residual	18	0.006		
(b) Proportion of Veligers (ANOVA)				
Treatment	3	0.030	12.03	0.003
Residual	8	0.003		
(c) Shell Size - Mean (RM)				
Treatment	2	337	36.80	0.0001
Replicates in Treatments	6	9.15		
Day	3	82.67	46.30	< 0.0001
Day x Treatment	6	3.40	1.90	0.137
Residual	18	1.79		
(d) Shell Size - CV (RM)				
Treatment	2	5.101	8.727	0.017
Replicates in Treatments	6	0.585		
Day	3	0.536	1.791	0.185
Day x Treatment	6	0.097	0.325	0.915
Residual	18	5.390		
Mytilus galloprovincialis – Expt. A				
(e) Survivorship (RM)				
Treatment	3	0.088	2.10	0.179
Replicates in Treatments	8	0.042		
Day	3	0.248	25.19	< 0.0001
Day x Treatment	9	0.014	1.45	0.221
Residual	24	0.010		
(f) Proportion of Veligers (ANOVA)				
Treatment	3	0.007	6.711	0.014
Residual	8	0.001		
(g) Shell Size - Mean (RM)				
Treatment	3	118.27	3.66	0.063
Replicates in Treatments	8	32.32		
Day	3	54.85	22.96	<0.0001
Day x Treatment	9	10.41	4.36	0.002
Residual	24	2.389		
(h) Shell Size - CV (RM)				
Treatment	3	10.528	5.745	0.021
Replicates in Treatments	8	1.872		
Day	3	0.448	0.794	0.51
Day x Treatment	9	0.53	0.939	0.513
Residual	24	12.414		

Table 5.S2. Analysis of variance (ANOVA) and repeated-measures ANOVA (RM) results on effects of low pHOx on (a, e) larval survivorship, (b, f) the proportion of veligers on day 2, (c, g) mean veliger size, and (d, h) coefficient of variation in shell size on *Mytilus californianus* and *M. galloprovincialis* during Expt. B. Treatments were ambient pH with ambient [O_2] and combined low pH with low [O_2].

Source	df	MS	F-ratio	P
Mytilus californianus – Expt. B				
(a) Survivorship (RM)				
Treatment	1	0.019	2.47	0.191
Replicates in Treatments	4	0.008		
Day	3	0.057	28.46	< 0.0001
Day x Treatment	3	0.002	1.24	0.339
Residual	12	0.002		
(b) Proportion of Veligers (ANOVA)				
Treatment	1	0.009	3.176	0.149
Residual	4	0.003		
(c) Shell Size - Mean (RM)				
Treatment	1	34.15	3.15	0.151
Replicates in Treatments	4	10.85		
Day	3	975	283	< 0.0001
Day x Treatment	3	2.94	0.855	0.491
Residual	12	3.44		
(d) Shell Size - CV (RM)				
Treatment	1	1.252	0.925	0.391
Replicates in Treatments	4	1.353		
Day	3	12.460	19.747	< 0.0001
Day x Treatment	3	0.366	0.580	0.640
Residual	12	7.571		
Mytilus galloprovincialis – Expt. B				
(e) Survivorship (RM)				
Treatment	1	0.0003	0.007	0.942
Replicates in Treatments	2	0.050		
Day	3	0.078	2.917	0.113
Day x Treatment	3	0.019	0.728	0.572
Residual	6	0.027		
(f) Proportion of Veligers (ANOVA)				
Treatment	1	0.011	0.487	0.558
Residual	2	0.022		
(g) Shell Size - Mean (RM)				
Treatment	1	113.99	7.55	0.111
Replicates in Treatments	2	15.09		
Day	3	207	87	< 0.0001
Day x Treatment	3	0.047	0.020	0.996
Residual	6	2.40		
(h) Shell Size - CV (RM)				
Treatment	1	1.9	5.124	0.1519
Replicates in Treatments	2	0.37		
Day	3	3.61	25.5	< 0.001
Day x Treatment	3	0.337	2.379	0.169
Residual	6	0.851		

Table 5.S3. Analysis of variance (ANOVA) and repeated-measures ANOVA (RM) results on the effects of low [O_2] (μmol kg^{-1}) versus low pH on (a, e) larval survivorship, (b, f) the proportion of veligers on day 2, (c, g) mean veliger size, and (d, h) coefficient of variation in shell size on *Mytilus californianus* and *M. galloprovincialis* during Expt. C.

Source	df	MS	F-ratio	P
Mytilus californianus - Expt. C				
(a) Survivorship (RM)				
Treatment	1	0.026	4.961	0.090
Replicates in Treatments	4	0.005		
Day	3	0.021	90.12	< 0.0001
Day x Treatment	3	0.002	0.772	0.532
Residual	12	0.002		
(b) Proportion of Veligers (ANOVA)				
Treatment	1	0.010	0.990	0.376
Residual	4	0.011		
(c) Shell Size - Mean (RM)				
Treatment	1	262	20.30	0.011
Replicates in Treatments	4	12.93		
Day	3	144	93.10	< 0.0001
Day x Treatment	3	0.58	0.38	0.771
Residual	12	1.55		
(d) Shell Size - CV (RM)				
Treatment	1	0.157	0.248	0.644
Replicates in Treatments	4	0.631		
Day	3	0.352	1.127	0.377
Day x Treatment	3	0.196	0.627	0.612
Residual	12	3.746		
Mytilus galloprovincialis – Expt. C				
(e) Survivorship (RM)				
Treatment	1	0.042	4.23	0.176
Replicates in Treatments	2	0.010		
Day	3	0.151	31.35	0.005
Day x Treatment	3	0.004	0.85	0.517
Residual	6	0.005		
(f) Proportion of Veligers (ANOVA)				
Treatment	1	0.055	13.87	0.065
Residual	2	0.004		
(g) Shell Size - Mean (RM)				
Treatment	1	99.19	1.15	0.396
Replicates in Treatments	2	86.54		
Day	3	240.09	20.30	0.002
Day x Treatment	3	0.62	0.05	0.983
Residual	6	11.83		
(h) Shell Size - CV (RM)				
Treatment	1	0.161	1.871	0.305
Replicates in Treatments	2	0.0859		
Day	3	2.286	1.832	0.242
Day x Treatment	3	0.415	0.3326	0.8027
Residual	6	7.489		

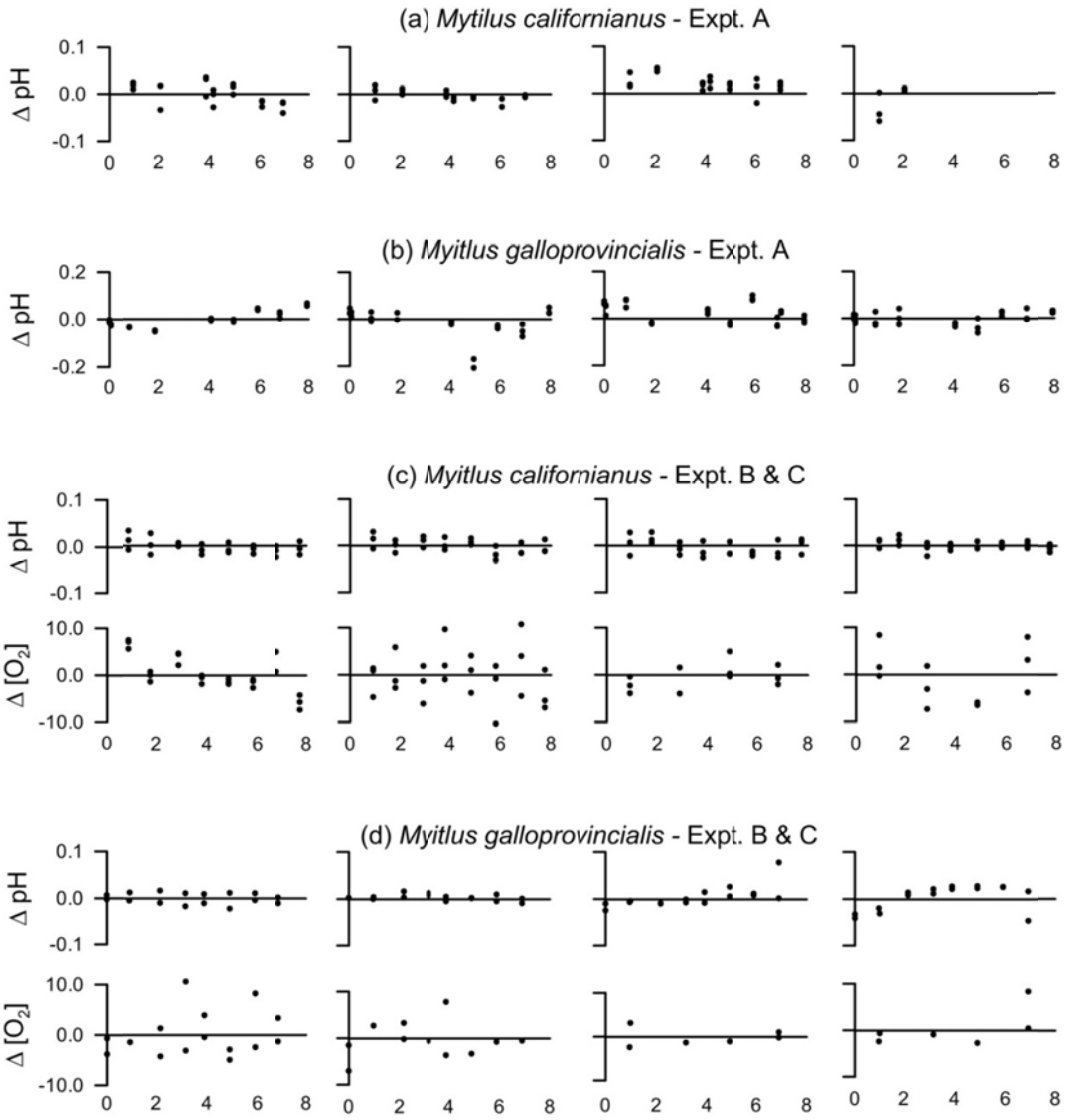

Figure 5.S1. Deviation of pH and $[O_2]$ (µmol kg^{-1}) from treatment set points (ΔpH and $\Delta[O_2]$) among replicate containers for each experiment. Each data point represents a discrete sample taken from larval culturing container and correspond with Fig. 5.2 & 5.3. The x-axes, in days post-fertilization, correspond with timing of discrete sampling. (a) *Mytilus californianus* Expt. A panels left to right are offsets in ambient pH, low pH, variable low pH and variable ambient pH treatments. (b) *M. galloprovincialis* Expt. A panels left to right are offsets in ambient pH, low pH, variable low pH and early low-pH exposure treatments. (c) *Mytilus californianus* Expt. B panels left to right are offsets in ambient pH and $[O_2]$ and low pHOx during Expt. B, and low pH and low $[O_2]$ during Expt. C. (d) *Mytilus galloprovincialis* Expt. B panels left to right are offsets in ambient pH and $[O_2]$ and low pHOx during Expt. B, and low pH and low $[O_2]$ during Expt. C.

CHAPTER 6

Geochemical signatures of larval carbonates reflect pH and oxygen exposure history

Abstract

Environmental conditions experienced by planktonic larvae are often unknown due to difficulties in tracking larval distributions. In the face of climate change, as oceanic dissolved oxygen ($[O_2]$) and pH continue to decrease, it will become increasingly useful to have larval shell-based geochemical proxies that reflect larval pH and oxygen exposure history. Such information, which is retained after settlement in molluscs and fishes, can provide insight into the influence of ocean acidification and deoxygenation on early life stages in their natural setting. In this study, we pursue proxy development by investigating pH and $[O_2]$-induced variation in single and multi-element signatures in larval carbonates of the mussels *Mytilus californianus* and *M. galloprovincialis*. Shells were produced from laboratory-based larval cultures under differing pH and $[O_2]$ levels. Our results demonstrated that U/Ca in *M. californianus* larval shell decreased by 6 ± 1 % per 0.1 pH unit increase from 7.51 to 8.04. Results from *M. galloprovincialis* larvae revealed a similar relationship, but U/Ca is on average 35% greater, and decreased by 12 ± 2 % per 0.1 pH unit increase from 7.59 to 7.95. Sr/Ca also decreased with increasing pH in both species along with multi-element signatures, represented as principal components, but these linear relationships were not as strong as for U/Ca and pH. Zn/Ca increased with increasing $[O_2]$ from 100 to 243 μmol kg^{-1}, but only in *M. californianus*, and multi-element signatures, represented as principal components, did not vary with $[O_2]$. All element ratios varied with larval size except for U/Ca, and this finding was

interpreted as an ontogenetic effect. Thus, we suggest that U/Ca is a geochemical proxy that may have great potential to reflect pH exposure histories of planktonic mussel larvae, and that a proxy for [O_2] is in need of further exploration. Further application of U/Ca was tested by comparing U/Ca in mussel larvae reared in situ in regions of differing upwelling intensity in the Southern California Bight. Larval-shell U/Ca was higher, putative for low-pH exposure, in a region of greater upwelling. Using U/Ca in carbonates to estimate pH-exposure history of elusive marine organisms will provide another lens with which the effects of changing ocean climates for marine populations can be assessed.

Introduction

For many sedentary marine species, movement is carried out by early life stages via free-dispersing planktonic larvae. Larval performance in the plankton can influence success after settlement and thus have profound ecological and evolutionary impacts on populations (reviewed by Cowen & Sponaugle, 2009), but environmental conditions experienced by a larva are often unknown due to a lack of information regarding larval distributions in space and time. Natural geochemical proxies in larval carbonate structures are one means by which environmental conditions can be estimated. Variations in the environment can be subsequently recorded into calcified structures (e.g., shells, otoliths and statoliths), and in molluscs and fishes these are retained in juvenile and adult stages (Thorrold *et al.*, 2007). Various geochemical proxies have been developed to reconstruct past ocean climate records including temperature, salinity and marine carbonate chemistry from biogenic carbonates (e.g.,Katz *et al.*, 2010). Their use

as a tool to reconstruct conditions experienced by larvae in the plankton has been much more limited (but see Levin, 2006).

Seawater chemistry, particularly pH and dissolved oxygen ($[O_2]$), can influence larval performance (Kurihara, 2008; Byrne, 2012; Eerkes-Medrano *et al.*, 2013). The effects on larvae could increase as anthropogenic activities and climate change continue to alter oceanic $[O_2]$ and pH levels. $[O_2]$ and pH are often considered in combination since they are tightly coupled in nearshore settings along upwelling margins (Booth *et al.*, 2012; Frieder *et al.*, 2012). Additionally, both parameters are influenced by present-day anthropogenic CO_2 accumulation in the atmosphere (Gruber, 2011). Reductions in sub-surface $[O_2]$ have been observed globally (Diaz & Rosenberg, 2008; Keeling *et al.*, 2010), and along upwelling margins (Whitney *et al.*, 2007; Chan *et al.*, 2008; Bograd *et al.*, 2008; Crawford & Peña, 2013). A decrease in pH has been observed in the open ocean (Bates *et al.*, 2012), along upwelling margins (Feely *et al.*, 2008), and is predicted to continue decreasing on a global scale and within the California Current due to ocean acidification (Meehl *et al.*, 2007; Hauri *et al.*, 2013). Studies of pH effects on mollusc larvae with calcified structures have revealed that most are sensitive to reduced seawater pH (reviewed by Kurihara, 2008; Byrne, 2012) associated with increased pCO_2, decreased $[CO_3^{2-}]$, and decreased $CaCO_3$ saturation state (Ω). Furthermore, negative carry-over effects of low-pH exposure for the larval to post-larval stages have been documented from molluscs (Hettinger *et al.*, 2012; Gobler & Talmage, 2013). Studies of $[O_2]$ effects on mollusc larvae with calcified structures have revealed a great deal of tolerance over a broad range of $[O_2]$ down to < 22 μmol kg^{-1} (0.5 ml l^{-1}) (but see Widdows *et al.*, 1989; Eerkes-Medrano *et al.*, 2013).

The development of geochemical proxies in larval carbonate structures for pH and $[O_2]$ could provide a means to determine when larvae have been exposed to potentially threatening pH and $[O_2]$ conditions, and to assess larval performance as a function of pH and $[O_2]$. Given that the larval shell component is retained during the early juvenile phase in molluscs and fishes, pH and $[O_2]$ proxies could also be utilized to evaluate carry-over effects of these parameters on post-larval growth and survival, and as a means to determine the range of pH and $[O_2]$ conditions experienced by larvae that have successfully recruited to adult populations.

Search for a geochemical proxy that reflects carbonate chemistry has intensified with growing interest in modern and past changes in ocean pCO_2 and pH. $\delta^{11}B$ and various trace and minor element-Ca ratios (*e.g.*, Mg/Ca, Sr/Ca, B/Ca, U/Ca) have been studied as possible proxies for low pH in planktic and benthic foraminifera, and invertebrates (Inoue *et al.*, 2011; Raitzsch *et al.*, 2011; Ries, 2011; LaVigne *et al.*, 2013). Of these, the most promising and consistent proxies for carbonate chemistry are $\delta^{11}B$ and U/Ca. The $\delta^{11}B$-pH proxy has been used to reconstruct past pH conditions since there is a pH dependence on the fractionation of $B(OH)_3$, which is enriched in ^{11}B, and $B(OH)_4^-$, enriched in ^{10}B (Xiao *et al.*, 2013). U/Ca in biogenic carbonates shows promise as a proxy for $[CO_3^{2-}]$ since uranium in seawater complexes with carbonate ions (Djogić & Branica, 1993). Development of proxies for oxygen from biogenic carbonates has largely been based on utilizing trace elements that are enriched in hypoxic sediments. Elements such as Ba, Cd, Ni, Zn, or Cu may be associated with organic matter enrichment, while Re, Mo, V and U are related to redox chemistry and may also be affected by pH (Gooday *et al.*, 2009). It is unclear whether these elements become enriched in carbonate laid

down within hypoxic sediments or even hypoxic waters. Limburg and colleagues (2011) and Thorrold and Shuttleworth (2011) found Mn/Ca ratios in otolith carbonate of two fish species, Baltic cod and Atlantic croaker, reflected changes in oxygen. The increase in Mn/Ca was attributed to reductive release of dissolved Mn^{2+} from anoxic sediments.

To date, pH or [O_2] proxies have not been developed for larval carbonate structures, but other environmental parameters are known to affect the elemental composition of larval carbonates. Most efforts have been to infer larval origins for a variety of taxa from multi-element signatures, and to identify salinity, temperature, proximity to land, exposure to hypoxia, pollution and upwelling experienced during the larval stage (reviewed by Levin, 2006). Endogenous factors are also known to influence element signatures; these include growth rates and ontogenetic effects (de Pontual *et al.*, 2003; Chittaro *et al.*, 2006).

The most reliable [O_2] or carbonate chemistry proxy would be primarily controlled by physicochemical principles and have limited influence from endogenous factors. To probe for such a geochemical proxy we allowed embryos of two mytilid mussel species to produce larval shells under differing [O_2] and pH levels and analyzed the shells for multiple trace and minor elements. The objectives of this study were (1) to determine if aragonitic mytilid larval shells precipitated in varying [O_2] and pH conditions have distinct single- or multi-element signatures, (2) to evaluate whether element accumulation was influenced by ontogenetic effects, represented by larval shell size, and (3) to compare element signatures of experimentally produced larval shells with those of field-produced larval shells with known pH and [O_2] exposure histories.

Methods

Laboratory-cultured shells and experimental conditions

Five separate larval culturing experiments were carried out, three with *Mytilus californianus* and two with *M. galloprovincialis*, to produce shells precipitated from differing combinations of pH and [O_2] (Table 6.1). We adopted *Mytilus californianus* and *M. galloprovincialis* larvae as model species because larval development patterns and transport are similar between the two species, but exposures might be different due to differing spawning seasons (Carson *et al.*, 2010). In southern California, *M. galloprovincialis* primarily spawns in the spring when upwelling conditions lower pH and [O_2] in subsurface waters; *M. californianus* primarily spawns in fall when there is less upwelling and higher subsurface pH and [O_2] (Nam *et al.*, 2011). Additionally, precise ablation techniques have been developed for larval shells in both species in the context of evaluating meta-population connectivity (Becker *et al.*, 2007; Carson *et al.*, 2010). Detailed spawning and larval culturing methods are provided in Chapter 5, along with explanations for chosen values of [O_2] and pH. Briefly, larvae were cultured in 4-liter replicate containers nested within a 7.5 liter bucket that received flow-through treatment seawater. There were three replicate containers per treatment for *M. californianus* experiments, and two replicate containers per treatment for *M. galloprovincialis* experiments. Larvae were fed *ad libitum* daily starting on day 2 a pre-mixed phytoplankton diet of *Isochrysis* sp., *Pavlova* sp., *Thalassiosira weissflogii*, and *Tetraselmis* sp. at 50,000 cells ml^{-1} during Expt. A (10 larvae ml^{-1}) and 100,000 cells ml^{-1} during Expt. B and C (50 larvae ml^{-1}). On day 8 post-fertilization, remaining larvae were frozen at -20 °C for later analysis.

Expt. A was designed to produce shells from a combination of pH conditions, and $[O_2]$ was not manipulated. Element data were collected only for *Mytilus californianus* and included three treatments: ambient pH (8.04), low pH (7.51), and low variable pH with semidiurnal fluctuations (7.51 ± 0.15) as occurs along the inner-shelf off California, USA (Table 6.1). Variable conditions were included to determine how trace and minor element signatures of shells vary with a semidiurnal signal relative to constant conditions. Elemental data were collected for both species during Expt. B and C. To test for interactive effects of low pH and low $[O_2]$ on the element signature of larval shells Expt. B was designed with two treatments: (1) ambient pH with ambient $[O_2]$ and (2) low pH with low $[O_2]$, termed low pHOx (Table 6.1). Experimental values with *M. californianus* were 7.90 pH units with 223 µmol O_2 kg^{-1}, and 7.68 with 104 µmol kg^{-1}. Experimental values with *M. galloprovincialis* were 7.91 pH units with 231 µmol O_2 kg^{-1}, and 7.61 with 86 µmol kg^{-1}. To compare element signatures in larval shells precipitated in low pH versus low $[O_2]$, Expt. C was designed with two treatments: (1) low pH with ambient $[O_2]$ and (2) low $[O_2]$ with ambient pH (Table 6.1). Experimental values with *M. californianus* were 7.64 pH units with 230 µmol O_2 kg^{-1}, and 8.00 with 101 µmol kg^{-1}. Experimental values with *M. galloprovincialis* were 7.59 pH units with 234 µmol O_2 kg^{-1}, and 7.95 with 87 µmol kg^{-1}. This combination of treatments was particularly important because it allowed discrimination between pH and $[O_2]$ contributions to variation in the observed shell-element ratios. These combinations of treatments among the three experiments tested pH levels between 7.51 and 8.04, and $[O_2]$ between 86 and 243 µmol kg^{-1}. Temperatures ranged between 15.8 and 16.5 °C in *M. californianus* experiments, and 16.9 and 17.2 °C in *M. galloprovincialis* experiments (Table 6.1). Experiments on *M.*

californianus were carried out between November 2012 and January 2013. Experiments on *M. galloprovincialis* were carried out during May 2012.

Manipulation of seawater carbonate chemistry and [O_2] have been described by Bockmon et al. (2013) and Chapter 5. Discrete samples were taken daily for determination of pH and [O_2], and A_T and salinity were determined at the beginning and end of each experiment. Detailed sampling and measurement procedures are provided in Frieder *et al.* (Submitted). pCO_2, aragonite saturation state (Ω_a) and [CO_3^{2-}] were calculated from average A_T and pH using the Matlab version of CO2SYS (van Heuven *et al.*, 2011) with dissociation constants from Mehrbach et al. (1973) as refit by Dickson and Millero (1987). Temperature, pH and oxygen were also measured continuously in one replicate per treatment with HOBO Pendant temperature data loggers, Honeywell Durafet III pH sensors, and Aanderra optodes.

Field-cultured shells and environmental conditions

To compare shell-element signatures of laboratory-cultured larvae with those of field-developed larvae, *M. californianus* embryos were cultured in the field to produce shell-bearing veligers. The field experiment was carried out from 19 - 27 November, 2011. Within 12 h, post-fertilization embryos were loaded into a larval "home" made from a poly-vinyl chloride plastic pipe capped with 35-μm nitex mesh at both ends (Becker *et al.*, 2007). The home was secured to a mooring line at 7 m water depth immediately offshore of a mussel aggregation at Bird Rock, 32.81°N 117.29°W. The larval home floated within 0.5 m of a seapHOx instrument package that continuously logged pH, [O_2], temperature, and salinity (Fig. 6.1). Details of instrumentation are

provided in Frieder *et al.* (2012). Upon retrieval, the contents of the home were frozen at -20 °C for later sorting and larval shell analysis. Environmental conditions corresponding with the larval outplant are provided in Table 6.1.

Sample Preparation and Analysis

All materials and containers coming into contact with larvae were seawater-leached or acid-leached for at least two weeks using 10% nitric acid and then rinsed thoroughly with ultra-pure water. All sample preparation steps below were carried out in a clean room environment using trace-metal-clean techniques. Larvae from each replicate were sorted into 1.5 ml acid-clean sample cups and rinsed with three aliquots of Milli-Q water to remove seawater and food-associated debris. Shells were soaked in a clean solution of 100 - 300 µl 15% Optima grade hydrogen peroxide (Fisher Chemical) buffered in 0.05 M Suprapur NaOH (EMD Chemicals) for 4.5 - 7 h to remove all organic material, were rinsed in ultra-pure water three times, and transferred to a depression slide and allowed to dry under a Class-100 laminar-flow hood. Dry shells were individually transferred to a petrographic slide covered in double-sided tape (3M Scotch Brand). Between 29 and 47 shells from each experimental replicate were mounted for analysis.

Shells were analyzed using a Thermo Element 2 single-collector ICP-MS operating in low-resolution mode with a New Wave Research UP-213 laser ablation unit (at the University of California Santa Barbara). Helium carrier gas moved ablated material from the laser unit into a "wet" sample chamber created using a 3% Optima nitric acid solution aspirated through a nebulizer. Element analysis of all larval shells

from both species and all experiments was conducted in one effort (3 days during March 2013) to minimize variability due to machine drift. Three standards were used to ensure proper calibration of the instrument: a solution-based dissolved $CaCO_3$ reference material (OTO), and two solid standards, NIST 612 and USGS MACS3 $CaCO_3$ standard. All reference materials, both solution- and solid-based, were analyzed at the beginning and the end of each run; mounting medium and instrument blanks were run multiple times during a sequence. Estimates of the external precision for standards, given as relative SD (%RSD) for the various isotopes, and detection limits are given in Table 6.S1.

Nine element isotopes were selected for analysis at low resolution: ^{24}Mg, ^{48}Ca, ^{55}Mn, ^{63}Cu, ^{66}Zn, ^{88}Sr, ^{138}Ba, ^{208}Pb, and ^{238}U. Isotopes were included in subsequent analyses if counts were > 3 standard deviations (SDs) of background levels when blanks were run. ^{55}Mn was rarely detected 3 SDs above background levels and so was not used for later analysis. During preliminary testing we also tried to detect ^{11}B at low resolution but values were inconsistently detected 3 SDs above background levels. All isotope data are given as concentration relative to ^{48}Ca in either mmol mol^{-1} or µmol mol^{-1} to control for differences in amount of material analyzed per sample. For ablations, laser settings were a single, 30-µm-long x 80-µm-wide line at 40% power, 10 Hz, and 8 µm s^{-1} scanning speed. These settings usually consumed the entire larval shell. The tape used to mount the shells had less than 5% of the average shell value for seven elements. There was significant contamination potential from analysis of mounting tape during shell ablation for two elements: Mg and Mn. Field-produced larvae were analyzed at an earlier date on the same instrument with the same standards and settings, excluding measurements for ^{63}Cu and ^{66}Zn.

Data Treatment and Statistical Analysis

Element-Ca ratios that were ± 5 SD were excluded, and resulted in the exclusion of seven shells out of a total of 969. Element ratios were transformed to normality or near-normality using square-root or log transformations when necessary to meet the normality and homogeneity of variance assumptions of analysis of variance (ANOVA) and regression analysis. All tests were conducted with averaged element-Ca ratios per replicate.

We first tested whether individual element-Ca ratios varied among ambient treatments across experiments using ANOVA because we were concerned that incorporation of some elements could be influenced by external factors (*e.g.*, experiments were conducted at different times when source waters may have had differing seawater chemistry). Mg/Ca ($F_{1,3} = 95$; $p < 0.01$), Ba/Ca ($F_{1,3} = 10$; $p = 0.05$), and Pb/Ca ($F_{1,3} = 80$; $p < 0.01$) were different between *M. californianus* shells from the two ambient treatments in Expt. A and B, and so were not examined for variation with pH or $[O_2]$. Since ambient treatments were not available to compare Expt. B with Expt. C for *M. galloprovincialis*, we were unable to test for an effect of conducting the two experiments at different times.

In order to determine whether there were relationships between pH or $[O_2]$ and individual element-Ca ratios in larval shells, simple linear regressions were performed. We then used simple linear regression to test whether there were ontogenetic effects (reflected by larval size) on individual element-Ca ratios. Larval size was measured as length of the veliger shell, anterior to posterior dimension parallel to the hinge line, on 30

veligers from within each replicate. Results of the effects of $[O_2]$ and pH on larval size itself are provided in Frieder *et al.* (Submitted). Data from all experiments were used for each of the linear regression tests described (n = 20 for *M. californianus* and n = 8 for *M. galloprovincialis*).

In order to examine the utility of a multi-element proxy, we then performed a principal component analysis (PCA) to produce a multi-element linear combination of the ratios Cu/Ca, Zn/Ca, Sr/Ca and U/Ca. Linear regression analyses were used to investigate the degree of association between the principal components and pH or $[O_2]$.

Results

Single-element ratios as a function of pH and $[O_2]$

Two element-Ca ratios varied as a function of pH in both species – U/Ca and Sr/Ca (Fig. 6.1). U/Ca was negatively correlated with pH in both species (Table 6.2), and ratios were 35% higher on average in *M. galloprovincialis* larval shells relative to *M. californianus* larval shells. Sr/Ca was also negatively correlated with pH in both species (Table 6.2), and ratios were 7% higher on average in *M. galloprovincialis* larval shells. Zn/Ca was positively correlated with $[O_2]$ in *M. californianus* (Table 6.2; Fig. 6.1). In *M. galloprovincialis*, none of the element-Ca ratios varied as a function of $[O_2]$.

Since Keul *et al.* (2013) revealed that incorporation of uranium in benthic foraminiferal calcite reflected $[CO_3^{2-}]$ we also performed regressions as a function of $[CO_3^{2-}]$. Regressions resulted in no precipitous change in the coefficient of determination, r^2, relative to pH as the predictor variable (Table 6.2). Since these experiments were designed to vary pH by changing C_T with constant A_T, there was a strong correlation

between pH and [CO_3^{2-}] among treatments and the range in alkalinity among all treatments was only 27 μmol kg^{-1} (Table 6.1). Thus we were unable to identify which aspect of carbonate chemistry changes were driving variation in uptake of U/Ca or Sr/Ca.

There was no influence of variable pH relative to stable pH conditions on the incorporation of any of the elements in the larval shells. During Expt. A on *M. californianus* the third treatment cycled pH by 0.3 units on a semidiurnal basis at a mean of 7.51. There were no differences between U/Ca and Sr/Ca precipitated in stable or cyclic pH (*t* test: $p = 0.412$ and $p = 0.942$, respectively). There was also no interaction of low [O_2] with pH on the incorporation of elements into shells for either species. To test for interactions of [O_2] comparisons were made between U/Ca and Sr/Ca from low pH treatments that were accompanied by ambient [O_2] or low [O_2], as well as comparisons between these element ratios from ambient pH treatments that were accompanied by ambient [O_2] or low [O_2]. For both species, there was no significant difference in U/Ca or Sr/Ca among any of the above treatment comparisons (*t* test: $p > 0.05$).

Element-Ca ratios as a function of size

In *Mytilus californianus*, element-Ca ratios varied with the length of the larval shell for all ratios except U/Ca (Fig. 6.3). All significant relationships had negative correlations except for Cu/Ca. The lack of a relationship between U/Ca and size indicates there is no ontogenetic effect on the incorporation of uranium, which provides further support for its utility as a proxy for pH. In contrast, there was a size effect on the incorporation of strontium, which could hinder the utility of Sr/Ca as a proxy for pH.

In *M. galloprovincialis*, none of the element-Ca ratios varied as a function of shell length (Figure 6.S1). Fewer degrees of freedom available for *M. galloprovincialis* regression tests, along with a lack of treatment or experimental effect on shell length (Frieder *et al.* Submitted) likely contributed to the lack of observation that element-Ca ratios varied with shell length in this species.

Multi-element ratios as a function of pH and [O_2]

For *Mytilus californianus*, PCA resolved three principal components (PC) which explained 97.7% of the total variance (Table 6.3).The values of the eigenvectors showed that all four element-Ca ratios had high loadings on the first PC (PC1), especially Sr/Ca. PC2 was related to Cu/Ca and Zn/Ca, and PC3 was related to Cu/Ca and U/Ca (Table 6.3). Regression analysis of the principal components against pH or [O_2] revealed a significant negative correlation between PC1 and pH, as well as PC3 and pH (Table 6.2; Fig. 6.3). None of the principal components varied with [O_2] ($p > 0.05$ for all regression tests).

For *M. galloprovincialis*, the PCA resolved three principal components (PC) which explained 97.4% of the total variance (Table 6.3).The values of the eigenvectors showed that Zn/Ca, Sr/Ca and U/Ca had high loadings on PC1. PC2 was related to Cu/Ca, and PC3 was related to Sr/Ca and U/Ca (Table 6.3). Regression analysis of the principal components against pH or [O_2] revealed a significant negative correlation between PC1 and pH (Table 6.2; Fig. 6.3). None of the principal components varied with [O_2] ($p > 0.05$ for all regressions).

Comparison with field-cultured larvae

Field-cultured *Mytilus californianus* larvae experienced average pH and [O_2] levels of 8.05 ± 0.04 and 232 ± 7 μmol kg^{-1}, respectively, based on SeapHOx data (Table 6.1). Average temperature during the outplant, 16.5 °C, was within the range of laboratory experiments, but salinity and alkalinity were slightly lower (Table 6.1). U/Ca in larval shells was comparable to laboratory-produced larval shells within the same pH range (Fig. 6.1). Estimated pH exposure based on the laboratory-derived linear relationship between U/Ca and pH was 7.91. Sr/Ca in field-cultured larval shells was higher than laboratory-cultured larval shells at similar pH levels (Fig. 6.1). The element-Ca ratio and size of the field-produced larvae matched well with those from laboratory-produced shells for all ratios except Sr/Ca (Fig. 6.2). We were unable to compare the principal components of field-produced shells because Cu/Ca and Zn/Ca were not measured in field-produced shells, and these ratios had high loadings in each of the laboratory-based principal components.

Discussion

Trace and minor element incorporation into biogenic calcified structures are known to reflect various properties of the water in which they are precipitated. Below we discuss element signatures of larval shells that reflected pH, but not [O_2], except in the case of Zn/Ca, compare our findings with those of previous studies, and further test their utility in natural settings by comparing U/Ca in larval shells that were precipitated along a spatial gradient of upwelling intensity.

Promising geochemical proxies that reflect pH and oxygen exposure for larval shells

Both U/Ca and Sr/Ca decreased with increasing pH in larval mytilid shells. In both species the relationship was stronger with U/Ca. When investigating the utility of multi-element signatures as pH proxies, represented as principal components, relationships were not as strong as those for U/Ca and pH. Principal components that varied as a function of pH had high loadings (*e.g.*, strong correlations between the components and the original ratios) with U/Ca and/or Sr/Ca. Changes in Sr/Ca with pH and $[CO_3^{2-}]$ have also been observed in planktic foraminifera, which precipitate calcite, but the relationship was positive, not negative (Russell *et al.*, 2004). Vital effects have been considered to influence the incorporation of strontium (e.g., Kuffner *et al.*, 2012). In this study we investigated size of the larval shell as a reflection of growth. All element-Ca ratios except uranium varied with larval shell size, and the relationship was strongest for Sr/Ca. The influence of growth and calcification on element incorporation has been observed in other taxa, and is often explained as a Rayleigh fractionation effect (e.g., Gaetani *et al.*, 2011). The lack of a relationship between U/Ca and shell size is important because it provides evidence that uranium incorporation into carbonate is independent of size or growth, which can be a function of many parameters, not just pH. Furthermore, there was no evidence that uranium incorporation varied between stable and fluctuating pH conditions (Expt. A) or as a function of high versus low $[O_2]$ at constant pH (Expt. B and C). Field-cultured larval shells with known pH histories had U/Ca in agreement with lab-produced larval shells. Thus, we suggest that U/Ca is a geochemical proxy that has great potential in reflecting the pH-exposure history of planktonic mollusc larvae.

Zn/Ca increased with increasing [O_2], but only in *Mytilus californianus* shells (Fig. 6.1c). This linear relationship was weaker than that of U/Ca or Sr/Ca with pH (Table 6.2). Zn/Ca also varied as a function of larval shell size, with lower ratios in larger shells (Fig. 6.2). Multi-element signatures, represented as principal components, did not vary with [O_2]. At this point, a promising geochemical proxy for [O_2] reflected in larval carbonate shells is still under exploration. The oxygen values chosen in this study were based on the estimated range experienced by the study species during its pelagic phase (Frieder *et al.* Submitted). Improvement in developing a proxy should consider a broader, more continuous range of [O_2], but it is also possible that larvae of *M. californianus* and *M. galloprovincialis* do not experience [O_2] low enough in the field to exert an influence on trace and minor element incorporation. Low [O_2] employed in this study also did not produce reductions in survivorship, delays in developmental or smaller shell size relative to those cultured at ambient [O_2] (Frieder *et al.* Submitted).

Comparison of U incorporation among taxa

Uranium in seawater occurs in a variety of physicochemical forms, including free ion forms and complexes with carbonate ions. The speciation of these various forms is dependent on the pH conditions and the concentration and availability of complexing ions (*e.g.*, carbonate). At pH of seawater, ~ 8.0, uranium is mostly present as the uranyl tricarbonate complex (Djogić & Branica, 1993). As pH decreases, the proportions of bicarbonate and monocarbonate uranyl complexes increase (Djogić *et al.*, 1986). These changes in speciation are matched with an increase in the free forms uranyl and uranyl hydroxide. It has been suggested that the free forms are more readily incorporated into

biogenic carbonates than the carbonate complexes (Keul *et al.*, 2013), while others have suggested that the relative increase in the bicarbonate and monocarbonate uranyl complexes are incorporated into calcium carbonate in preference to the tricarbonate complex (Russell *et al.*, 2004; Inoue *et al.*, 2011).

While the underlying mechanism resulting in the increased incorporation of uranium into biogenic carbonates remains ambiguous, the trend is consistent across corals, foraminifera and mussels (Table 6.5). Between polymorphs of calcium carbonate there is an overall increase in the U/Ca in aragonite relative to calcite. This trend has been observed in authigenic carbonates, and is attributed to the more stable coordination provided for uranyl by the aragonite structure relative to calcite (Reeder *et al.*, 2000). Differences in U/Ca within a polymorph may be the result of species-specific fractionation against uranium during calcification and underscores the need for species-based calibrations when applying U/Ca to reconstruct past [CO_3^{2-}] or pH or to develop present-day pH exposure histories. Within this study, *M. galloprovincialis* had higher U/Ca than *M. californianus*. Furthermore, there was a greater increase in U/Ca in *M. galloprovincialis* per 0.1 pH unit increase and 100 μmol kg^{-1} increase in [CO_3^{2-}] (Table 6.5). This percent change metric has been developed for comparability among studies (Russell *et al.*, 2004). The expected change in U/Ca per 0.1 pH unit increase is -6 ± 1% in *M. californianus* and -12 ± 2% in *M. galloprovincialis*; the expected change in U/Ca per 100 μmol kg^{-1} increase in [CO_3^{2-}] is -31 ± 5% in *M. californianus* and -68 ± 10% in *M. galloprovincialis*. These values correspond well with changes in U/Ca as a function of pH and [CO_3^{2-}] observed for other species, and is much higher than the only other aragonite-precipitating taxon studied to date (Table 6.5).

In this study, pH and [CO_3^{2-}] were manipulated by altering total dissolved inorganic carbon (C_T) and keeping A_T constant. As a result we were unable to distinguish whether pH or [CO_3^{2-}] directly influenced uranium incorporation into larval aragonitic shells. Others have explored this uncertainty by conducting a series of experiments that decouple carbon system parameters; C_T-stable manipulations that vary pH and [CO_3^{2-}] and pH-stable manipulations that vary C_T and [CO_3^{2-}] (Keul *et al.*, 2013). From these experiments, Keul and colleagues (2013) concluded that [CO_3^{2-}] is the parameter affecting U/Ca. This finding should be considered when applying U/Ca to estimate pH exposures of living fauna. Along upwelling margins, [CO_3^{2-}] and pH covary because changes in carbon chemistry are driven by gradients in C_T with relatively small changes in A_T (Feely *et al.*, 2008; Frieder *et al.*, 2012), and so utilizing U/Ca to estimate pH in these types of settings is likely more reliable. On the other hand, application of U/Ca in systems in which both A_T and C_T vary, such as estuaries influenced by freshwater input or coral reefs with high calcification rates and long residence times, should be approached with caution (e.g., Cao *et al.*, 2011; Shaw *et al.*, 2012).

Variation in larval shell U/Ca along a spatial gradient of upwelling intensity

We further evaluated the utility of larval shell U/Ca as an indicator of spatial gradients in pH by comparing larval shells from regions of varying upwelling intensity. The San Diego County coastline extends over 70 km. Spatial variation in upwelling in the inner shelf is influenced by factors such as flow-topography interactions and inner-shelf hydrodynamics (Kirincich *et al.*, 2005; McPhee-shaw *et al.*, 2007). We used temperature as an index for thermal upwelling (e.g., as in Tapia *et al.*, 2009), which is accompanied

by low pH and low [O_2] (Feely *et al.*, 2008; Frieder *et al.*, 2012). During May 2007, the South Coast region was 2 °C cooler than the Central and North Coast regions (Fig. 6.4). A week-long outplant of *Mytilus galloprovincialis* larvae at eight sites along the coastline were examined for spatial differences in U/Ca (Becker *et al.*, 2007; Carson *et al.*, 2010; see Supplemental Methods). U/Ca ratios were higher in shells from the South Coast region relative to the Central and North Coast regions (Fig. 6.4). The average pH exposure history of shells from South Coast based on the laboratory-derived U-pH proxy was 7.80. The average pH exposure history of those from North and Central Coast regions was 8.09 and 8.16, respectively.

This is the first documentation of a spatial gradient in pH resulting in differing pH exposure histories of planktonic larvae. Spatial patchiness in pH conditions could translate into variation in larval performance and result in carry-over effects. This patchiness, driven by changes in upwelling intensity along the coast, highlights the need to further characterize larval distributions in natural settings. Field surveys have observed larvae of *Mytilus* spp. distributed close to shore (< 5 km), and below the surface Eckman layer (> 10 m) (Shanks & Shearman, 2009), which would expose nearshore larval populations to low pH during upwelling events (Frieder *et al.*, 2012). Furthermore, pH conditions that elicit larval sensitivities are predicted to occur with increasing frequency by 2050 (Hauri *et al.*, 2013). U/Ca in larval carbonates could be a reliable pH proxy in other taxa that retain larval carbonates after metamorphosis, such as fishes and molluscs.

Conclusions

As climate change alters oceanic oxygen and pH levels, their influence on biology becomes increasingly important and appreciated. For many marine organisms and life stages, pH and oxygen exposure histories are largely unknown (*e.g.*, planktonic larvae). The development of geochemical proxies for larval carbonate structures retained at settlement is one means to estimate exposure histories. In this study we determined which trace and minor elements varied with pH and $[O_2]$ in larval shells. The most promising geochemical proxy for pH was U/Ca, which may be directly influenced by $[CO_3^{2-}]$. There were no individual or multi-element signatures that varied with $[O_2]$ without larval size effects. A U-pH proxy was further tested in natural settings to determine whether U/Ca varied in shells precipitated along a spatial gradient of upwelling intensity. Further applications can now be developed and tested to address important larval ecology questions. Examples include what phenomena expose larvae to threatening pH levels? What is the range of larval pH exposure that results in successful recruitment? Is there an effect of pH exposure history (as determined by U/Ca in the larval shell component retained in the juvenile phase) on post-larval growth and survival? This biogenic carbonate-based proxy also has potential beyond larval ecology and could be used to determine changes in pH experienced by populations along a depth, latitudinal or upwelling gradient, or temporal variation in pH exposure in species that exhibit ontogenetic migration. These studies will aid in further assessing the threat of ocean acidification for marine populations.

Acknowledgements

Special thanks to G. Paradis at University of California Santa Barbara for guidance with shell ICPMS analyses. We thank A. G. Dickson and T. R. Martz for providing access to their laboratory facilities to run A_T, salinity, and $[O_2]$ samples. The experimental system used in Expt. A was developed in partnership with Brian Cregger at Safe Harbor Associates LLC. The experimental system used in Expt. B and C was developed by A. G. Dickson and E. E. Bockmon. This research was supported by NSF-OCE Award Nos. 0927445 and 1041062, and under NOAA Grant NA10OAR4170060, California Sea Grant College Program Project R/CC-02EPD and R/CC-04, through NOAA'S National Sea Grant College Program, U.S. Dept. of Commerce; and was supported in part by the California Natural Resources Agency. The statements, findings, conclusions and recommendations are those of the authors and do necessarily reflect the views of California Sea Grant, state agencies, NOAA or the U.S. Dept. of Commerce. This chapter, in part, is currently being prepared for submission for publication of the material. Frieder, Christina A.; Levin, Lisa A. The dissertation author was the primary investigator and author of this material.

References

Bates NR, Best MHP, Neely K, Garley R, Dickson AG, Johnson RJ (2012) Detecting anthropogenic carbon dioxide uptake and ocean acidification in the North Atlantic Ocean. *Biogeosciences*, **9**, 2509–2522.

Becker BJ, Levin LA, Fodrie FJ, McMillan PA (2007) Complex larval connectivity patterns among marine invertebrate populations. *Proceedings of the National Academy of Sciences*, **104**, 3267–72.

Bockmon EE, Frieder CA, Navarro MO, White-Kershek LA, Dickson AG (2013) Controlled experimental aquarium system for multi-stressor investigation: carbonate chemistry, oxygen saturation, and temperature. *Biogeosciences Discussions*, **10**, 3431–3453.

Bograd SJ, Castro CG, Di Lorenzo E, Palacios DM, Bailey H, Gilly W, Chavez FP (2008) Oxygen declines and the shoaling of the hypoxic boundary in the California Current. *Geophysical Research Letters*, **35**, L12607.

Booth JAT, McPhee-Shaw EE, Chua P, *et al.* (2012) Natural intrusions of hypoxic, low pH water into nearshore marine environments on the California coast. *Continental Shelf Research*, **45**, 108–115.

Byrne M (2012) Global change ecotoxicology: Identification of early life history bottlenecks in marine invertebrates, variable species responses and variable experimental approaches. *Marine Environmental Research*, **76**, 3–15.

Cao Z, Dai M, Zheng N, *et al.* (2011) Dynamics of the carbonate system in a large continental shelf system under the influence of both a river plume and coastal upwelling. *Journal of Geophysical Research*, **116**, G02010.

Carson HS, López-Duarte PC, Rasmussen L, Wang D, Levin LA (2010) Reproductive timing alters population connectivity in marine metapopulations. *Current Biology*, **20**, 1926–31.

Chan F, Barth JA, Lubchenco J, Kirincich A, Weeks H, Peterson WT, Menge BA (2008) Emergence of anoxia in the California current large marine ecosystem. *Science*, **319**, 920.

Chittaro PM, Hogan JD, Gagnon J, Fryer BJ, Sale PF (2006) In situ experiment of ontogenetic variability in the otolith chemistry of Stegastes partitus. *Marine Biology*, **149**, 1227–1235.

Cowen RK, Sponaugle S (2009) Larval dispersal and marine population connectivity. *Annual Review of Marine Science*, **1**, 443–466.

Crawford WR, Peña MA (2013) Declining oxygen on the British Columbia continental shelf. *Atmosphere-Ocean*, **51**, 88–103.

Diaz RJ, Rosenberg R (2008) Spreading dead zones and consequences for marine ecosystems. *Science*, **321**, 926–9.

Dickson AG, Millero FJ (1987) A comparison of the equilibrium constants for the dissociation of carbonic acid in seawater media. *Deep-Sea Res.*, **34**, 1733–1743.

Djogić R, Branica M (1993) Study of uranyl(VI) ion reduction at various ionic strengths of sodium perchlorate. *Analytica Chimica Acta*, **281**, 291–297.

Djogić R, Sipos L, Branica M (1986) Characterization of uranium(VI) in seawater. *Limnology and Oceanography*, **31**, 1122–1131.

Eerkes-Medrano D, Menge BA, Sislak C, Langdon CJ (2013) Contrasting effects of hypoxic conditions on survivorship of planktonic larvae of rocky intertidal invertebrates. *Marine Ecology Progress Series*, **478**, 139–151.

Feely RA, Sabine CL, Hernandez-Ayon JM, Ianson D, Hales B (2008) Evidence for upwelling of corrosive "acidified" water onto the continental shelf. *Science*, **320**, 1490–1492.

Frieder CA, Nam SH, Martz TR, Levin LA (2012) High temporal and spatial variability of dissolved oxygen and pH in a nearshore California kelp forest. *Biogeosciences*, **9**, 3917–3930.

Gaetani GA, Cohen AL, Wang Z, Crusius J (2011) Rayleigh-based, multi-element coral thermometry: A biomineralization approach to developing climate proxies. *Geochimica et Cosmochimica Acta*, **75**, 1920–1932.

Gobler CJ, Talmage SC (2013) Short- and long-term consequences of larval stage exposure to constantly and ephemerally elevated carbon dioxide for marine bivalve populations. *Biogeosciences*, **10**, 2241–2253.

Gooday AJ, Jorissen F, Levin LA, *et al.* (2009) Historical records of coastal eutrophication-induced hypoxia. *Biogeosciences*, **6**, 1–39.

Gruber N (2011) Warming up, turning sour, losing breath: ocean biogeochemistry under global change. *Philosophical Transactions of the Royal Society A*, **369**, 1980–96.

Hauri C, Gruber N, Vogt M, *et al.* (2013) Spatiotemporal variability and long-term trends of ocean acidification in the California Current System. *Biogeosciences*, **10**, 193–216.

Hettinger A, Sanford E, Hill TM, *et al.* (2012) Persistent carry-over effects of planktonic exposure to ocean acidification in the Olympia oyster. *Ecology*, **93**, 2758 – 68.

Inoue M, Suwa R, Suzuki A, Sakai K, Kawahata H (2011) Effects of seawater pH on growth and skeletal U/Ca ratios of Acropora digitifera coral polyps. *Geophysical Research Letters*, **38**, L12809.

Katz ME, Cramer BS, Franzese A, Honisch B, Miller KG, Rosenthal Y, Wright JD (2010) Traditional and emerging geochemical proxies in foraminifera. *The Journal of Foraminiferal Research*, **40**, 165–192.

Keeling RF, Körtzinger A, Gruber N (2010) Ocean deoxygenation in a warming world. *Annual Review of Marine Science*, **2**, 199–229.

Keul N, Langer G, de Nooijer LJ, Nehrke G, Reichart G-J, Bijma J (2013) Incorporation of uranium in benthic foraminiferal calcite reflects seawater carbonate ion concentration. *Geochemistry, Geophysics, Geosystems*, **14**, 102–111.

Kirincich AR, Barth JA, Grantham BA, Menge BA, Lubchenco J (2005) Wind-driven inner-shelf circulation off central Oregon during summer. *Journal of Geophysical Research*, **110**, C10S03.

Kuffner IB, Jokiel PL, Rodgers KS, Andersson AJ, Mackenzie FT (2012) An apparent "vital effect" of calcification rate on the Sr/Ca temperature proxy in the reef coral *Montipora capitata*. *Geochemistry, Geophysics, Geosystems*, **13**, Q08004.

Kurihara H (2008) Effects of CO_2-driven ocean acidification on the early developmental stages of invertebrates. *Marine Ecology Progress Series*, **373**, 275–284.

LaVigne M, Hill TM, Sanford E, *et al.* (2013) The elemental composition of purple sea urchin (*Strongylocentrotus purpuratus*) calcite and potential effects of pCO_2 during early life stages. *Biogeosciences*, **10**, 3465–3477.

Levin LA (2006) Recent progress in understanding larval dispersal: new directions and digressions. *Integrative and Comparative Biology*, **46**, 282–97.

Limburg KE, Olson C, Walther Y, Dale D, Slomp CP, Høie H (2011) Tracking Baltic hypoxia and cod migration over millennia with natural tags. *Proceedings of the National Academy of Sciences*, **108**, E177–82.

McPhee-shaw EE, Siegel DA, Washburn L, Brzezinski MA, Jones JL, Leydecker A, Melack J (2007) Mechanisms for nutrient delivery to the inner shelf: Observations from the Santa Barbara Channel. *Limnology and Oceanography*, **52**, 1748–1766.

Meehl GA, Stocker TF, Collins WD, *et al.* (2007) Global climate projections. In: *Climate Change 2007: The Physical Science Basis. Contribution of Working Group I to the Fourth Assessment Report of the Intergovernmental Panel on Climate Change* (eds: Solomon S, Qin D, Manning M, *et al.*), Canbridge, UK and New York, NY, USA.

Mehrbach C, Culberson CH, Hawley JE, Pytkowicz RN (1973) Measurement of the apparent dissociation constants of carbonic acid in seawater at atmospheric pressure. *Limnology and Oceanography*, **18**, 897–907.

Nam S, Kim H-J, Send U (2011) Amplification of hypoxic and acidic events by La Niña conditions on the continental shelf off California. *Geophysical Research Letters*, **38**, L22602.

de Pontual H, Lagardère F, Amara R, Bohn M, Ogor A (2003) Influence of ontogenetic and environmental changes in the otolith microchemistry of juvenile sole (*Solea solea*). *Journal of Sea Research*, **50**, 199–211.

R Thorrold S, Shuttleworth S (2000) In situ analysis of trace elements and isotope ratios in fish otoliths using laser ablation sector field inductively coupled plasma mass spectrometry. *Canadian Journal of Fisheries and Aquatic Sciences*, **57**, 1232–1242.

Raitzsch M, Kuhnert H, Hathorne EC, Groeneveld J, Bickert T (2011) U/Ca in benthic foraminifers: A proxy for the deep-sea carbonate saturation. *Geochemistry, Geophysics, Geosystems*, **12**, Q06019.

Reeder RJ, Nugent M, Lamble GM, Tait CD, Morris DE (2000) Uranyl incorporation into calcite and aragonite: XAFS and luminescence studies. *Environmental Science & Technology*, **34**, 638–644.

Ries JB (2011) Skeletal mineralogy in a high-CO_2 world. *Journal of Experimental Marine Biology and Ecology*, **403**, 54–64.

Russell AD, Hönisch B, Spero HJ, Lea DW (2004) Effects of seawater carbonate ion concentration and temperature on shell U, Mg, and Sr in cultured planktonic foraminifera. *Geochimica et Cosmochimica Acta*, **68**, 4347–4361.

Shanks AL, Shearman RK (2009) Paradigm lost? Cross-shelf distributions of intertidal invertebrate larvae are unaffected by upwelling or downwelling. *Marine Ecology Progress Series*, **385**, 189–204.

Shaw EC, McNeil BI, Tilbrook B (2012) Impacts of ocean acidification in naturally variable coral reef flat ecosystems. *Journal of Geophysical Research*, **117**, C03038.

Tapia FJ, Navarrete SA, Castillo M, *et al.* (2009) Thermal indices of upwelling effects on inner-shelf habitats. *Progress in Oceanography*, **83**, 278–287.

Thorrold SR, Zacherl DC, Levin LA (2007) Population connectivity and larval dispersal: Using geochemical signatures in calcified structures. *Oceanography*, **20**, 32–41.

Whitney FA, Freeland HJ, Robert M (2007) Persistently declining oxygen levels in the interior waters of the eastern subarctic Pacific. *Progress in Oceanography*, **75**, 179–199.

Widdows J, Newell RIE, Mann R (1989) Effects of hypoxia and anoxia on survival, energy metabolism, and feeding of oyster larvae (*Crassostrea virginica*, Gmelin). *Biological Bulletin*, **177**, 154–166.

Xiao J, Xiao Y k., Jin Z d., He M y., Liu C q. (2013) Boron isotope variations and its geochemical application in nature. *Australian Journal of Earth Sciences*, **60**, 431–447.

Table 6.1. Experimental conditions for Experiment A, B and C used to rear mussel larvae of *Mytilus californianus* and *M. galloprovincialis*.

Species	Experiment	Treatment (Reps)	pH	$[O_2]$ (μmol kg^{-1})	Temperature (°C)	Salinity	A_T (μmol kg^{-1})	pCO_2 (μatm)	Ω_a	$[CO_3^{2-}]$ (μmol kg^{-1})
M. californianus	A	Ambient pH (3)	8.04	243*	16.5	33.53	2235	399	2.4	155
		Low pH (3)	7.51	243*	16.5	33.53	2241	1542	0.81	52
		Low Variable pH (3)	7.51 ± 0.15	243*	16.5	33.53	2240	1542 ± 574	0.81 ± 0.27	52 ± 17
	B	Ambient pH & O_2 (3)	7.90	223	15.9	33.49	2228	576	1.78	115
		Low pHOx (3)	7.68	104	15.8	33.49	2227	1006	1.13	73
	C	Low pH (3)	7.64	230	16.3	33.55	2233	1116	1.06	68
		Low O_2 (3)	8.00	101	16.1	33.54	2232	443	2.19	142
	Field [+]	Larval Outplant	8.05	232	16.5	33.23	2225	387	2.42	156
M. galloprovincialis	B	Ambient pH & O_2 (2)	7.91	231	17.2	33.64	2250	567	1.93	124
		Low pHOx (2)	7.61	86	17.2	33.65	2252	1216	1.04	67
	C	Low pH (2)	7.59	234	16.9	33.6	2240	1269	0.98	63
		Low O_2 (2)	7.95	87	17.1	33.62	2241	509	2.07	134

[+] Environmental data for field-cultured larvae were collected with seapHOx instrumentation that recorded pH, $[O_2]$, temperature and salinity every 15 minutes. pCO2, Ω_{arag}, and $[CO_3^{2-}]$ were calculated from pH along with A_T determined from a discrete sample taken at the beginning of the outplant.

* $[O_2]$ was not controlled or measured during Expt. A; values were calculated assuming 100% saturation at corresponding temperature and salinity conditions.

Table 6.2. Summary of element-Ca and principal component linear relationships with pH, $[CO_3^{2-}]$ (μmol kg^{-1}), and $[O_2]$ (μmol kg^{-1}) in *Mytilus californianus* and *M. galloprovincialis.* All regressions and statistics are based on averaged shells from replicates (not means of treatments as plotted in figures). Units for U/Ca are μmol mol^{-1}, and units for all other element-Ca ratios are mmol mol^{-1}. Only relationships that are statistically significant ($p < 0.05$) are included.

Species	Response	Relationship	r^2	p
Mytilus californianus	log(U/Ca)	1.093(±0.15) - 0.116(±0.019) pH	0.67	<0.0001
	log(Sr/Ca)	0.994(±0.184) - 0.066(±.024) pH	0.30	0.012
	PC1	35.0(±10.9) - 4.52(±1.41) pH	0.37	0.005
	PC3	17.7(±5.7) - 2.29(±0.73) pH	0.35	0.005
	log(U/Ca)	0.247(±0.010) - 0.0006(±0.0001) $[CO_3^{2-}]$	0.65	<.0001
	log(Sr/Ca)	0.511(±0.013) - 0.0003(±0.0001) $[CO_3^{2-}]$	0.22	0.038
	log(Zn/Ca)	0.123(±0.121) + 0.001(±0.0006) $[O_2]$	0.23	0.034
Mytilus galloprovincialis	log(U/Ca)	2.925(±0.439) - 0.339(±0.057) pH	0.86	0.001
	log(Sr/Ca)	1.61(±0.27) - 0.140(±0.034) pH	0.74	0.006
	PC1	49.2(±17.1) - 6.34(±2.20) pH	0.58	0.028
	log(U/Ca)	0.466(±0.030) - 0.002(±0.0003) $[CO_3^{2-}]$	0.86	<.0001
	log(Sr/Ca)	0.588(±0.018) - 0.0007(±0.0002) $[CO_3^{2-}]$	0.74	0.006

Table 6.3. Principal component analysis based on Cu/Ca, Zn/Ca, Sr/Ca and U/Ca for (a) *Mytilus californianus* and (b) *M. galloprovincialis* larval shell composition. All experiments and treatments are included in principal components analysis. Variables with high loadings on each of the principal components are indicated in boldface.

(a) *Mytilus californianus*			
	PC1	PC2	PC3
Eigenvalues	2.41	0.86	0.64
Percent (%)	60.3	21.4	16.0
Cum. percent (%)	60.3	81.7	97.7
Element	Eigenvectors		
log(Cu/Ca)	**-0.462**	**0.578**	**0.534**
log(Zn/Ca)	**0.416**	**0.796**	-0.203
log(Sr/Ca)	**0.624**	0.033	-0.088
log(U/Ca)	**0.473**	-0.177	**0.816**
(b) *Mytilus galloprovincialis*			
	PC1	PC2	PC3
Eigenvalues	2.25	1.14	0.51
Percent (%)	56.2	28.5	12.8
Cum. percent (%)	56.2	84.6	97.4
Element	Eigenvectors		
lug(Cu/Ca)	0.162	**-0.840**	0.517
log(Zn/Ca)	**-0.496**	0.364	0.755
log(Sr/Ca)	**0.634**	0.172	**0.109**
log(U/Ca)	**0.571**	0.364	**0.388**

Table 6.4. Summary of studies investigating the influence of carbonate chemistry on U/Ca incorporation into biogenic carbonates. Blank cells indicate data not reported or tested.

Species	Taxon	Life stage characteristic	$CaCO_3$ polymorph	pH studied	$[CO_3^{2-}]$ (μmol kg^{-1}) studied	U/Ca (nmol/mol)	D_U	Percent change with + 0.1 pH unit	Percent change with + 100 μmol kg^{-1} CO_3^{2-}	Reference
Acropora digitifera	coral	primary polyps	aragonite	6.44 - 8.03	7 - 220	1120 - 1428		-1.5		Inoue et al. 2011
Globigerina bulloides	Foraminifera	planktic	calcite	7.74 - 8.65	76 - 469	8 -17		-15 ± 10	-25 ± 23	Russell et al. 2004
Orbulina universa	Foraminifera	planktic	calcite	7.93 - 8.66	111 - 480	5 - 15		-12 ± 3	-25 ± 7	Russell et al. 2004
Ammonia sp.	Foraminifera	benthic	calcite	7.60 - 8.32	21 - 563	32 - 797	0.023 - 0.584		-54	Keul et al. 2013
Planulina wuellerstorfi	Foraminifera	benthic	calcite		85 - 110	5 - 23	0.0034 - 0.0165		-242 §	Raitzsch et al. 2011
Cibicidoides mundulus	Foraminifera	benthic	calcite		86 - 107	3 - 21	0.0024 - 0.015		NS	Raitzsch et al. 2011
Mytilus californianus	Mollusc	planktonic larvae	aragonite	7.51 - 8.04	52 - 155	430 -750	0.33 - 0.62	-6 ± 1	-31 ± 5	this study
Mytilus galloprovincialis	Mollusc	planktonic larvae	aragonite	7.51 - 7.95	63 - 134	570 - 1150	0.44 - 1.16	-12 ± 2	-68 ± 10	this study

Partition coefficient $D_U = (U/Ca_{shell})/(U/Ca_{seawater})$. For this study $U/Ca_{seawater}$ was estimated from salinity using Owens et al. (2011) ^{238}U-salinity relationship in seawater.

NS = relationship not significant

§ Percent change not provided in reference; estimated based on slope of linear relationship and mean U/Ca reported.

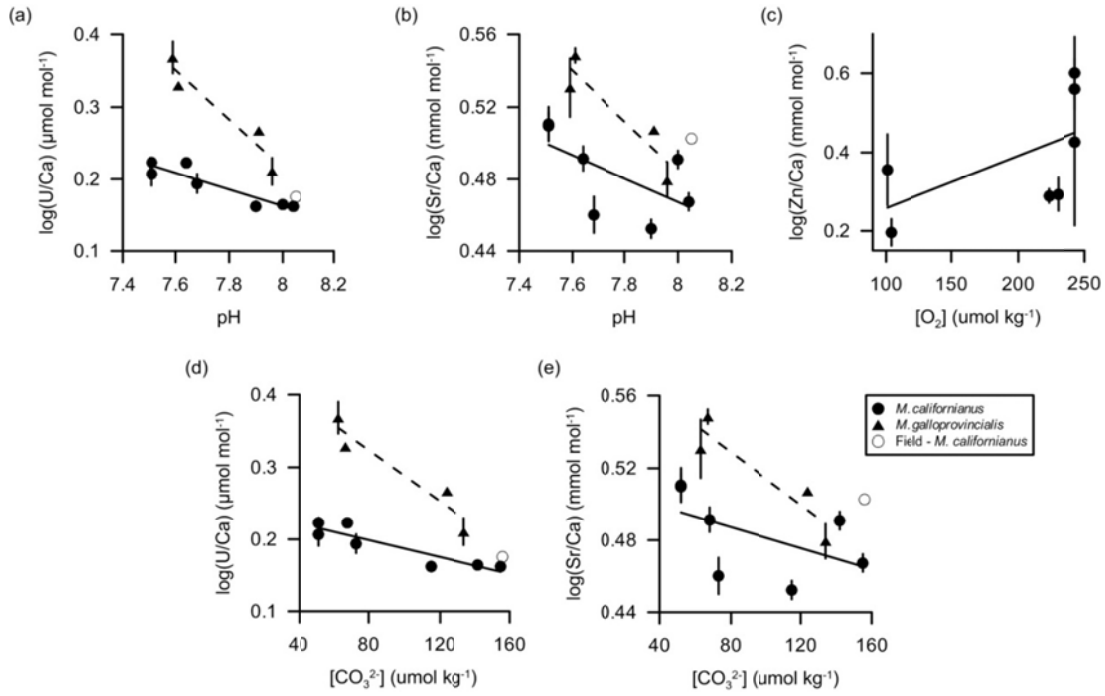

Figure 6.1. Element-Ca ratios as a function of pH for *Mytilus californianus* larval shells (closed circle) and *M. galloprovincialis* larval shells (triangle). Element-Ca of field-cultured *M. californianus* larval shells (open circle) are added to the plot for comparison but not included in statistical analysis. Error bars are ± 1 SE.

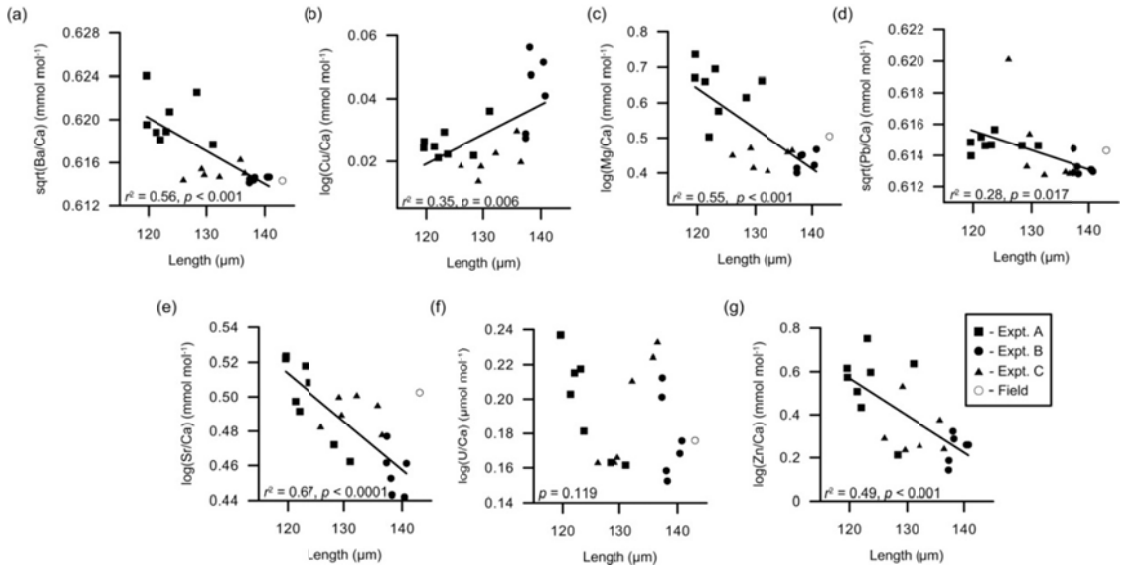

Figure 6.2. Element-Ca ratios as a function of larval length in *Mytilus californianus*. Experiments are designated by differing symbols. Each data point represents the average of multiple larvae measured from a replicate. Lines indicate significant linear regressions.

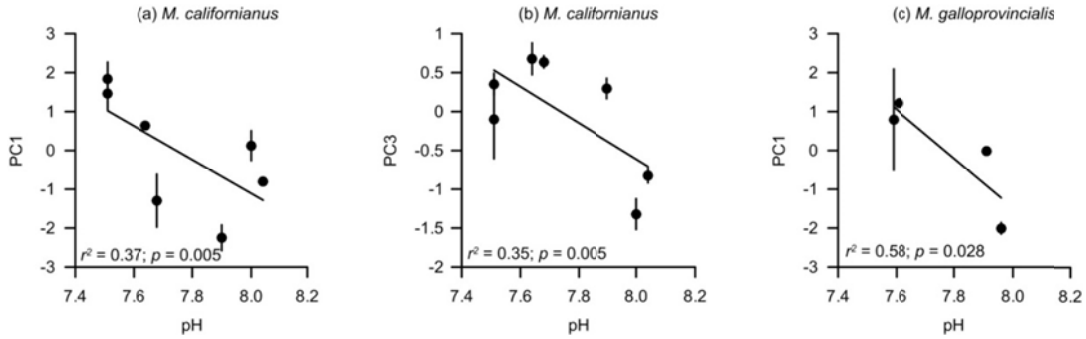

Figure 6.3. Significant linear regressions between principal components and pH. (a, b) *Mytilus californianus* points are means of 3 replicates of principal components derived from averaged multi-element signatures, and (c) *M. galloprovincialis* are means of 2 replicates of principal components derived from averaged multi-element signatures. Error bars are ± 1 SE.

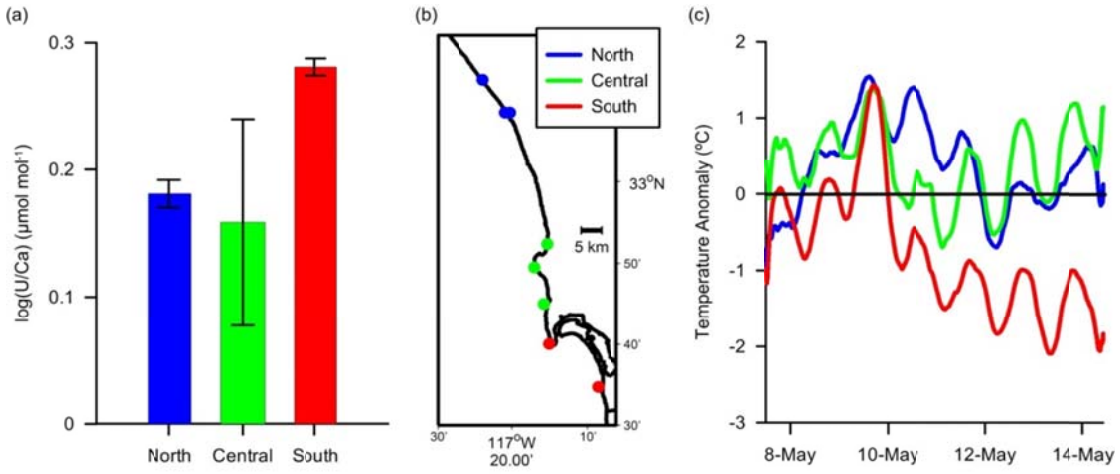

Figure 6.4. (a) Comparison of U/Ca in *Mytilus galloprovincialis* larval shells from three regions precipitated during May 2007 along the San Diego County coastline. pH estimates based on the laboratory-developed U-pH proxy were 8.09, 8.16 and 7.80 for the North, Central and South Region, respectively. (b) Map of sites from the North (n = 3 stations), Central (n = 3 stations), and South (n = 2 stations) regions along the San Diego County coastline. (c) Temperature anomalies for each region during the larval outplant indicate changes in upwelling intensity between the South and other regions. The South was characterized by temperatures up to 2 °C cooler than the Central or North Region.

Supplemental Material: Methods, 1 Table and 1 Figure

Supplemental Methods

To test for spatial variation in U/Ca of larval shells from regions of differing upwelling intensity, shell elemental data were derived from a trace-element fingerprinting study of realized population connectivity for *Mytilus californianus* and *M. galloprovincialis* (Carson et al. 2010). The outplant conducted during May 2007 was chosen because shells were analyzed on the same instrument as utilized in this study (Table 6.S1). Only data from *M. galloprovincialis* were available. Sites from this outplant were split into three regions, and only open coast sites were included to avoid salinity influences on uranium (Carson et al. 2013). The North County region included Agua Hedionda, Oceanside Harbor and Agua Lagoon. The Central County region included Dike Rock, La Jolla and Ocean Beach. The South County region included Imperial Beach and Cabrillo. Larval shell U/Ca was averaged from 20 individual shells for each site, except for Oceanside Harbor and Dike Rock (n = 6 and 13 larval shells, respectively). Temperature data were recorded with the use of a HOBO Pendant® temperature data logger located next to larval home at each site.

Table 6.S1. Estimates of external precision for standards, given as relative SD (%RSD) for the various isotopes and detection limits for analyses made during March 2013, along with %RSD and detection limits for uranium from *Mytilus galloprovincialis* shells analyzed during Feb. 2009 that were generated during the May 2007 outplant.

	MACS 3	NIST 612	OTO	Detection Limit (mmol mol^{-1} Ca)
Mg	7.35	4.11	6.51	0.162
Cu	8.66	8.47	4.34	0.031
Zn	15.11	22.82	11.45	0.022
Sr	10.50	3.33	2.67	0.565
Ba	14.53	7.05	4.72	0.063
Pb	23.17	12.20	8.08	0.033
U (Mar. 2013)	25.68	12.09	9.47	0.003
U (Feb. 2009)	4.03	4.55	0.97	0.063

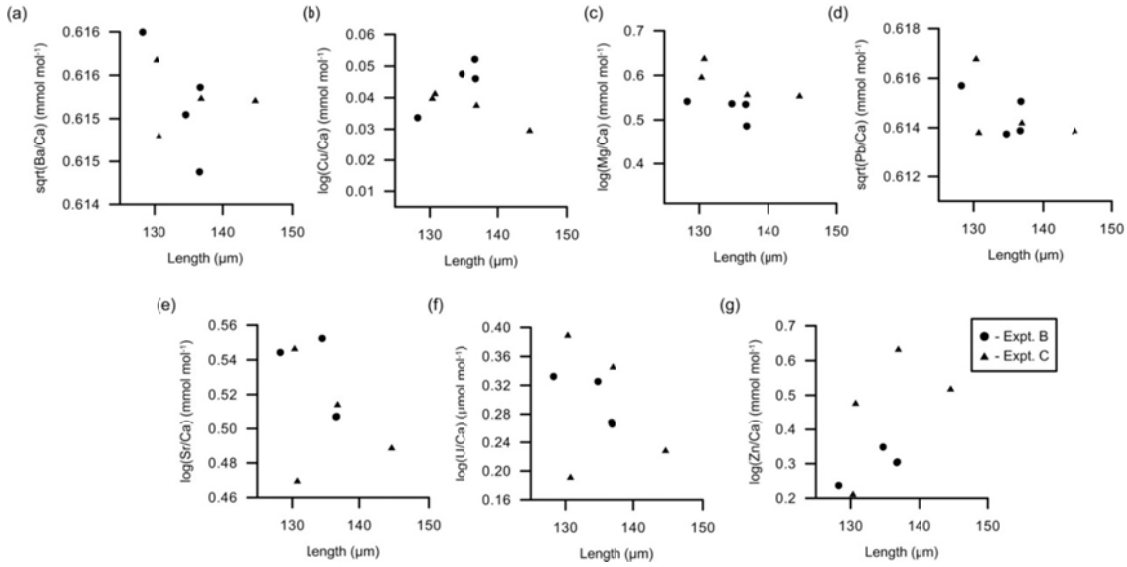

Figure 6.S1. Element-Ca ratios as a function of larval length in *Mytilus galloprovincialis*. Experiments are designated by differing symbols. Each data point represents the average of multiple larvae measured from a replicate. None of the linear regressions were significant ($p > 0.05$).

CHAPTER 7

Conclusions

Within the chapters of this dissertation are tests of the potential threats of oxygen and pH for invertebrate early life stages along upwelling margins. Special consideration was made to incorporate the natural oxygen and pH conditions of nearshore habitats within the Southern California Bight along with region-specific projections of pH change. Emphasis was placed on gamete performance and fertilization success in echinoids, and larval stages in both echinoids and mytilid mussels. Four major conclusions have been identified that were common among the chapters. (1) The tolerance of individuals to a stress, pH in this case, is species-specific and there were no obvious, unifying characteristics (*e.g.*, genetic relatedness, habitat type, depth distribution, time of spawning) to predict magnitude of a response to pH. (2) High-frequency pH variability is an underappreciated source of pH-stress alleviation that could have increasing importance in future, low-pH oceans. (3) Spatial variability in pH that is present now and will continue into the future results in differing exposure histories of organisms. And, (4) a first-level evolutionary response of a population to ocean acidification could be reflected by increased variance of a response variable. In addition, there was no evidence that low oxygen altered larval performance either as an individual stressor or in combination with low pH, indicating that along upwelling margins oxygen is not a threat for early life stages of mytilid mussels within the ranges that presently occur in nearshore settings.

Many researchers have attempted to identify unifying characteristics among taxa that will allow prediction of winners and losers to ocean acidification (e.g., Kroeker *et*

al., 2010). Often these characteristics are associated with calcium carbonate polymorphs that have differing solubility products, or the ability of a group to maintain homeostasis, or even habitat type. On the other hand, many experimental studies have identified a great deal of variability in responses among species that fall within these generalities (reviewed by Doney *et al.*, 2009). Responses that were species-specific were a common finding among my studies. Fertilization in three of the four echinoids studied in Chapter 3 were largely robust to reduced pH, but *Strongylocentrotus francsicanus* fertilization was sensitive to modest reductions in pH even though it inhabits the same environment as *S. purpuratus* and is within the same genus as two of the echinoids studied. In Chapter 4, *Paracentrotus lividus* larvae were particularly sensitive, as demonstrated by shrinking of the larval arms and body, to extreme low pH (≤ 7.48) at CO_2 vents in the Mediterranean. On the other hand, larval size of *Arbacia lixula* did not vary with pH at the vents. Lastly, in Chapter 5, while the effect of pH on larval size of *Mytilus californianus* and *M. galloprovincialis* was similar, their response to semidiurnal fluctuations at low pH was different. *M. galloprovincialis* benefitted from pH fluctuations suggesting that larvae of this species might better cope with ocean acidification in variable environments than those of *M. californianus*. Altogether, these examples highlight the presence of both striking and subtle differences in species-specific responses to ocean acidification, even in closely related species with overlapping distributions, and suggest that grouping organisms based on common traits may be yielding misguided generalities about winners and losers.

Another important conclusion based on similar findings among the chapters is the importance of the interaction of high-frequency pH variability with reduced pH. The

dominance of semidiurnal and diurnal pH fluctuations in nearshore environments along upwelling margins was well established in Chapter 2, published as Frieder *et al.* (2012). Daily ranges in pH and oxygen were observed to be as large as 0.36 units and 220 μmol kg^{-1} at 7 m water depth, and average daily ranges were 0.11 pH units and 63 μmol kg^{-1}, respectively. Incorporation of high-frequency pH variability into ocean acidification experiments revealed that the negative effect of reduced pH on developmental rate in both mytilid mussel species was alleviated, but the effect of reduced pH on larval size was alleviated in only *M. galloprovincialis*. Additionally, seasonality in reproductive timing of *Mytilus californianus* and *M. galloprovincialis* might also dictate larval sensitivity in each species. *M. californianus* predominantly spawns during the fall when seasonal pH is higher along the coast, and *M. galloprovincialis* predominantly spawns during the spring when seasonal pH is at its lowest along the coast. Further consideration of present-day variability suggests that fertilization success of *Strongylocentrotus franciscanus* could be decreasing by as much as 21% when natural, present-day conditions are at their lowest. Thus timing of spawning, predominantly during the spring for *S. franciscanus*, may become increasingly important over time.

Spatial pH variability also plays an important role in providing alleviation to pH stress much in the same way that temporal pH variability does. There are present-day latitudinal pH gradients along upwelling margins; along the northeastern Pacific margin, regional differences in upwelling drive spatial gradients in pH (Feely *et al.*, 2008; Hauri *et al.*, 2009), likely resulting in different pH-exposure histories of populations that span this biogeographic range (LaVigne *et al.*, 2013). Meso-scale variability in upwelling putatively reflected differing pH-exposure histories of mussel larvae in Chapter 6, as

revealed by U/Ca in larval carbonates originating from different regions along the San Diego coastline. Plus, natural environments exhibit spatial gradients in many environmental factors, not just pH. In the field experiments at natural CO_2 vents there was extensive variability in the size response of echinoid larvae among sites, even in the face of extreme reductions in pH. This suggests that laboratory-based experiments overestimate larval sensitivity to reduced pH, and in natural settings larval performance is an integration of many environmental parameters with influence from pH being just one of many factors.

Increased variance in a population in response to a stressor can represent the first steps in the evolution of a population to a changing environment, and a population's resilience could be dependent on increased phenotypic variance (Orlando & Guillette, 2001). In Chapter 3, variance in gamete performance of individual males resulted in variable pH effects on fertilization success in both *Strongylocentrotus purpuratus* and *S. franciscanus*. Gametes of males that are less sensitive to reductions in pH may be dominant fertilizers during low pH conditions. In Chapter 5, *Mytilus galloprovincialis* had an increase in size variance of 76% at low pH relative to ambient pH and *M. californianus* had an increase of 49%. This leads to the possibility that *M. galloprovincialis* will have greater resilience to reductions in pH than *M. californianus*.

The development of geochemical proxies of oxygen and pH exposure from larval carbonates in Chapter 6 provides a new direction for the field of ocean acidification research. U/Ca in larval carbonates was demonstrated to have potential to accurately reflect pH-exposure histories of planktonic mussel larvae. Provided that environmental conditions experienced by larvae are often unknown due to the elusive nature of larval

trajectories, developing a proxy that estimates pH-exposure histories will become increasingly useful as ocean acidification progresses. Being able to estimate pH conditions experienced by the larval stage in the field can result in unique and previously unavailable ways to explore what phenomena expose larvae to threatening pH levels, the range of larval pH exposure that results in successful recruitment, and the effect of larval pH-exposure history on post-larval growth and survival.

In conclusion, reductions in pH appear to be a greater threat than reductions in oxygen for early life stages of mussels inhabiting nearshore environments along upwelling margins, and moderate reductions in pH were only a threat for fertilization in one of four echinoid species. Accurate assessment of pH effects for broadcast spawners and planktonic larvae requires appreciation for species-specific tolerances along with temporal and spatial gradients in pH which provide heterogeneous exposure of distinct planktonic larval populations.

References

Doney SC, Fabry VJ, Feely RA, Kleypas JA (2009) Ocean acidification: The other CO_2 problem. *Annual Review of Marine Science*, **1**, 169–192.

Feely RA, Sabine CL, Hernandez-Ayon JM, Ianson D, Hales B (2008) Evidence for upwelling of corrosive "acidified" water onto the continental shelf. *Science*, **320**, 1490–2.

Hauri C, Gruber N, Plattner G-K, Alin S, Feely RA, Hales B, Wheeler PA (2009) Ocean acidification in the California Current system. *Oceanography*, **22**, 60–71.

Kroeker KJ, Kordas RL, Crim RN, Singh GG (2010) Meta-analysis reveals negative yet variable effects of ocean acidification on marine organisms. *Ecology Letters*, **13**, 1419–34.

LaVigne M, Hill TM, Sanford E, *et al.* (2013) The elemental composition of purple sea urchin (*Strongylocentrotus purpuratus*) calcite and potential effects of pCO_2 during early life stages. *Biogeosciences*, **10**, 3465–3477.

Orlando EF, Guillette LJ (2001) A re-examination of variaiton associated with environmentally stressed organisms. *Human Reproduction Update*, **7**, 265–272.